การศึกษาเปรียบเทียบเทคนิคการสังเคราะห์ผงอลูมินาต่อสมบัติทางกายภาพและทางแสงของอลูมินาเซรามิกที่เติมแต่งสี

นางสาวธนิษฐา ประสิทธิวุฒิศักดิ์

วิทยานิพนธ์นี้เป็นส่วนหนึ่งของการศึกษาตามหลักสูตรปริญญาวิศวกรรมศาสตรมหาบัณฑิต
สาขาวิศวกรรมเคมี ภาควิชาวิศวกรรมเคมี
คณะวิศวกรรมศาสตร์ จุฬาลงกรณ์มหาวิทยาลัย
ปีการศึกษา 2547

ISBN 974-53-1418-8

COMPARATIVE STUDY OF ALUMINA POWDER SYNTHESIS TECHNIQUES TO THE PHYSICAL AND OPTICAL PROPERTIES OF COLORED ALUMINA CERAMICS

Miss Tanitta Prasitwuttisak

A Thesis Submitted in Partial Fulfillment of the Requirements
for the Degree of Master of Engineering in Chemical Engineering
Department of Chemical Engineering
Faculty of Engineering
Chulalongkorn University
Academic Year 2004

ISBN: 974-53-1418-8

Thesis Title	COMPARATIVE STUDY OF ALUMINA POWDER SYNTHESIS TECHNIQUES TO THE PHYSICAL AND OPTICAL PROPERTIES OF COLORED ALUMINA CERAMICS
By	Miss Tanitta Prasitwuttisak
Field of Study	Chemical Engineering
Thesis Advisor	Varong Pavarajarn, Ph.D.

Accepted by the Faculty of Engineering, Chulalongkorn University in Partial Fulfillment of the Requirements for the Master's Degree

…..……..…… Dean of the Faculty of Engineering
(Professor Direk Lavansiri, Ph.D.)

THESIS COMMITTEE

…… Chairman
(Associate Professor Suttichai Assabumrungrat, Ph.D.)

……. Thesis Advisor
(Varong Pavarajarn, Ph.D.)

……. Member
(Associate Professor Tawatchai Charinpanitkul, Ph.D.)

……. Member
(Joongjai Panpranot, Ph.D.)

ธนิษฐา ประสิทธิวุฒิศักดิ์: การศึกษาเปรียบเทียบเทคนิคการสังเคราะห์ผงอลูมินาต่อสมบัติทางกายภาพและทางแสงของอลูมินาเซรามิกที่เติมแต่งสี (COMPARATIVE STUDY OF ALUMINA POWDER SYNTHESIS TECHNIQUES TO THE PHYSICAL AND OPTICAL PROPERTIES OF COLORED ALUMINA CERAMICS) อ. ที่ปรึกษา: ดร. วรงค์ ปวราจารย์, 107 หน้า. ISBN: 974-53-1418-8

ผงอัลฟาอลูมินาที่มีขนาดผลึกในระดับนาโนเมตร สามารถสังเคราะห์ได้จากวิธีตกตะกอน วิธีโซลเจล และวิธีโซลโวเทอร์มอล โดยมีขนาดผลึก 9.65 9.52 และ 9.74 นาโนเมตรตามลำดับ ผลิตภัณฑ์ที่สังเคราะห์ได้จากแต่ละวิธีสามารถเปลี่ยนเป็นเฟสอัลฟาโดยการให้ความร้อนที่อุณหภูมิ 1150 องศาเซลเซียสเป็นเวลา 3 ชั่วโมง ลักษณะของผงที่ผ่านการให้ความร้อนแล้วพบว่ามีการเกาะกันอย่างหลวมๆ ซึ่งสามารถลดขนาดอนุภาคลงได้โดยการบด นอกจากนี้ได้ทำการศึกษาปัจจัยต่างๆ ที่มีผลต่อขนาดและการกระจายขนาดของอนุภาคในวิธีตกตะกอน ได้แก่ ความเร็วในการผสม อุณหภูมิ และค่าพีเอชของระบบที่เกิดปฏิกิริยา นอกจากนี้ได้ทำการสังเคราะห์ผงอลูมินาที่เติมแต่งสีด้วยโลหะโครเมียมความเข้มข้นต่างๆ ในช่วง 0.05 ถึง 0.5 เปอร์เซ็นต์ของสารประกอบโครเมียม การให้ความร้อนแก่ผลิตภัณฑ์ส่งผลให้ได้ผงอลูมินาที่มีความเข้มแตกต่างกันตามปริมาณโครเมียมที่เข้าไปในโครงสร้างของอลูมินาโดยอยู่ในรูปของโครเมียมไอออน(III) นอกจากนี้ได้ทำการศึกษาเปรียบเทียบความหนาแน่นของอลูมินาที่สังเคราะห์ และอลูมินาที่สังเคราะห์โดยมีการเติมโลหะโครเมียม โดยเทียบกับอลูมินาทางการค้า ชิ้นงานที่ขึ้นรูปได้ถูกเผาผนึกในอากาศที่อุณหภูมิ 1550 องศาเซลเซียส เป็นเวลา 2 ชั่วโมงพบว่า ค่าความหนาแน่นของอลูมินาที่สังเคราะห์ได้ทั้งในแบบที่เติมโลหะโครเมียมและไม่เติมโลหะโครเมียม อยู่ในช่วงร้อยละ 93-98 ของความหนาแน่นทางทฤษฎีของอลูมินา

ภาควิชา....วิศวกรรมเคมี..... ลายมือชื่อนิสิต.....

สาขาวิชา....วิศวกรรมเคมี..... ลายมือชื่ออาจารย์ที่ปรึกษา.....

ปีการศึกษา.....2547..... ลายมือชื่ออาจารย์ที่ปรึกษาร่วม.....

4670690121 : MAJOR CHEMICAL ENGINEERING
KEY WORDS : SOL-GEL, PRECIPITATION, SOLVOTHERMAL, ALUMINA, CHROMIUM DOPED

TANITTA PRASITWUTTISAK: COMPARATIVE STUDY OF ALUMINA POWDER SYNTHESIS TECHNIQUES TO THE PHYSICAL AND OPTICAL PROPERTIES OF COLORED ALUMINA CERAMICS. THESIS ADVISOR: VARONG AVARAJARN, Ph.D., 107 pp. ISBN: 974-53-1418-8.

α-alumina with nanocrystallite size can be successfully synthesized by precipitation, sol-gel and solvothermal method with crystallite size of 9.65, 9.52 and 9.74 nm, respectively. As-synthesized product from these methods can be completely transformed to α-phase by heat treatment at 1150^{o}C for 3 h. The morphology of calcined product is found to be loosely agglomerated powder that can be broken off by milling. For precipitation method, many factors affect size and size distribution of powder, including the speed of mixing, the reaction temperature and pH of the reaction system. Furthermore, all synthesis techniques can be employed for the preparation of chromium-doped alumina in various chromium concentrations, in the range of 0.05-0.5 wt% of chromium precursor. Heat treatment of the obtained samples results in wide range of red-colored alumina, which suggests different amount of chromium ions residing in alumina matrix in Cr^{3+} form. Fabrication of undoped alumina and chromium-doped alumina are also investigated and compared with commercial alumina. The compacted bodies were sintered at 1550°C for 2 h in air. The relative density of sintered specimens prepared from various techniques were in the range of 93-98% of theoretical density.

Department …Chemical Engineering….. Student's signature ……
Field of Study ……Chemical Engineering…….. Advisor's signature ……
Academic year ……2004……. Co-advisor's signature ……...

ACKNOWLEDGEMENTS

The author would like to express her sincere gratitude and appreciation to her advisor, Dr. Varong Pavarajarn, for his invaluable suggestions, stimulating, useful discussions throughout this research and devotion to revise this thesis otherwise it can not be completed in a short time.

The author is similarly grateful to Professor Shigetaka Wada, Mr. Nirut Wangmuklang and Mr. Soontorn Tansungnoen for their kind suggestion throughout this work. In addition, the author would also be grateful to Associate Professor Suttichai Assabumrungrat, as the chairman, and Associate Professor Dr. Tawatchai Charinpanitkul and Dr. Joongjai Panpranot, as the members of the thesis committee.

The author would like to acknowledge to Thailand Research Fundd (TRF), Thailand Japan Technology Transfer Project (TJTTP), Graduate School of Chulalongkorn University and National Nano-Technology Center (NANOTEC) for their financial support.

The author wishes to thank the members of the Center of Excellence on Catalysis and Catalytic Reaction Engineering, Department of Chemical Engineering, Faculty of Engineering, Chulalongkorn University for their assistance especially Dr. Okorn Mekasuwandumrong and Miss Patta Soisuwan.

Finally, the author would like to express her highest gratitude to her parents who always pay attention to her all the times for suggestions and have provided her support and encouragement. The most success of graduation is devoted to her parents.

CONTENTS

PAGE

LIST OF TABLES

LIST OF FIGURES

FIGURE **PAGE**

FIGURE **PAGE**

CHAPTER I

INTRODUCTION

Alumina (Al_2O_3) is an important material in ceramic industry. It has been considered as one of the most promising advanced materials for varieties of applications because of its good properties. It has high surface area with the fine particle size, high melting point (above 2000°C), high purity, good adsorbent, and good catalytic activity. Alumina can be used in many applications, i.e. as absorbents, ceramic tools, fillers, wear-resistant ceramic, catalyst, catalyst support, ceramic coatings, soft abrasives, medium balls, crucibles and saggers for high temperature refractory applications. Many preparation methods have been developed to prepare alumina powder that possesses the required characteristics. Examples of these method are sol-gel synthesis [1], hydrothermal synthesis [2], microwave synthesis [3], emulsion evaporation [4-5], precipitation from solution [6] and solvothermal synthesis [7-14]. In such methods, the required characteristics are obtained by controlling the crystal type, crystal size, particle shape, particle size distribution, degree of agglomeration and porosity [15-22].

Alumina is not only fabricated and used in its pure, single-phase configuration Al_2O_3, but there exists a wide series of material compositions which start from Al_2O_3 as a base material. It may appear as a single-oxide component or in combination with various ceramics oxides or even metallic phase. The improvement of facilities and techniques has strongly contributed to an improvement of the quality of ceramic products. Since alumina is conventionally produced in powder form, shape forming process is necessary for the fabrication of an alumina article. During forming process, alumina raw material should be compacted and formed into desired shape at the same time. Compacting is necessary for bringing the particles as close together as possible in order to eliminate pores in the specimen by the surface tension during sintering. There are many kinds of the forming process, for instance, dry pressing, hydrostatic molding, extrusion, injection molding, and hot pressing. Applications of each forming technique depends upon dimension and shape of part to be fabricated, quantity of parts, and the requirements of the final product. Subsequent sintering results in alumina article having properties suitable for variety of applications.

Ceramic pigment is one of the important applications in ceramic industry. Thermally stable ceramic pigments can be produced by heating intimate mixture of metal oxides colorant with alumina at temperature sufficiently high for obtaining color development. Various colored gemstones have been developed from alumina by adding the appropriate oxides to precursors during the synthesis of alumina, for instance, to the feed in the Verneuil process [23] or to the nutrient alumina in the solution-grown processes. Spinel formation and the Chemical Vapor Deposition technique (CVD) are also effective methods for to achieve a range of brilliant colors from metal oxides, for use as ceramic stains and pigments.

This research is a comparative study of different synthesis methods, which are precipitation method, sol-gel method, and solvothermal method, for producing alumina nanopowders. Doping of metal oxide colorant during alumina synthesis according to all mentioned methods is also investigated. All alumina nanoparticles are fabricated into alumina articles and sintering at high temperature in order to investigate the effect of the synthesis powders on properties of the sintered article.

CHAPTER II

THEORY AND LITERATURE REVIEW

Study of alumina has been a subject of great interest for many decades. Alumina is widely used as ceramics, catalyst, catalyst support, wear-resistance material, abrasives, medicinal material, and adsorbent, because of its distinctive chemical, mechanical and thermal properties. The basic knowledge of alumina including its crystal structure, preparation techniques, and phase transformation of transition alumina is described in this chapter. Furthermore, shape forming technique and sintering are also described.

2.1 Crystal Structure of α-alumina

The extensive crystallographic researches on the each phase of alumina have been conducted by many researchers. For instance, a very detailed crystallographic description of sapphire single crystals was given by Kronberg et al.,(1957). The structure of α-alumina consists of close packed planes of the large oxygen ions stacking in A-B-A-B sequence, thus forming hexagonal close packed array of anions. The aluminium cations are located at octahedral sites of this basic array and form another type of close packed planes between the oxygen layers. To maintain neutral charge, however, only two third of the available octahedral sites are filled with cations. Figure 2.1 illustrates the packing of Al and O atoms in the basal plane. Since the vacant octahedral sites also form regular hexagonal array, three different types of cation layer can be defined, namely a, b, and c layer, depending on the position of the vacant cation site within the layer. These layer are stacked in a-b-c-a-b-c sequence in the structure of alumina.

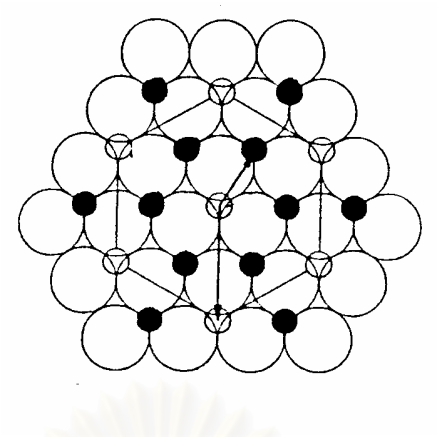

Figure 2.1 Illustration of Al and O atoms packing in the basal plane [24].

2.2 Phase Transformation

Alumina can exist in many metastable phases before transforming to the stable α-alumina (corundum form). There are six principal metastable phases of alumina designated by the Greek letters chi (χ), kappa (κ), eta (η), theta (θ), delta (δ), and gamma (γ), respectively. Although the range of temperature in which each transition phase is thermodynamically stable has been reported by many researchers, it depends upon various factors such as degree of crystallinity of sample, amount of impurities in the starting materials, and thermal history of sample. Most of the studies on phase transformation of alumina was conducted by calcinations of alumina precursor. It was found that difference in the phase transformation sequence is resulted from the difference in the precursor structure [25-26]. Moreover, the transformation sequence is irreversible. The nature of the product obtained by calcination depends on the starting hydroxide and on the calcination condition.

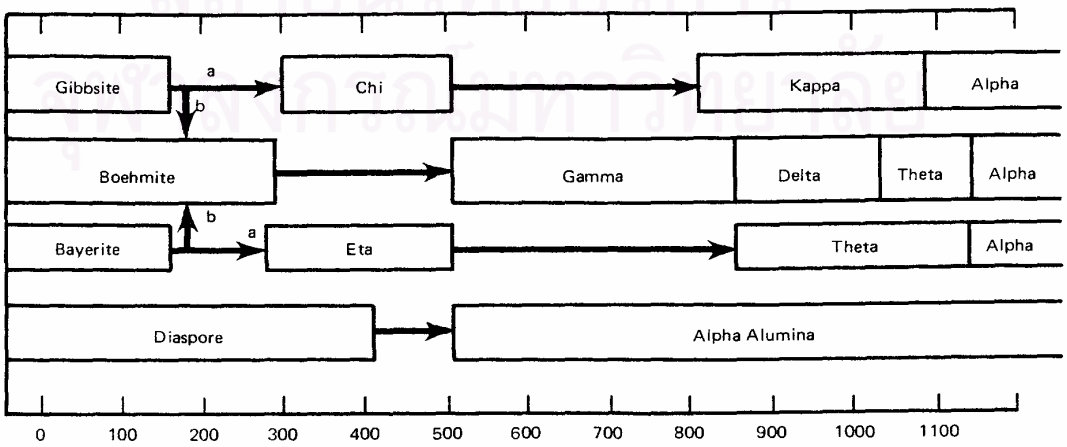

Figure 2.2 Transformation sequence of aluminum hydroxides [27].

The phase transformation sequence normally starts with aluminum hydroxide ($Al(OH)_3$ and AlOOH) transforming to low-temperature phase of alumina (η and χ) at temperature around 150-500^oC, and subsequently to high temperature phase (δ, θ, κ) at temperature around 650-1000^oC. Finally, the thermodynamically stable phase, α-alumina, is formed at temperature around 1100-1200^oC. It is generally believed that α-phase transformation takes place through the nucleation and growth mechanism.

Normally, transition alumina start to lose their surface area even at temperature below 800^oC due to the elimination of micro-pores. However, drastic loss occurs at temperature higher than 1000^oC when the crystallization to the thermodynamically stable α-alumina occurs [28].

Several studies have been carried out on the direct phase transformation of alumina. The mechanism of direct phase transformation and the direct phase transformation from γ-alumina to α-alumina involving the conversion of the cubic close packing of oxygen ions into a stable hexagonal close packing which have been examined [29, 30]. Morinaga et al (2000) [31] studied the phase transformation that occurred during the thermal decomposition of ammonium aluminum carbonate hydroxide into α-alumina. Amorphous, γ-, θ-alumina were identified as intermediate products. They have found that the atmosphere affects the grain size distribution of the final α-alumina particles

2.3 Preparation Methods for Al_2O_3 Powder

There are many methods which have already been used to prepare alumina powder. Many techniques are developed to prepare alumina powder which are sol-gel synthesis [1], hydrothermal synthesis [2], microwave synthesis [3], emulsion evaporation [4, 5], precipitation from solution [6] and solvothermal synthesis [7-14] . In this research, solvothermal, sol-gel, and precipitation method are investigated because of their advantages that would be further discussed in this section. The products from these methods are different in quality and properties.

2.3.1 Solvothermal method

Solvothermal synthesis is improved from the hydrothermal synthesis by using organic solvent as the reaction medium instead of water. This method is based on the decomposition of metal alkoxide at elevated temperature (200-300^{o}C) under autogenous pressure. It is particularly suited for the synthesis of alumina in phase that is unstable at high temperature. It is also a useful technique for growing single crystals. In this method, parts or all of the reactants can dissolve in the organic solvent under high pressure. This feature enables the reaction to take place at lower temperature.

Generally, solvothermal equipment is basically a tube, usually made of steel, closed at one end. The other end has a screw cap with a gasket of soft copper to provide a seal. Alternatively, the “bomb” may be connected directly to an independent pressure source, such as a hydraulic ram. This is known as the “cold seal” method. The reaction mixture with appropriate amount of solvent are placed inside the bomb, which is then sealed and placed inside an oven at the required temperature, in the range of 100-500^{o}C. Pressure is controlled either externally or by the degree of filling in the sealed bomb.

Alumina can also be synthesized by the solvothermal method. Inoue et al. has developed technique to synthesize inorganic materials by using organic media at elevated temperature (200-300^{o}C) under autogeneous pressure of organic for many years (1988-2002). It has been found that many oxides and mixed oxides can be crystallized in organic media at temperature lower than that required by the hydrothermal reaction. In 1988, they have reported that the glycothermal treatment (the use of glycol instead of water for hydrothermal treatment) of gibbsite at 250^{o}C yielded glycol derivative of boehmite [13]. In 1992, they have found that the reaction of aluminum isopropoxide (AIP) in toluene at 300^{o}C resulted in χ-alumina [9]. Mekasuwandumrong, et al., (2003) have reported that thermal decomposition of aluminum isopropoxide in mineral oil at 250-300^{o}C over 2 h resulted in χ-alumina powder having high thermal stability and could be transformed directly to α-alumina at temperature higher than 1000^{o}C [32].

In this work, aluminum isopropoxide (AIP) is used as a precursor which is dissolved in mineral oil (organic solvent). The stoichiometry of the reaction has been proposed by analyzing the recovered solvent by gas chromatography. The overall reaction can be written as follows:

$$Al(OCH(CH_3)_2)_3 \xrightarrow{\text{Mineral oil}} 1/2Al_2O_3 + 3C_3H_6 + 3/2H_2$$

2.3.2 Sol-gel method

Basically, the sol-gel process means the synthesis of an inorganic network by chemical reactions in solution at low temperature. The most obvious feature of this reaction is the transition from liquid (solution or colloidal solution) into solid (di- or multiplasic gel) leading to the expression “sol-gel process”. Nevertheless, this type of reaction is not necessarily restricted to an aqueous system, although reactions in aqueous solution have been known for a very long time. Any precursor, which is able to form reactive “inorganic” monomers or oligomers, can be used for sol-gel techniques. It is very difficult to foresight type of precursor to be used for a specific aim. The reactivity of the precursor does not only depend on its chemical nature but also on the applied reaction conditions. Even finely divided silica particles can be peptisized and used for preparation of sols. However, it is necessary to generate appropriate surface charges in order to prevent coagulation and precipitation. Most work in the sol-gel has been done by using alkoxides as precursors. Alkoxides provide a convenient source for “inorganic” monomers which in most cases are soluble in common solvents. Another advantage of the alkoxide route is possibility to control rate by controlling hydrolysis and condensation by chemical means, not by surface or colloid chemistry. In the case of a few metals, it might not be convenient to use alkoxides due to their unavailability and/or difficulties in synthesis, alternative precursors may have to be employed. Metal salts provide a viable alternative, because of the advantage in their solubility in organic solvents from the initial stage or during the sol-gel processing. However, care has to be exercised to choose such precursors since they can be converted easily to oxide by thermal or oxidative decomposition. Among the inorganic salts, metal nitrates are probably the best candidates as other salts such as sulfate or chloride are more thermally stable and therefore, it may be difficult to remove the anionic portion effectively from the final ceramic product [33].

Sol-gel preparation is widely used in glass and ceramic industries as well as in catalyst preparation. There are many routes of sol-gel preparation starting with different precursors such as inorganic salt or metal alkoxide. Sol, which is suspension of nanosized or micron-sized solid particles in liquid, can be obtained by hydrolysis and partial condensation of the precursor. Further condensation of sol particles result in three-dimensional network called gel, which is a diphasic material with solids encapsulating solvent [34]. Alternatively, gel can be produced by destabilizing the solution of preformed sols. Therefore, control of the gelation condition is important. Operation at low temperature is the major advantage of this method. Furthermore, the obtained products are uniform. Sol-gel derived alumina offers a number of advantages such as high purity, high degree of homogeneity, well-define nanostructure, large surface area and superior mechanical properties.

The most often cited process for making alumina gel, developed by Yoldas [35, 36], is to hydrolyze aluminum isopropoxide or sec-butoxide in large excess of water, with an acid catalyst in the ratio of 0.07 mole acid/mole Al. If the reaction is carried out at room temperature, the product is an amorphous gel that can be converted to bayerite [$Al(OH)_3$] over a period of 24 h. At 80^oC, the reaction produces boehmite [AlO(OH)]. If the process is starts at room temperature and continue heating to 80^oC, the product obtained is bayerite.

In order to synthesized α-alumina with controlled morphology and particle-size distribution, additive can be introduced to the reaction system. Phase transformation temperature of the powder obtained from sol-gel method into α-alumina, which is typically greater than 1200^oC, can be reduced by adding CuO and Fe_2O_3 [37-39] or α-alumina seed [40-43] before gelation. In this case, the transformation was observed at 1050^oC. Another alternative is the modification of the sol formulation, which allows the conversion to α-alumina without additive or seeding [44-48]. In common practice, powder obtained from sol-gel method transform to α-alumina through the formation of θ-Al_2O_3, which is relatively stable. Therefore, the phase transformation from θ- to α- Al_2O_3 takes place at relatively high temperature [42]. Tsay et al., [47] demonstrated that sols that have been prepared with reduced amount of water can be directly transformed to α-Al_2O_3, whereas the water-

containing sol transforms through several transition phases, such as γ-Al_2O_3 and θ-Al_2O_3. Indeed, the measured activation energy of the θ-Al_2O_3-> α-Al_2O_3 transition is 650 kJ/mol, which is in contrast to that of the induced γ-Al_2O_3->α-Al_2O_3 transformation (360-431 kJ/mol) [46, 49]. Therefore, the key to achieve the α-Al_2O_3 transformation at lower temperature is to avoid the transition via θ-alumina.

N. Bahlawane [49] has investigated the preparation of an organic and viscous aluminum oxide sol with high stability. This sol allowed complete conversion to α-alumina at a temperature of 950^{o}C with a single transition via γ-alumin. Furthermore, to prevent the effect of nucleation and growth on phase transformation by causing a rapid growth of θ-alumina before the formation of α-alumina, the specific surfactant, such as oleic acid, has been selected to modify surface properties. Lin et al., (2002) [50] have proposed a method to form ultrafine α-alumina powder by mixing $Al(OH)_3$ gel with surfactant (oleic acid) to obstruct grain growth during the formation of α-Al_2O_3. The average crystallite diameter of the product obtained was 60 nm.

Many precursors can be used in sol-gel technique, for instance, salts, oxides, hydroxides, complexes and alkoxides. Buelna and Lin (1999) [51] have prepared stable boehmite sols from alkoxide precursor and they have found the important parameters affecting the final pore structure were the precursor type and the acid concentration in the sol. Higher acid concentration yielded alumina with lower surface area, pore volume and pore size.

2.3.3 Precipitation method

Precipitation method involves growth of crystals from solvent of different composition. The reactants may or may not be in the same phase before the precipitation takes place. If the reactants are in the same phase, the precipitation is homogeneous, otherwise, it is heterogeneous. The homogeneous precipitation is often preferred because its behavior is more controllable [52]. Homogeneous precipitation of alumina precursor can be carried out by heating aqueous solution containing excess urea and aluminum salt approximately up to its boiling temperature [53, 54].

Basically, all process parameters influence quality of the final product of the precipitation. It is usually desired to get the precipitates with specific properties. These properties may involved physical properties of particle such the nature of the phase formed, chemical composition, purity, particle size, surface area, pore size, pore volumes, and separability from the mother liquor. On the other hand, it may include the demands which are imposed by the requirement of downstream processes, such as drying, palletizing or calcinations. It is therefore necessary to optimize the parameters in order to produce the desired material. Figure 2.3 summarizes the parameters which can be adjusted in precipitation processes and the properties which are mainly influenced by these parameters.

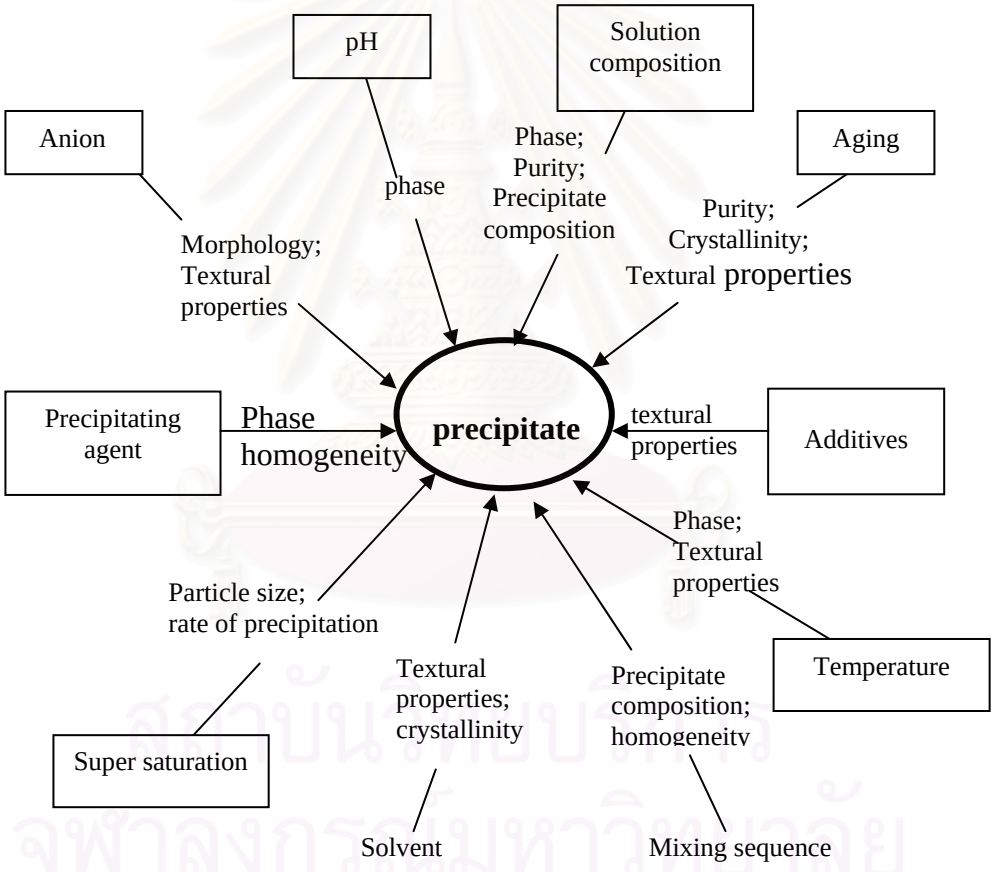

Figure 2.3 Parameters affecting property of the precipitate [55].

As stated above, precursors, which can be easily decomposed to volatile products, are usually chosen. There are preferably the nitrates of metal precursors and ammonia or sodium carbonate as the precipitating agent. Since nucleation rate is extremely sensitive to temperature change, precipitation temperature is a decisive factor in controlling properties of the precipitate such as primary crystallite size,

surface area, and phase. However, it is very difficult to state how the precipitation temperature should be adjusted to achieve a product with specific properties. The optimum precipitation temperature is usually a parameter which has to be determined experimentally. In general, most precipitation process is carried out above room temperature, often close to 100^{o}C. Furthermore, pH directly controls the degree of supersaturation, at least in case that hydroxides are precipitated. Therefore, it is one of the crucial factors in precipitation process. As for many other parameters, the influence of pH is not straight forward and it has to be investigated experimentally for a specific system.

Alumina powder has been prepared from ammonium aluminum carbonate hydroxide via the precipitation method as reported by Kato et al [56]. A soluble aluminun salt was gradually added to a solution of ammonium hydrogen carbonate, subsequently allowing the mixed solution to age for a prescribed period of time to permit growth of crystals. Then, the precipitate was separated by filtration and drying. The ammonium aluminum carbonate hydroxide obtained is decomposed at temperature in a range of 1250 to 1300^{o}C to form α-alumina.

The main advantages of precipitation method are the potential to create very pure material and the flexibility of the process with respect to quality of final product.

2.4 Method for Shape Forming

There are various methods to form shaped article from ceramic powder, for instance, dry pressing, hydrostatic molding, extrusion, injection molding, and hot pressing. The choice of the forming process depends on dimension and shape of parts to be fabricated, quantity of parts, and requirements of the final product. The forming pressure to be applied should be approximately 100 MN/m^2 , but it is usually adaptable in each type of the forming process. Bulk density of the green compacted body, as well as density of the final product after sintering, increases with increasing in forming pressure (figure 2.4). If the forming pressure is too low, then final product will not achieve the full density. On the contrary, excessive pressure, which has the same effect as insufficient plastification or inhomogeneous distribution of the plasticizer, can lead to defects such as flaws and cracks in the compacted bodies.

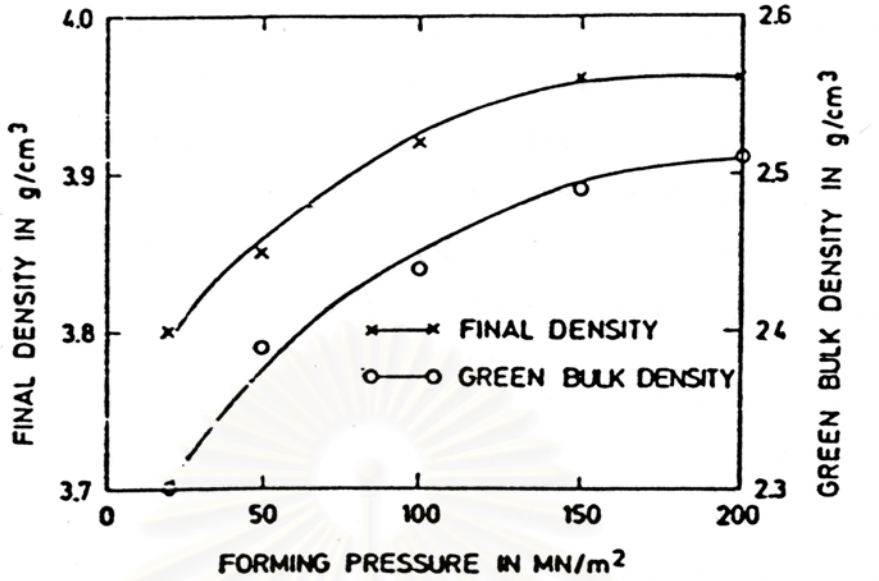

Figure 2.4 Correlation between green bulk density, final density, and forming pressure of high-purity alumina ceramics [57].

The dry pressing technique is the most common and most economical compaction process for the fabrication of high alumina ceramics. It is restricted, however, to parts with simple shape and to wall thickness greater than 1 mm. Dry pressing is unidirectional. Figure 2.5 illustrates the dry pressing operation using a simple ring, as well as a ring with a flange, under a pressure of 150 MN/m^2. The procedure is carried out in three basic steps. In order to development of internal stresses, the following requirements should be met.

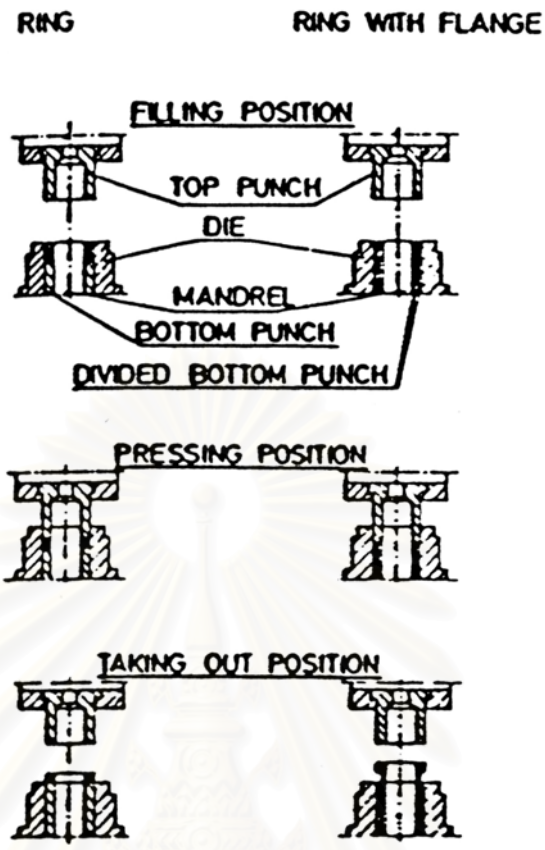

Figure 2.5 Steps of dry pressing operation [57].

1. It is important to get homogeneous distribution of the powder when the die is filled. This can be achieved by using suitably prepared free-flowing alumina powder and by filling the die evenly, for example, by means of a fill shoe.
2. In the pressing position, a homogeneous compaction of the powder within the desired shape should be ensured.
3. Removal of the part from the die should be simple, without any risk of damage.

Due to the substantial tool wear caused by the extremely abrasive alumina powder, all parts of the die which are exposed to wear, such as mandrels and punches, are preferably made of cemented carbides.

The isostatic pressing is a process to form ceramic components from dry powder by uniform pressing from all directions. It is also used for other materials,

such as metals, plastics, graphite, and carbon. The process is accomplished by enclosing the powder in a deformable mold and then collapsing the mold by using a hydrostatic pressure exerted from fluid medium. For cold isostatic pressing (CIP), the process carried out at or near room temperature. On the other hand, hot isostatic pressing (HIP) is performed at elevated temperature. Cold isostatic pressing is used extensively on both laboratory and production scales. In production, it is used to form diverse array of parts, including spark plug insulator, oxygen sensor, large refractory component, and dinnerware.

The general advantages of cold isostatic (CIP) pressing are :

- Very few size or dimensional limitations, because the uniform application of pressure associated with this process obviates the size limitations of many other processes, particularly the length-to-diameter problems of dry pressing.
- Very uniform pressed compacts, due to the uniform application of pressure, which leads to very consistent density and shrinkage resulting in a reproducible process.
- Generally moderate tooling costs particularly in case of prototype and low-volume production, where the tooling can be quite simple.
- Short overall process time, which do not require long binder burnout or drying period.

On the other hand, the general advantages of hot isostatic pressing (HIP) are :

- Void, particularly large ones, in most materials can be efficiently reduced in size and frequency.
- Ceramics can be densified at relatively low temperature.
- Extremely difficult to sinter ceramics can be fully densified, for example high-purity silicon-nitride powders.
- The reduced sintering temperature means that grain growth and undisirable reactions can be controlled or avoided.
- A very high uniformity in properties, i.e. density, can be obtained.

2.5 Sintering

Sintering is the process by which small particles of material are bonded together by solid-state diffusion. In ceramic manufacturing, this thermal treatment results in the transformation of a porous compact into a dense, coherent product. In the sintering process, particles are coalesced by solid-state diffusion at very high temperatures yet lower than melting point of the compound being sintered [58]. In sintering, atomic diffusion takes place between the contacting surfaces of the particles so that they become chemically bonded together, as shown in Figure 2.6 [59]. As the process proceeds, larger particles are form at the expense of the smaller ones, while the porosity of the compacts decreases [60]. Finally, at the end of the process, an "equilibrium grain size" is attained.

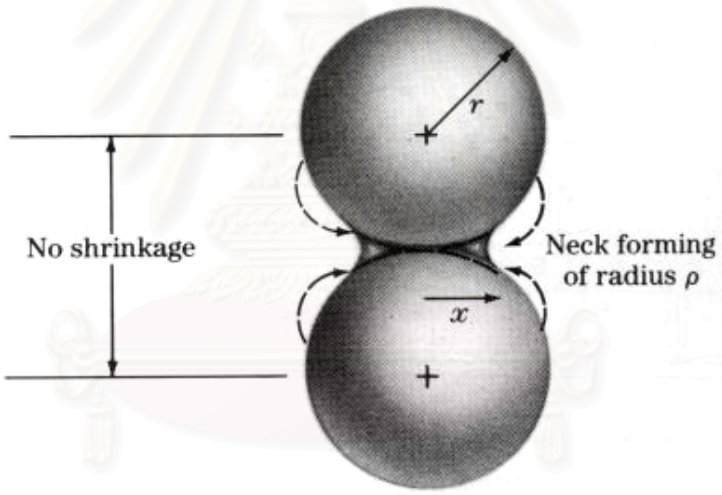

Figure 2.6 Formation of a neck during the sintering of two fine particles.

Densification, recrystallization, and grain growth occur in the same temperature range. Therefore, strict control of the sintering process as well as small addition of grain growth inhibitor, e.g. MgO, to the alumina powders is essential to achieve a fully dense sintered body with fine-grained microstructure. In the course of sintering, the density increases with the logarithm of time, and the grain size increases with the one-third powder of time.

As illustrated in Figure 2.7, the density increase linearly, according to the densification process during sintering, until it reaches saturation, where the specimen approaches its final-density. A further increase in the sintering time does not improve either the density or the mechanical properties. On the contrary, it promotes grain growth which reduces the mechanical strength. Therefore, the sintering process should be stopped as soon as the final density is obtained. Sintering in air can achieve a maximum final density of about 99% of the theoretical density which corresponds to minimum residual porosity of about 1% from trapped air. Beyond the saturation point there is a decrease of density, due to volume-increasing reactions between the individual additives. It is very slight in the case of high-purity alumina ceramics and larger in case of alumina ceramics with high density.

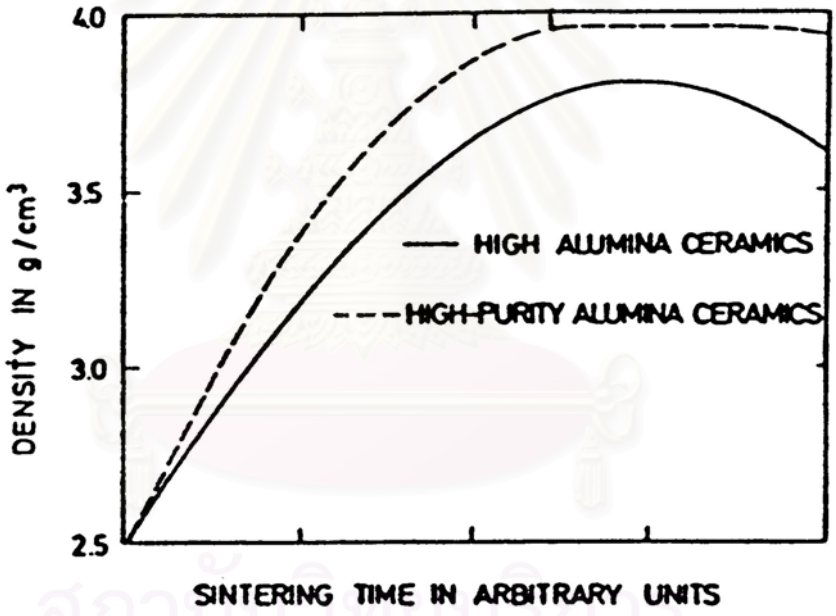

Figure 2.7 Development of the density of alumina ceramics during sintering [57].

The nature of the sintering atmosphere may influence the rate of sintering and the residual porosity. Many additives other than temporary binders have been used in sintering process for several purposes, such as crystal growth repression, crystal growth acceleration, acceleration of sintering or shrinkage rate, reduction in maturing temperature, porosity alteration, changes in physical or chemical properties, and removal of impurities. Many researchers have studied the effects of sintering additives on the sintering process in order to improve properties of material obtained.

The choice of sintering temperature, which is usually between 1600 and 1800^{o}C, depends on surface energy, grain size distribution, and the additives of the alumina powder. The sintering time and particularly the heating rate should be adapted to the size and the wall thickness of the body to be sintered. Larger parts require a longer sintering time and a slower rate of heating-up. Smaller parts can be heated up more quickly, allowing a much shorter sintering time.

2.6 Desirable Powder Characteristics in Ceramics [61]

Traditional ceramics generally require less specific property than advanced ceramics. They can be chemically inhomogeneous and can have complex microstructures. Unlike the case of advanced ceramics, chemical reaction during firing is often a requirement. On the other hand, advanced ceramics must meet very specific property requirements, and therefore their chemical composition and microstructure must be well controlled.

For advanced ceramics, the important powder characteristics are the size, size distribution, shape, state of agglomeration, chemical composition, and phase composition. The structure and chemistry of the surface are also important. The most profound effect of the particle size, however, is on the sintering. The rate at which the body densifies increases strongly with a decrease in particle size. Normally, if other factors do not cause severe difficulties during firing, a particle size of less than ≈1 μm allows the achievement of high density within a reasonable time. Whereas powder with a wide distribution of particle size may lead to higher packing density in the green body, this benefit is usually vastly outweighed by difficulties in the control of the microstructure during sintering. A common problem is that the large grains coarsen rapidly at the expense of the smaller grains, making the attainment of high density with controlled grain size impossible. Homogeneous packing of a powder with a narrow size distribution (i.e., a neatly monodisperse powder) generally allows greater control of the microstructure. A spherical or equiaxial particle shape is beneficial for controlling the uniformity of the packing.

Agglomerates lead to heterogeneous packing in the green body, which in turn leads to differential sintering (different regions of the body sintering at different rates) during the firing stage. This can cause serious problems such as the development of large pores and voids in the fired body. Furthermore, the rate at which the body densifies is roughly similar to that for a coarse-grained body with a particle size equivalent to that of the agglomerates. An agglomerated powder therefore has serious consequences for the fabrication of ceramics when high density coupled with a fine-grained microstructure is desired. Agglomerates are classified into two types : soft

agglomerates in which the particles are held together by weak van der Waals forces and hard agglomerates in which the particles are chemically bonded together by strong bridges. The ideal situation is the avoidance of agglomeration in the powder. However, in most cases this is not possible. In such cases, we would prefer to have soft agglomerates rather than hard agglomerates. Soft agglomerates can be broken down relatively easily by mechanical method (e.g., pressing or milling) or by dispersion in a liquid. Hard agglomerates cannot be easily broken down and therefore must be avoided or removed from the powder.

Surface impurities may have a significant influence on the dispersion of the powder in a liquid, but the most serious effects of variations in chemical composition and microstructure are encountered in the firing stage. Impurities may lead to the presence of a small amount of liquid phase at the sintering temperature, which causes selected growth of large individual grains. In such a case, the achievement of a fine uniform grain size would be impossible. Chemical reactions between incompletely reacted phases can also be a source of problems. We would therefore like to have no chemical change in the powder during firing. For some materials, polymorphic transformation between different crystalline structures can also be a source of severe difficulties for microstructure control. To summarize, the desirable powder characteristics for the fabrication of advanced ceramics are listed in Table 2.1.

Table 2.1 Desirable powder characteristics for advanced ceramics

Powder characteristic	Desired property
Particle size	Fine (< 1 μm)
Particle size distribution	Narrow
Particle shape	Spherical or equiaxial
State of agglomeration	No agglomeration or soft agglomerates
Chemical composition	High purity
Phase composition	Single phase

2.7 Color-Doped Alumina

Corundum is composed of aluminum oxide (Al_2O_3) which, in its pure state, is completely colorless. However, pure corundum is rare in nature. Instead, small amount of metal impurity may impart color, either individual metal, or in combination [62].

In synthetic corundum, many different coloring agents have been used. Most color results from a peculiar group of transition elements, which also produce color in many different substances besides minerals. Electron structure of these elements contains inner unpaired electrons which can be excited to higher energy levels by absorption of visible light. The first series of transition elements in the periodic table are chromium, iron, titanium, vanadium, manganese, and copper. These are the most important instigator of gemstone coloration, which is responsible for the color of ruby, sapphire, emerald, alexandrite, tanzanite, and tsavorite.

White light or sunlight is made up of a balanced mixture of the spectral colors which are violet, blue, green, yellow, orange, and red. An object does not really posses color itself. Instead, it is merely a perception based upon interaction between the light source, object, and eye. Table 2.2 shows causes of color in corundum. The color of ruby is one of the magnificent accidents of nature. Ruby is not only by its body color due to absorption of blue and green light, but ruby also fluoresces red to daylight. This supercharges the hue into levels of intensity unmatched by other red stones. Ruby's rich crimson hue is due to electron transitions involving the Cr^{3+} ion, which substitutes for Al in amounts approximating 0.1 – 3 atomic %. Ability to absorb visible light of this ion is due to its outer electron suborbitals, in which the energy gaps correspond to the energy of visible light. In ruby, two absorption mechanisms occur when white light passes through it. The first one involves electron transition from the ground state $^4A_2$ to the $^4T_2$ level (2.2 eV), which is corresponding to the absorption of yellow-green light. The second mechanism involves a transition to the $^4T_1$ level by absorbing 3.0 eV radiation or violet light. These absorption areas are actually bands rather than narrow lines and somewhat overlapped. Thus, there is only slight transmission in the blue, but strong transmission in the red, giving ruby its rich red color with slight purplish stones.

Table 2.2 Causes of color in corundum

Color	Cause(s)	Reference
Red (including pink)	Electronic transition on dispersed Cr^{3+} ions in octahedral coordination which have replaced Al^{3+} in the corundum structure.	Fritsch & Rossman (1987) [63]
Blue	Intervalence charge transfer (Fe^{2+}+ Ti^{4+} ---> Fe^{3+} + Ti^{3+};sometimes written Fe^{2+}-O-Ti^{4+} --> Fe^{3+}-O-Ti^{3+}) , where the Fe^{2+} and Ti^{4+} have replaced Al^{3+} in the corundum structure and are in close proximity to one another.	Ferguson & Fielding (1972) [63] Fritsch & Rossman (1987) [63]
	Intervalence charge transfer (Fe^{2+} ---> Fe^{3+}), where the Fe^{2+} and Fe^{3+} have replaced Al^{3+} in the corundum structure and are in close proximity to one another.	Schmetzer ,K.(1987) [64]
Yellow	Ion pair transition on individual ions of a pair (Fe^{3+}- Fe^{3+}).	Ferguson & Fielding (1972) [65]
	Color center (point defect) hole pair resulting from insufficient charge when any divalent impurity (such as Mg^{2+}) replaces Al^{3+} in the corundum lattice. When sapphire is heat treated under highly oxidizing atmosphere, if combines with the divalent impurity, producing the +3 charge needed at the lattice site. Apparently this divalent impurity-hole pair absorbs light.	Emmett & Douthit (1993) [66]
	A variety of color centers of unknown structure.	Nassau & Valente (1987) [67]
	Color associated with an unknown element diffusing outward from exsolved particles of unknown composition.	Koivula(1987) [68] John Emmett, pers.comm. (July 5, 1994)
	Unreported mechanism involving dispersed Ni ion (synthetic only).	Nassau (1980) [69]
Orange	Combination of red color (Cr^{3+}) and one or more of the yellow cause above.	Emmett & Douthit (1993) [66]
Violet/purple	Combination of red color (Cr^{3+}) and one or more of the blue cause above.	Fritsch & Rossman (1988) [63]
Green	Ion pair transition on individual ions of a pair (Fe^{3+}- Fe^{3+}), plus Intervalence charge transfer (Fe^{2+}+ Ti^{4+} ---> Fe^{3+} + Ti^{3+}), as described above.	Emmett & Douthit (1993) [66]
	Unreported mechanism involving Co (strong reducing conditions), V and Ni ions which have replaced in the corundum structure (synthetic only).	Nassau (1980) [69]

Color	Cause(s)	Reference
	Combination of one or more of the blue and yellow causes described above.	Nassau, K. (pers. Comg. 19, 1994)
Color-change	Electronic transition of dispersed V^{3+} ions in octahedral coordination which have replaced Al^{3+} in the corundum structure. Due to balanced transmission in both the red and blue – green, the gem shifts color depending on the composition of the light source.	Schmetzer & Bank (1980) [70]
Dark Brown	Mechanical color due to dark brown color of exsolved hematite plates (mainly black star sapphire).	Weibel & wessicken (1981) [71]

In blue sapphire, iron and titanium both substitute for aluminum in the corundum structure. Iron resides either in a ferrous (Fe^{2+}) or ferric (Fe^{3+}) state, while titanium is found as Ti^{4+}. If both Fe^{2+} and Ti^{4+} lie in close proximity, it results in blue color. When stimulated by light, a single electron transfers from iron to the titanium ion. This is illustrated by the following equation.

$$Fe^{2+} + Ti^{4+} \longrightarrow Fe^{3+} + Ti^{3+}$$

The intervalence charge transfer mechanism which produces blue color in sapphire is a far more efficient than the Cr^{3+} ion in ruby. Ruby requires about 0.4 – 2 atomic % of chromium for a deep red color, while only a few hundredth of one percent of iron and titanium are needed to achieve a similar depth of color in sapphire. Many sapphires posses the necessary iron and titanium, but do not have for deep blue color because the iron is in improper electronic state. Heat treatment under reducing condition can change Fe^{3+} to the required Fe^{2+} ion. Then, with Ti^{4+} already presents in the structure, a pale and cloudy stone becomes clear, with deep blue color.

For synthetic color-doped alumina, When Al_2O_3 powder is sintered with coloring agents at high temperature of 1700^{o}C or higher, metal ions diffuse into the lattice and exchange with the Al ion, resulting in the change in ceramic color after sintering. However, when Al_2O_3 is sintered at such high temperature, the grain of Al_2O_3 grows over several microns. As the result, the Al_2O_3 does not show good

transparency. Therefore, it is very important to synthesize alumina powder in which some metal ions have already dissolved in lattice without formation of undesired porosity.

Verneuil method is known as a very popular method for synthesizing Al_2O_3 single crystal. It employs ammonium alum as starting material to prepare feed powder. $(NH_4)Al(SO_4)_2.12H_2O$ is dissolved in hot distilled water and subsequently filtered to remove solid matter. On cooling, crystals of alum form out of the solution and impurities are left in the solution. After this process has been repeated several times, the purity of the crystals is high enough to allow the powder to be used in the crystal growth process. Chromium alum $(NH_2)Cr(SO_4)_2.12H_2O$ is purified in the same way to give the dopant for ruby. Two alum precursor are mixed together and fired at a temperature about 1000-1200^oC to give the final feed powder. The feed powder needs to flow freely in the Verneuil reactor and therefore it is sieved before use. The feed powder is melted to give a characteristic boule which is a single crystal. The smooth flow of feed powder is ensured by tapping the powder container with a hammer, and the heating is achieved by a very hot flame, produced from an oxygen stream and a stream of coal gas which was available in Verneuil's time. The powder drops down through the flame. The flame touched a ceramic pedestal upon which the powder builds up a sintered cone whose tip melts and enlarges. The pedestal is lowered to give a start to the formation of the boule. The gas flow is maintained while the oxygen flow is monitored to control growth. Transparency is achieved by allowing slow growth in layers from the bottom of the boule. To prevent the formation of bubbles in the melt in many crystal and to stop cracking of the contact area of the sintered cone, the boule has to be kept small [72].

In 1817, Gay-Lussac reported that pure aluminium oxide could be obtained by heating ammonium alum. This allowed progress toward the final successful corundum growth. The work of Edmond Fremy is important because he was the first to produce clear red, though small, rubies. By using large fireclay crucibles held in heat for 20 days, thin ruby crystals were obtained [23]. Ballman, (1961) [73] described a method for growing synthetic rubies in corundum seed in an aqueous medium containing chromium compound.

As recently, LÓpez-Navarrete and Ocaña have shown the use of the spray pyrolysis technique for the synthesis of several pigment systems such as Cr-SnO_2 [74], Cr-$SnCaSiO_2$ [75], and Pr-CeO_2 [76]. In 2003, they have prepared manganese-doped α-alumina pink pigments by spray pyrolysis technique [77]. They have found that the temperature required for the fully development of corundum was much lower (900^{o}C) than that in the traditional ceramic procedure (1300^{o}C). Nevertheless, the newly developed procedure yielded more intense color, since the amount of Mn incorporated to the corundum lattice increased with decreasing preparation temperature. In addition, the pigments obtained by this procedure require no grinding. They were consisted of uniformly shaped grains with controlled and reproducible size distribution. Furthermore, López-Navarrete, et al., (2003) [77] have investigated on the Mn valence in the Mn-alumina pigments. They have mainly used x-ray photoelectron (XPS) and X-ray adsorption spectroscopy for characterization. It was found that pink color of the pigments is mainly due to Mn(III) species dissolved in the corundum lattice, in which they form cluster containing ~2 Mn cations. The more intense color presented by the sample prepared in the presence of fluxes is due to the incorporation of a higher amount of Mn into the alumina lattice as a consequence of liquid phase presented in the system which favors the diffusion process involving in the solid solution formation.

CHAPTER III

EXPERIMENTAL

This chapter describes experimental system procedures for alumina and chromium doped-alumina preparation. This can be divided into four parts; chemicals and equipment are shown in section 3.1 and 3.2, respectively. Preparation and characterization of all obtained products are explained in section 3.3 and 3.4 respectively.

3.1 Chemicals

All chemicals using in this experiment are as following :

1. Ammonium aluminum sulfate (99%+) ($NH_4Al(SO_4)_2.12H_2O$) available from Merck Co., Ltd., Germany.
2. Ammonium hydrogencarbonate (98%) (NH_4HCO_3) available from Unilab.
3. Aluminium nitrate (98%) ($Al(NO_3)_3.9H_2O$) available from Aldrich Chemical Company, USA.
4. Urea (99.5%) available from Univar, Australia.
5. Ethyl alcohol absolute anhydrous available from Mallinckrodt Baker Co.,Ltd.
6. Aluminum isopropoxide (98%+) (AIP, $((CH_3)_2CHO)_3Al$) available from Aldrich Chemical Company, USA.
7. Mineral oil available from Merck Co., Ltd., Germany.
8. Chromium (III) nitrate nonahydrate (99.99%+) ($Cr(NO_3)_3.9H_2O$) available from Aldrich Chemical Company, USA.
9. Chromium (III) acetylacetonate (97%) ($(CH_3COCHCOCH_3)_3Cr$) (available from Aldrich Chemical Company, USA.

3.2 Equipment

Alumina preparation by sol-gel method and precipitation method employs only conventional laboratory glassware. On the contrary, solvothermal requires an autoclave reactor with the following specifications.

Autoclave reactor

- Made from stainless steel
- Volume of 200 cm^3
- Maximum temperature of 350^oC
- Pressure gauge in the range of 0-300 bar
- Relief valve used to prevent runaway reaction
- Test tube was used to contain the reagent and solvent
- A temperature program controller was connected to a thermocouple attached to the reagent in the autoclave.
- Electrical furnace (heater) supplied the required heat to the autoclave for the reaction.
- Nitrogen was set with a pressure regulator (0-150 bar) and needle valves are used to release gas from autoclave.

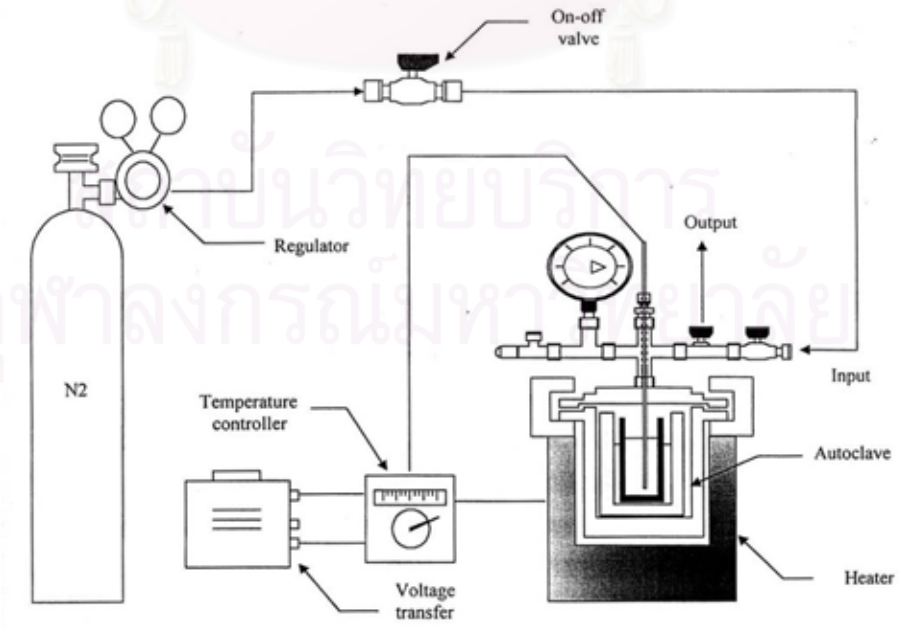

Figure 4.1 Autoclave reactor and gas controlling system

3.3 Experimental Procedures

3.3.1 Synthesis of alumina and color-doped alumina

3.3.1.1 Sol-gel method

A mixture of aluminium nitrate nonahydrate and ethanol used as starting solution was prepared by dissolving 24 g of aluminium nitrate in 50 cc of ethanol at room temperature. A homogeneous solution was obtained after mixing for approximately 10 minutes using magnetic stirrer. The experiment was conducted in the reflux-condenser reactor at the temperature about 70-80^{o}C for 18 h. Then, urea solution, which consist of 60 grams of urea and 50 ml of distilled water, was added to adjust pH of sol. The mixture was rested at the same temperature for 24 h to be gelled at neutral condition. For Cr-doped alumina, $Cr(NO_3)_3.9H_2O$ was addded to the starting solution at the concentration in the range of 0.05-0.5 wt % of chromium precursor to aluminium precursor. Then, above procedure were repeated.

The obtained product was calcined with 2 steps heating rate to avoid overflowing of gel during calcination, i.e. 3^{o}C/min from room temperature to 500^{o}C and continue heating at 5^{o}C/min to 1150^{o}C. Then, temperature was hold for 3 h.

3.3.1.2 Precipitation method

The method to manufacture alumina from ammonium aluminum carbonate hydroxide ($NH_4AlCO_3(OH)_2$) has been invented by Kato Shuzo et.,al since 1975. Ammonium aluminum carbonate hydroxide, is produced from the reaction between a solution of ammonium hydrogencarbonate and aluminum salt solution, according to the following equation [56]:

$$8NH_4HCO_3\,(aq) + 2(NH_4)\,Al\,(SO_4)_2\,(aq) \longrightarrow 2NH_4AlCO_3(OH)_2\,(s) + 2H_2O\,(aq) + 4(NH_4)_2SO_4\,(aq) + 6CO_2\,(g)$$

Ammonium aluminium sulfate solution (AAS solution) was gradually added to ammonium hydrogencarbonate aqueous solution (AHC solution) with concentration ratio of AAS solution to AHC solution 0.2 : 2.0 mol/l at the temperature in a range of 40-45^{o}C. The speed of mixing is 450 rpm and rate of addition of AAS solution to AHC solution is 3 cc/min. The pH value of reaction is constant at 9. The mixed solution was aged for 15 minutes to permit growth of crystals. Then, the aluminum compound was produced. White precipitates formed were separated from the final solution by centrifuging, repeatedly washed with methanol and dry in the oven at 110^{o}C over night. For Cr-doped alumina, $Cr(NO_3)_3.9H_2O$ used as chromium source was added into AAS which before droping into AHC solution. Amount of $Cr(NO_3)_3.9H_2O$ used was adjusted to get the same concentration as in sol-gel method.

After these preparation procedures, The obtained products were calcined in depleted-oxygen atmosphere in a box furnace at 1150^{o}C for 3 h with heating rate 10^{o}C/min for transformation to α-Al_2O_3.

3.1.1.3 Solvothermal method

An appropriate amount of aluminum isopropoxide (AIP), approximately 25 g, was suspended in 100 ml of mineral oil in a test tube. This test tube was then placed in an autoclave which was added with 30 ml of mineral oil. The autoclave was purged completely by nitrogen before heating up to 300^{o}C at a rate of 2.5^{o}C/min, and held at that temperature for 2 h. After the system was cooled down, the resulting products were repeatedly washed with acetone and dried in air over night. For Cr-doped alumina, Chromium (III) acetylacetonate was added by suspending in test tube before the reaction tool place. The concentration of chromium precursor to aluminium precursor was adjust to be 0.05-0.5 wt %.

For some experiments, a different drying was applied as follows. After the reaction, the valve of the autoclave was slightly opened to release the organic solvent from the autoclave by flash evaporation while keeping at the reaction temperature. The valve was opened until the pressure inside the autoclave was decreased to

atmospheric level. Dry products were obtained directly after the assemble was cooled down without the step of washing by methanol and centrifugation. The obtained products were calcined in the box furnace in the same manner as described in section 3.3.1.2.

3.3.2 Vary conditions during precipitation method

3.3.2.1 Concentration of both precursors

The concentration of both precursors has been varied from 0.5, 1.0, and 2.0 mol/l for ammonium hydrogencarbonate solution (AHC solution) and 0.1, 0.2, 0.3, 0.4, and 0.6 mol/l for ammonium aluminum sulfate solution (AAS solution). Amount of reagents used were adjusted to maintain the molar ratio of AAS solution : AHC solution equal to 1:4 (see calculation in Appendix A). The concentration is fixed in this range because of the limited solubility of both precursors. The solubility of AAS solution is 180 g/l , while the solubility of AHC solution is 220 g/l.

3.3.1.2 Speed of mixing or stirring speed

Magnetic stirrer was used for mixing with controlled speed. The stirring speed was varied from 0, 300 and 450 rpm for each batch of reaction.

3.3.1.3 Rate of addition

A solution of ammonium aluminum sulfate is dropwisely added to the solution of ammonium hydrogencarbonate at different rate of addition by using 50 cc Burette. The adding rate was varied from 1, 3, 10 cc/min.

3.3.1.4 Reaction temperature

The range of reaction temperature has been varied from 30-35, 40-45, 75-80^{o}C by using water bath for holding temperature at desired value.

3.3.1.5 pH value of reaction system

The pH of reaction has been varied from 5, 7 and 9 by adding acetic acid and potassium sodium orthophosphate buffer solution to control pH of reaction. At pH 9, it was not necessary to add any chemical because the pH value of AHC solution is 9 and it maintained constant throughout the reaction.

3.3.3 Fabrication of alumina article

The obtained powders from all techniques were milled by using ball mill (See Appendix D) and dried in an oven for 24 h. The dried powders were sieved through a 100 mesh screen. Sieved powders were mixed with organic binder (PVA with 9000-10000 MW) in content of 6 wt% and passed through a 50 mesh screen. The mixture was biaxial pressed into a pallet of 13 mm in diameter followed by cold isostatic press at the pressure of 200 MPa. The green compact was dried in the oven at 105°C for 2 h.

The dried green bodies were sintered at 1550°C for 2 h under air atmosphere. In some cases, the sintered specimen was followed by hot isostatic press (HIP) at the pressure 150 MPa and the temperature 1300^{o}C.

3.4 Characterizations

3.4.1 X-ray diffraction (XRD)

The X-ray diffraction (XRD) patterns of powder were performed by a X-ray diffractometer SIEMENS D5000 connected with a computer with Diffract ZT version 3.3 program for fully control of the XRD analyzer. The experiments were carried out by using Ni-filtered CuKα radiation. Scans were performed over the 2θ ranges from 10^{o} to 70^{o}. The crystallite size was estimated from line broadening according to the Scherrer equation. The value of shape factor, K, was taken to be 0.9 and α-alumina was used as an external standard.

3.4.2 Scanning electron microscopy (SEM)

The morphology and the size of secondary particle of the samples were observed on JSM-5410LV scanning electron microscope at the scientific and Technological Research Equipment Center (STREC), Chulalongkorn University.

3.4.3 Infrared Spectroscopy (IR)

The functional group in the samples was determined by using Nicolet impact 400 Infrared spectroscopy. Before measurement, the sample was mixed with KBr and then was formed into a thin pellet.

3.4.4 Laser Particle Size Distribution Analyzer

The particle size and particle size distribution was analyzed by using Laser Particle Size Distribution Analyzer (Mastersizer S model) at Scientific and Technological Research Equipment Centre, Chulalongkorn University.

3.4.5 X-Ray Photoelectron Spectra (XPS)

The content of chromium on the surface of powder was determined by using X-ray photoelectron (Amicus) at Petrochemical Engineering Laboratory, Chulalongkorn University.

3.4.6 UV/Visible Spectrometer

The absorption range and transparency of sample was determined by using Lambda 650 UV/Visible spectrometer at Petrochemical Engineering Laboratory, Chulalongkorn University and Ocean Optic USB 2000 UV/Visible spectrometer at Mahidol university.

3.4.7 Low-Temperature Electron Spin Resonance (ESR)

Chemical state of metal ion was indicated by using Electron Spin Resonance (JES-RE2X) at Scientific and Technological Research Equipment Centre, Chulalongkorn University.

CHAPTER IV

RESULTS AND DISCUSSION

In this chapter, the experimental results and discussions are described. The can be divided into 3 sections as follow :

Section 4.1 describes structure and morphology of alumina powder prepared from different techniques, i.e. precipitation, sol-gel and solvothermal methods. Further investigation on effects of various factors such as concentration of precursors, speed of mixing, dropping and stirring rate, temperature and finally pH of the reaction system, on morphology of powder synthesized by the precipitation method are also investigated.

Section 4.2 describes effect of chromium doping into alumina structure. The discussion includes chromium content and oxidation state, in both surface and bulk of alumina powder.

Section 4.3 discusses application of synthesized alumina powder in ceramic field by measuring relative density and structure of fabricated alumina specimen. The result are compared with commercial alumina powder.

4.1 Undoped alumina powder

4.1.1 Structure and morphology of synthesis products

As-synthesized products from precipitation, sol-gel and solvothermal methods are different in crystal structure as shown in Figure 4.1.

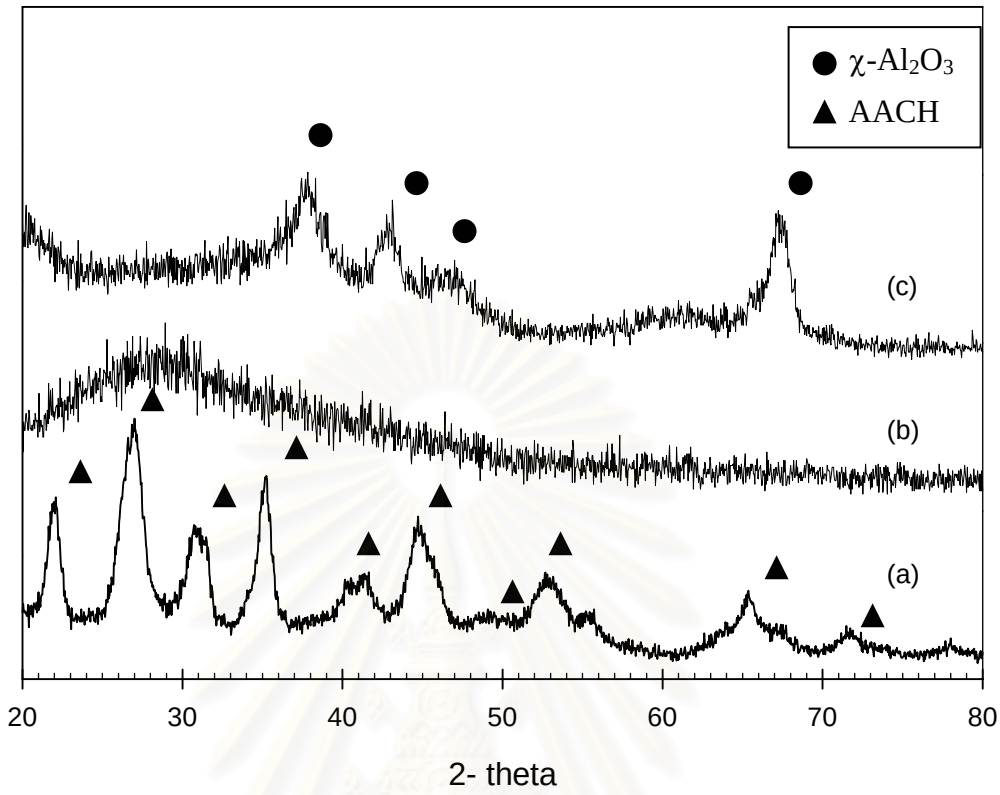

Figure 4.1 The XRD patterns of as-synthesized product from various techniques : (a) precipitation method, (b) sol-gel method, (c) solvothermal method.

According to the XRD patterns of as-synthesized products, it can be seen that all pre-calcined products have different crystal structure. Amorphous gel is obtained from sol-gel method, while powders obtained from both precipitation and solvothermal methods are crystalline. XRD analysis indicated that the powder from solvothermal method is χ-alumina. All diffraction peaks are broad, indicating that the crystallites are very small and imperfect. This is in agreement with the previous finding in the literature [32]. On the other hand, XRD pattern of the product from precipitation method does not match any polymorph of alumina. It is in fact corresponding to the reflection of ammonium aluminium carbonate hydroxide (AACH). The peaks for this precipitate is more narrow than that from solvothermal method which implies higher crystallinity of the product.

After calcination, all products transform to α-alumina as indicated by XRD analysis in Figure 4.2.

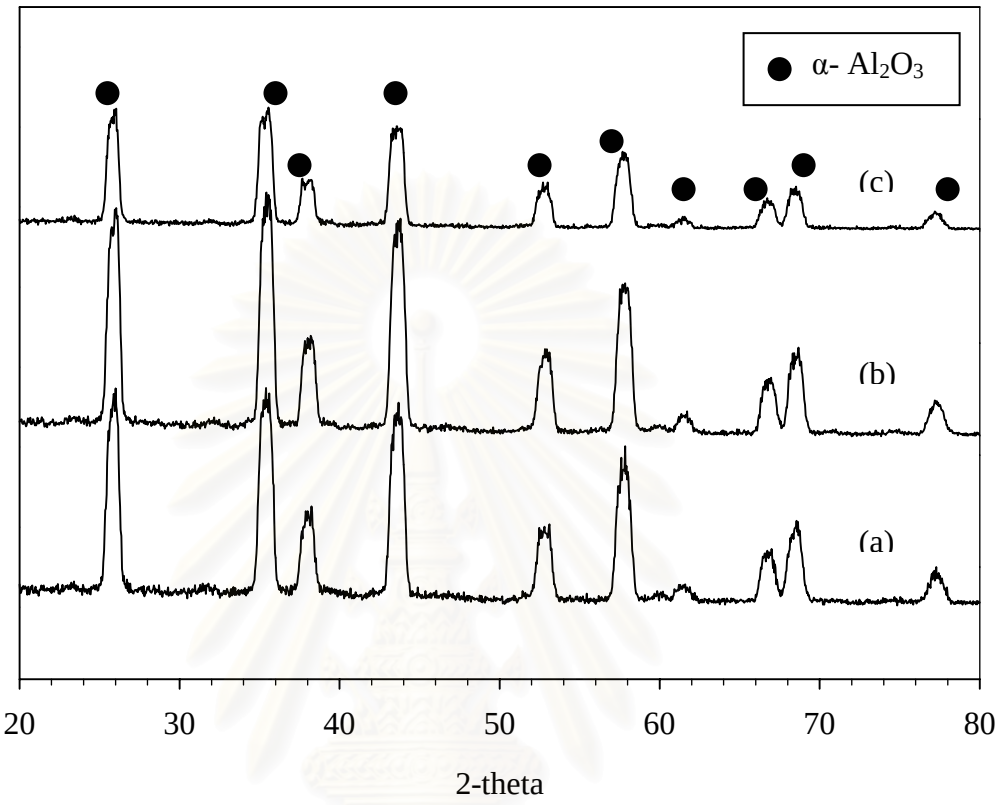

Figure 4.2 The XRD patterns of calcined product produced from various techniques: (a) precipitation method, (b) sol-gel method, (c) solvothermal method.

As mentioned earlier, the calcination for all products was conducted at 1150^{o}C for 3 h. This condition is satisfactory with conditions reported in literature for complete phase transformation or decomposition to α-alumina. Mekasuwandumrong et al [32] reported that majority of χ-alumina synthesized via solvothermal method transforms directly to α-alumina after 1 h calcination at 1150^{o}C. The χ-to-α phase transformation is completed within 1 h of calcination at 1200^{o}C. According to Figure 4.2, it can be seen that, the phase transformation can be completed at 1150^{o}C if the holding period is prolonged to 3 h. No sigh of χ-alumina is formed after the calcination. The same observation is also witnessed for the products synthesized by both precipitation and sol-gel techniques. Although it has been reported that phase transformation of the amorphous gel, as well as the result from thermal decomposition

of ammonium aluminum carbonate hydroxide crystals, proceeds through various form of alumina such as γ- and δ-phase, no other phase is detected in the XRD patterns [78]. The crystallite size of all samples calculated from Scherrer equation are summarized in Table 4.1.

Table 4.1 Structure and crystallite size of calcined products.

Synthesis method	Structure of as-synthesized product	Structure of calcined product	Crystallite size before calcination (nm)	Crystallite size after calcination (nm)
Precipitation	$NH_4AlCO_3(OH)_2$	α - Al_2O_3	4.08	9.65
Sol-gel	amorphous	α - Al_2O_3	-	9.52
Solvothermal	χ-Al_2O_3	α - Al_2O_3	5.37	9.74

The calcined powders from all methods are corundum (α-Al_2O_3) with crystallite size in nanometer range, shown in Table 4.1. For solvothermal method, the crystallite size after calcination (9.74 nm) is bigger than the crystallite size of the as-synthesized product (5.37) because of the crystal growth during phase transformation and heat treatment in the calcination. The same result also achieved for the calcined-product synthesized by precipitation method. The crystallite size of powder after calcination is 9.65, which is greater than that before calcination (4.08).

The IR spectra of as-synthesized and calcined products are shown in Figure 4.3-4.4, respectively. For the white precipitation obtained from precipitation method, strong H_2O peak at wave number around 3450 cm^{-1} disappears after calcination. Moisture trapped between crystals are removed during heat treatment. Moreover organic groups such as CO_3^{2-} and NH_4^+ which have absorption band at 860 and 1425 cm^{-1}, are also eliminated during calcination. For product from sol-gel method, the absorption peaks at 1400, 1700, and 3500 cm^{-1} disappear after calcination which indicates that NO_3^- ion and organic groups are removed. Lastly, solvothermal method, the characteristic absorption bands of boehmite observed at 773 and 615 cm^{-1} from the as-synthesized product disappear after calcination. It should be noted that boehmite is resulted from the present small amount of water which is by-product from AIP decomposition [32]. Therefore, the IR analysis confirms that the products obtained

after calcination are pure alumina without contamination of residual organic moiety, regardless of the synthesis technique.

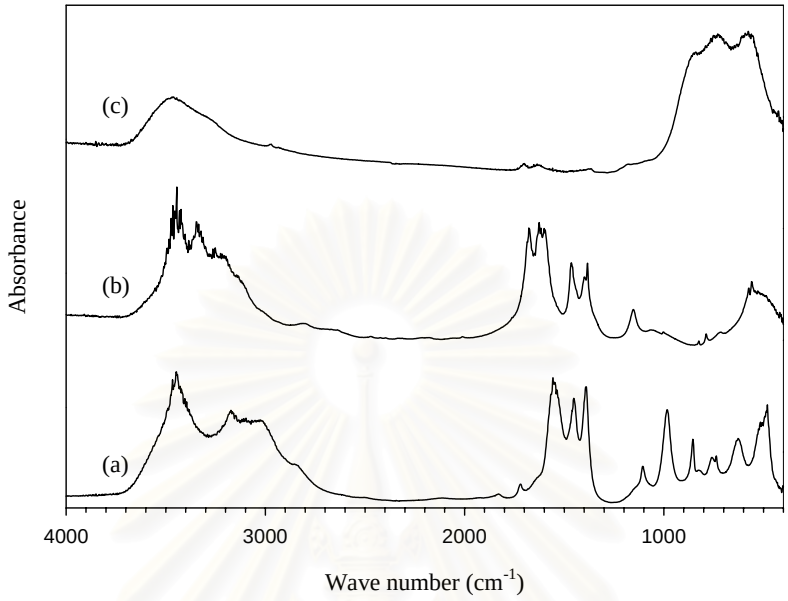

Figure 4.3 The IR spectra of as-synthesized product from: (a) precipitation method, (b) sol-gel method, (c) solvothermal method.

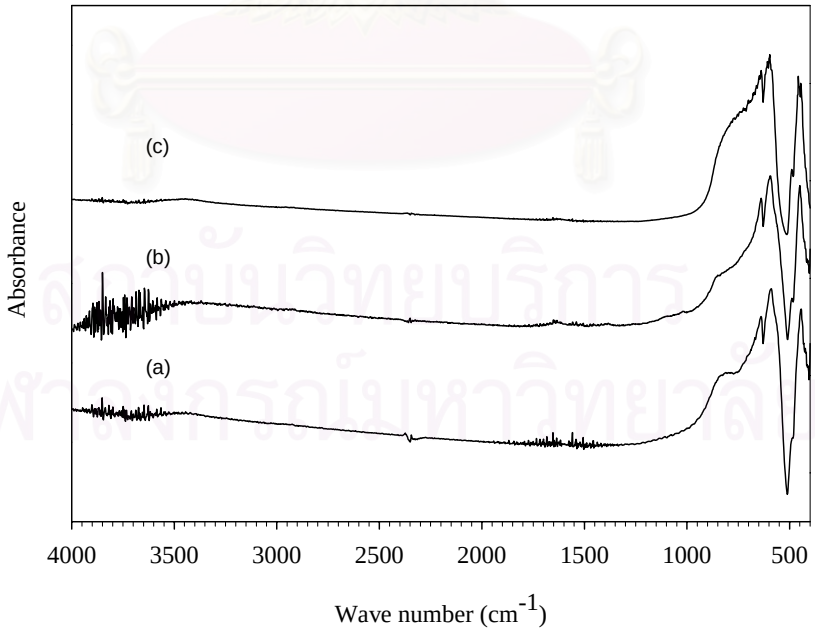

Figure 4.4 The IR spectra of calcined product synthesized via : (a) precipitation method, (b) sol-gel method, (c) solvothermal method.

Morphologies of the calcined product, observed by SEM, are shown in Figure 4.5. It is obvious that particles shown are much bigger than the crystallite size calculated from XRD line broadening. This is due to agglomeration of alumina powders into larger particle, called secondary particle. Size of the secondary particle for all samples are different as shown in Figure 4.5. The secondary particle size of powder synthesized by precipitation method is much smaller than these synthesized via sol-gel or solvothermal method. The median sizes of the particles synthesized by precipitation, solvothermal and sol-gel technique are 0.42, 3.62 and 4.07 μm, respectively. It should be noted that the particle size is measured by using laser scattering technique. Nevertheless, since the average size of the secondary particles can be decreased by milling as shown in Table 4.2, it is suggested that the secondary particles are loosely agglomerated.

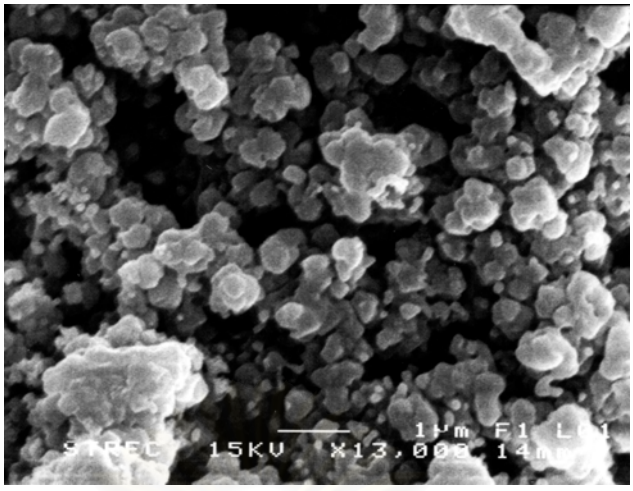

(a) Calcined powder from precipitation method.

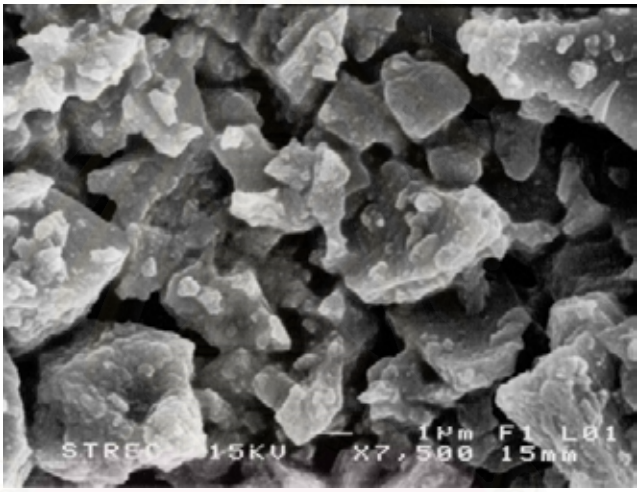

(b) Calcined powder from sol-gel method.

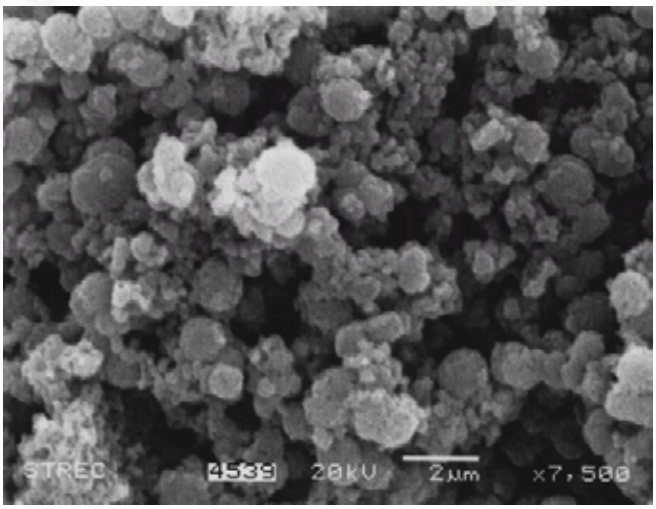

(c) Calcined powder from solvothermal method.

Figure 4.5 SEM images of calcined-powders from various techniques.

Table 4.2 Particle size of calcined products after milling for various time.

Synthesized method	Median diameter (μm) at various milling time			
	0 h	24 h	48 h	72 h
Precipitation	0.42	0.33	0.34	0.33
Sol-gel	4.07	0.38	0.54	0.36
Solvothermal	3.62	2.44	0.39	0.38

The calcined powders from different synthesis methods were milled by using ball mill for 72 h. Samples were taken at various milling times for particle size distribution analysis. The results are shown in Figure 4.6-4.8. It is found that the longer the milling time, the narrower the particle size distribution. However, it is found that particle size distributions of powder synthesized from different methods are different. All of the curves in Figure 4.6 are unimodal, especially at milling time 24 and 72 h, in which the range of distribution is very narrow. It implies that the powders synthesized by precipitation are very uniform in size. On the contrary, the particle size distribution of calcined powder in sol-gel method is bimodal. It is decreased to unimodal by milling for 24 h, as shown in Figure 4.7, attributing to soft agglomeration of powder. For the solvothermal method, the powders obtained also have bimodal size distribution, However, as shown in Figure 4.8, the particle size distribution after milling at 24 h is still large and bimodal. The size distribution turns into unimodal after 48 h of milling. The particle size can also be reduced under longer milling time. The suggests that although the powder from solvothermal method is packed more tightly than that from sol-gel method, the particle size is still under soft agglomeration and can be broken by milling.

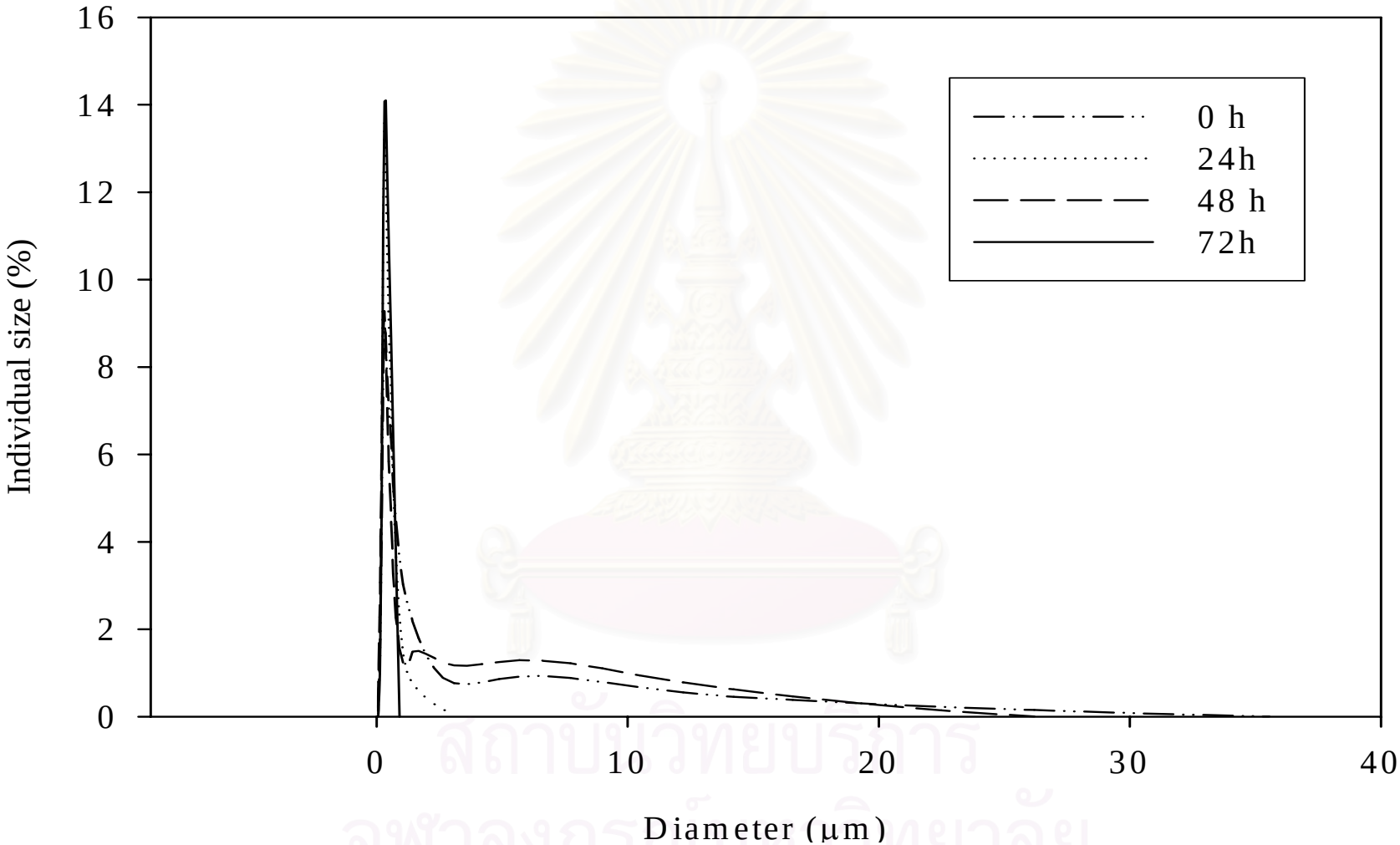

Figure 4.6 The particle size distribution of powder from precipitation method at various milling time.

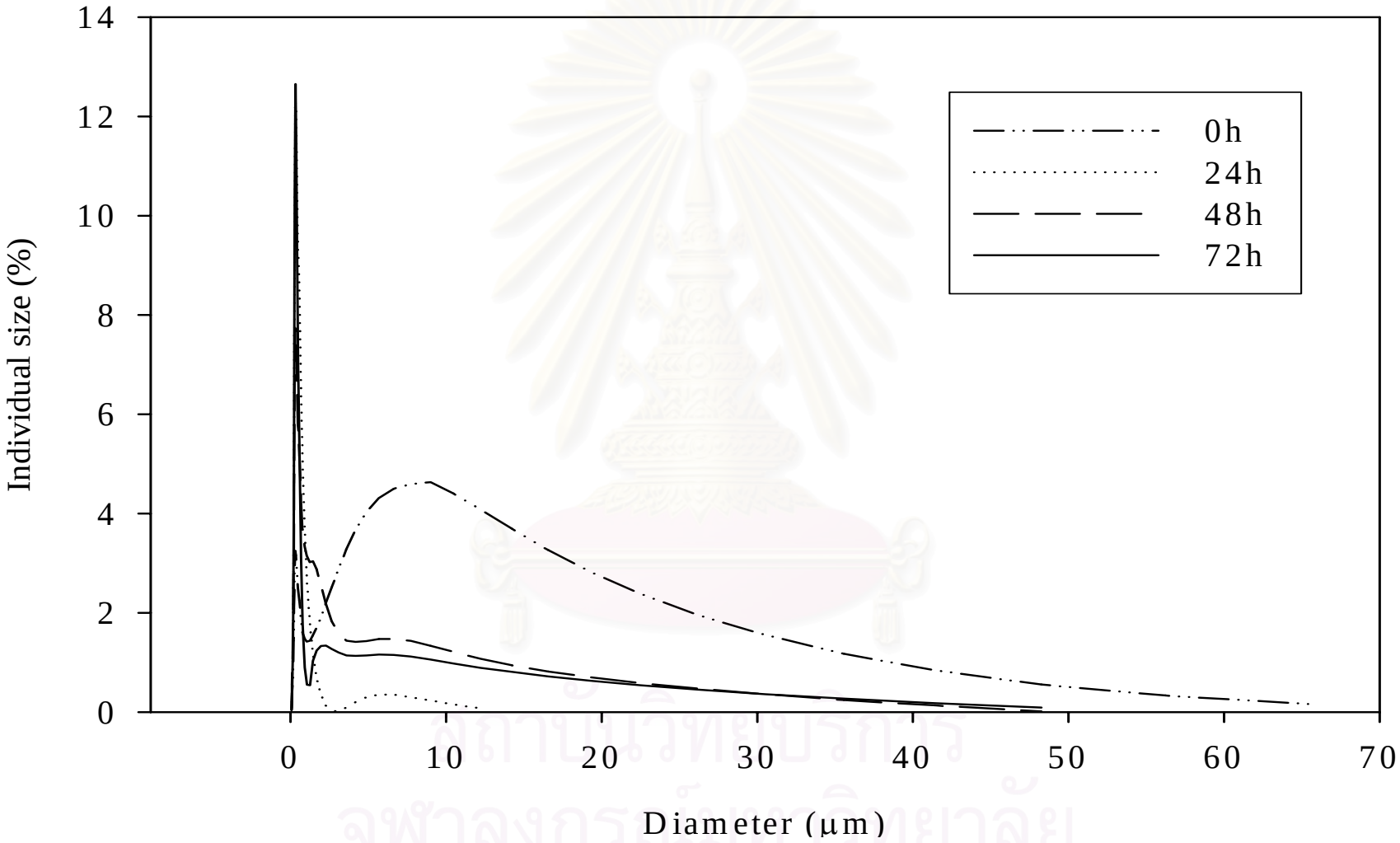

Figure 4.7 The particle size distribution of powder from sol-gel method at various milling time.

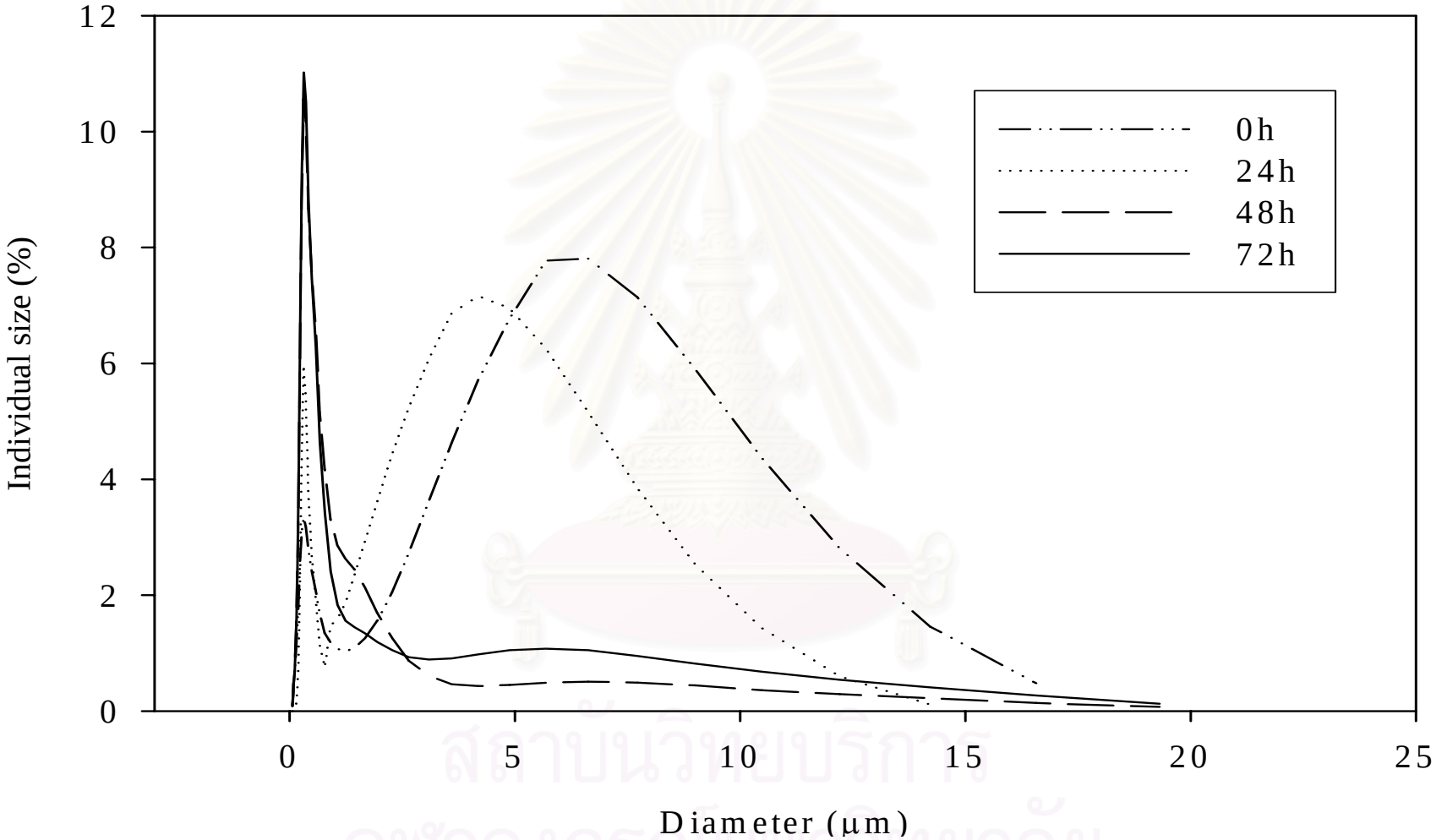

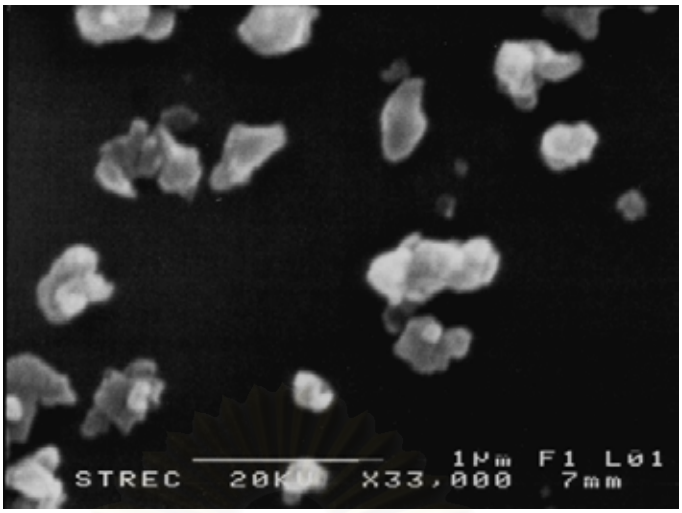

(a) Precipitation method (24 h milling time)

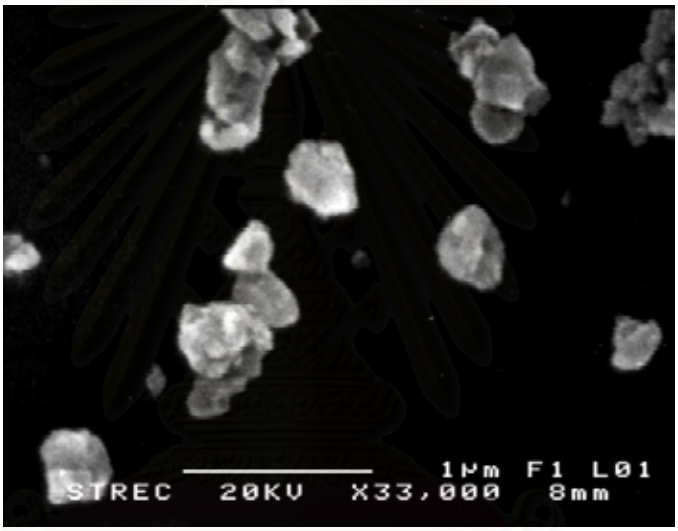

(c) Sol-gel method (24 h milling time)

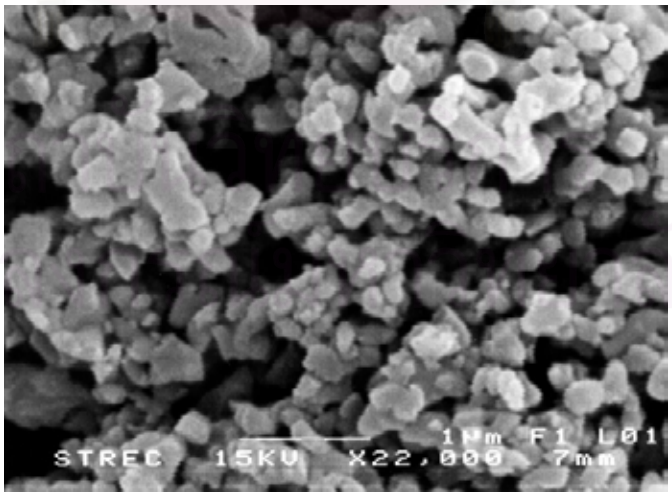

(c) solvothermal method (48 h milling time)

Figure 4.9 SEM images of alumina powder which is milled at various time.

Figure 4.9 shows morphology of alumina powder milled for reasonable time, which is considered from their size distribution and median diameter. For precipitation and sol-gel methods, 24 h milling time is suitable because small particle size and narrow size distribution are achieved within a short milling time. For solvothermal method, longer milling time of 48 h is required to achieve the same narrow size distribution as other methods.

4.1.2 Effects of preparation conditions for precipitation

According to morphology and particle size distribution discussed in prior sections, it is apparent that precipitation method is preferable for alumina nanocrystal synthesis since high purity α-alumina with small particle size can be easily synthesized within relatively short time. The powders obtained are readily uniform and need no milling. Therefore, detailed study on the effect of preparation conditions in the formation of ammonium aluminum carbonate hydroxide by this method is investigated. The concerned factors include the concentration of both reactants, the speed of mixing, the rate of the addition of aluminium precursor, the reaction temperature and the pH value of the reaction system.

4.1.2.1 Effects of reactant concentration

The concentration of both reactants has been varied. The median diameter of all obtained powders at different concentration are shown in Table 4.3. It should be noted that the particle size measurement was done after the calcination of the obtained powders.

Table 4.3 Median diameter of synthesized powders using various concentration of reagents.

Concentration of AHC Solution	Median diameter at various concentration of AAS solution (μm)				
	0.1 M	0.2 M	0.3 M	0.4 M	0.6 M
0.5 M	0.4	0.37	0.41	0.35	0.4
1 M	0.4	0.36	0.39	0.34	0.41
2 M	0.41	0.42	0.39	0.39	0.47

According to Table 4.3, the particle size of all powders synthesized from reagents at various concentrations are not much different. It suggests that the concentration of both solutions in this range has no effect to median diameter of the calcined-powder. However, it affects the particle size distribution of the powder, as shown in Figure 4.10-4.12.

From the particle size distribution curve in Figure 4.10, where the concentration of AHC solution is fixed at 0.5M, it is found that the curve apparently splits into bimodal distribution at high concentration of AAS solution. On the other hand, at the lower AAS concentration, the distribution curve is nearly unimodal. The same behavior is also observed when the concentration of AHC solution is increased to 1.0 and 2.0M (Figure 4.11 and 4.12, respectively), in which the distribution curve also split into bimodal mode at the highest concentration of AAS solution. The size distribution of all samples are broad, except at the AAS concentration of 0.2 mol/l, which is narrow and unimodal.

All curves in Figure 4.10-4.12 indicate that the concentration of both reactants affects the particle size distribution, although it has no effect on the median diameter of particles. This is attribute to the fact that the reaction system undergoes gelation when high concentration reactant is employed. Consequently, washing of the obtained product is more difficult and therefore it fails to acquire high purity of ammonium aluminum carbonate hydroxide. The remaining impurities act as nucleation sites for rapid crystal growth, which cause large particle and broad size distribution of the calcined powder.

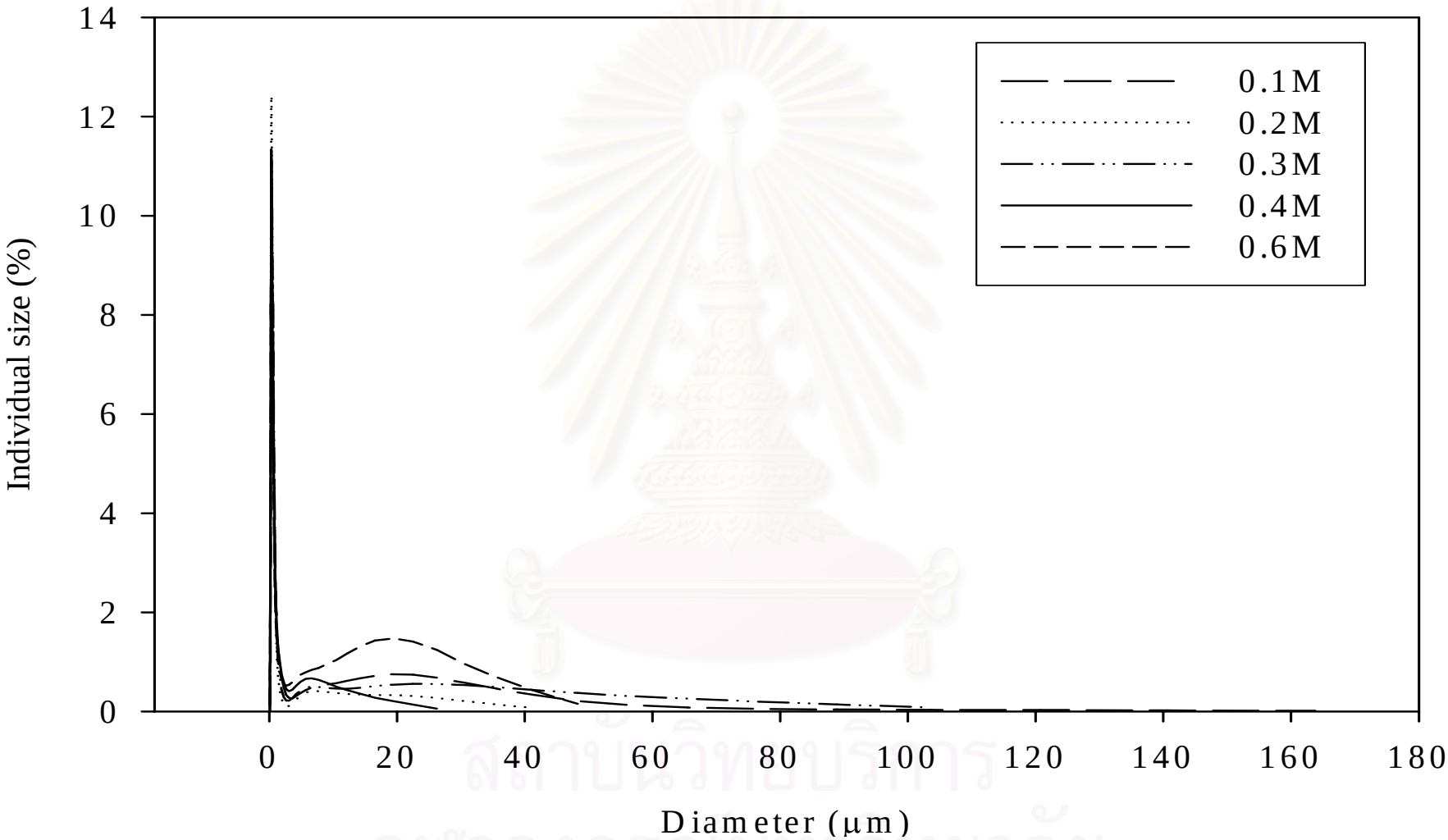

Figure 4.10 The particle size distribution of powder synthesized by precipitation method, using 0.5 M of AHC solution and various concentration of AAS solution.

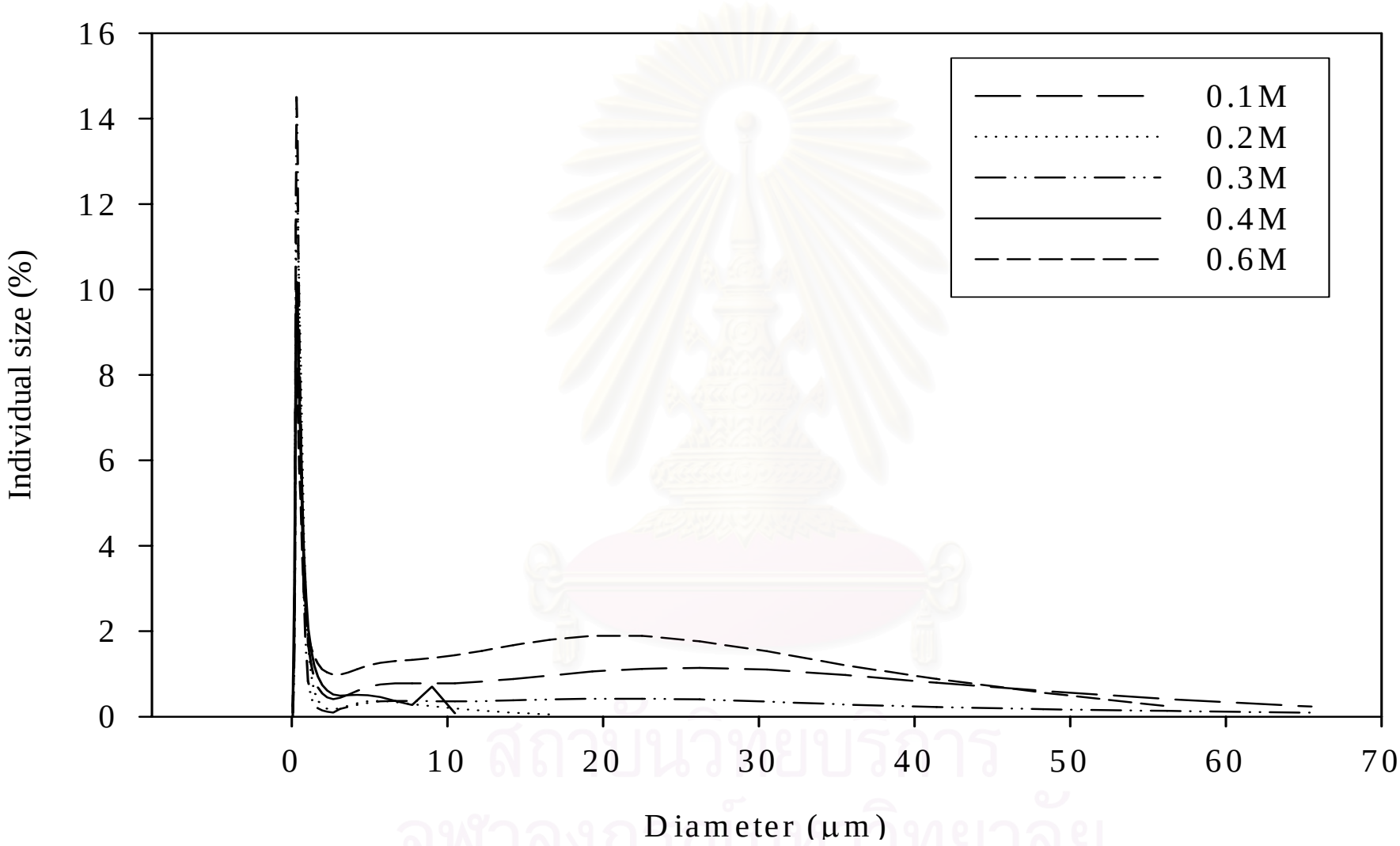

Figure 4.11 The particle size distribution of powder synthesized by precipitation method, using 1.0 M of AHC solution and various concentration of AAS solution.

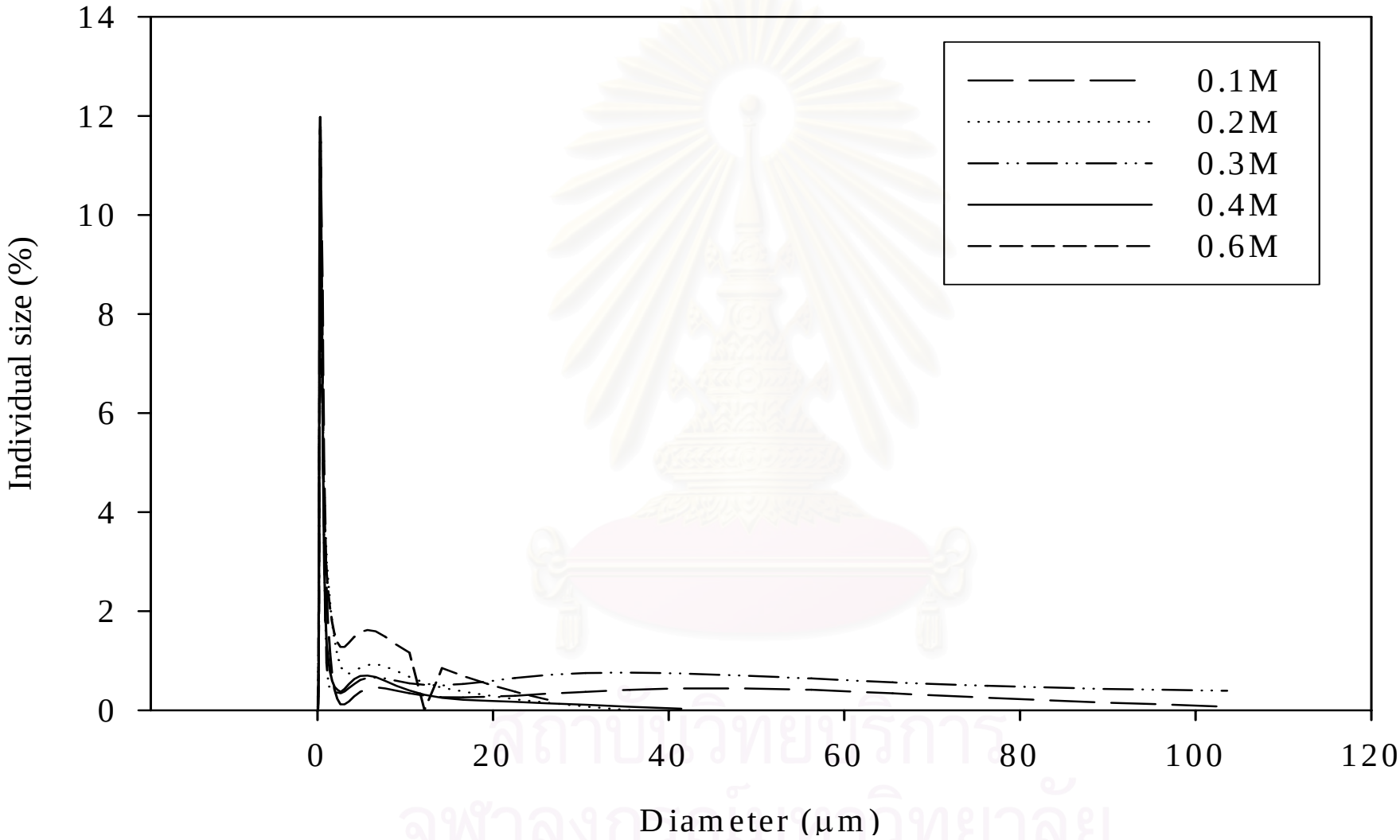

Figure 4.12 The particle size distribution of powder synthesized by precipitation method, using 2.0 M of AHC solution and various

4.1.2.2 Effects of pH

The effect of pH are presented in Table 4.4 and Figure 4.13 When the pH of reaction system is adjusted to 5 by adding acetic acid, the reaction does not proceed because H^+ from acidic solution reacts with the reactants, resulting in an undesired product. At pH 7, the powder obtained is large in median diameter as well as the size distribution. This indicates that neutral reaction condition is not suitable to produce powder with fine particle size. However, pH value of reaction system constant at 9, where the reaction proceed spontaneously and do not need additional chemical to adjust pH of the system, the median diameter of the obtained powder becomes small. The range of particle size distribution is also found to be narrow and unimodal.

Table 4.4 Median diameter at various pH of reaction system

pH	Median diameter (μm)
5	No reaction
7	2.62
9	0.42

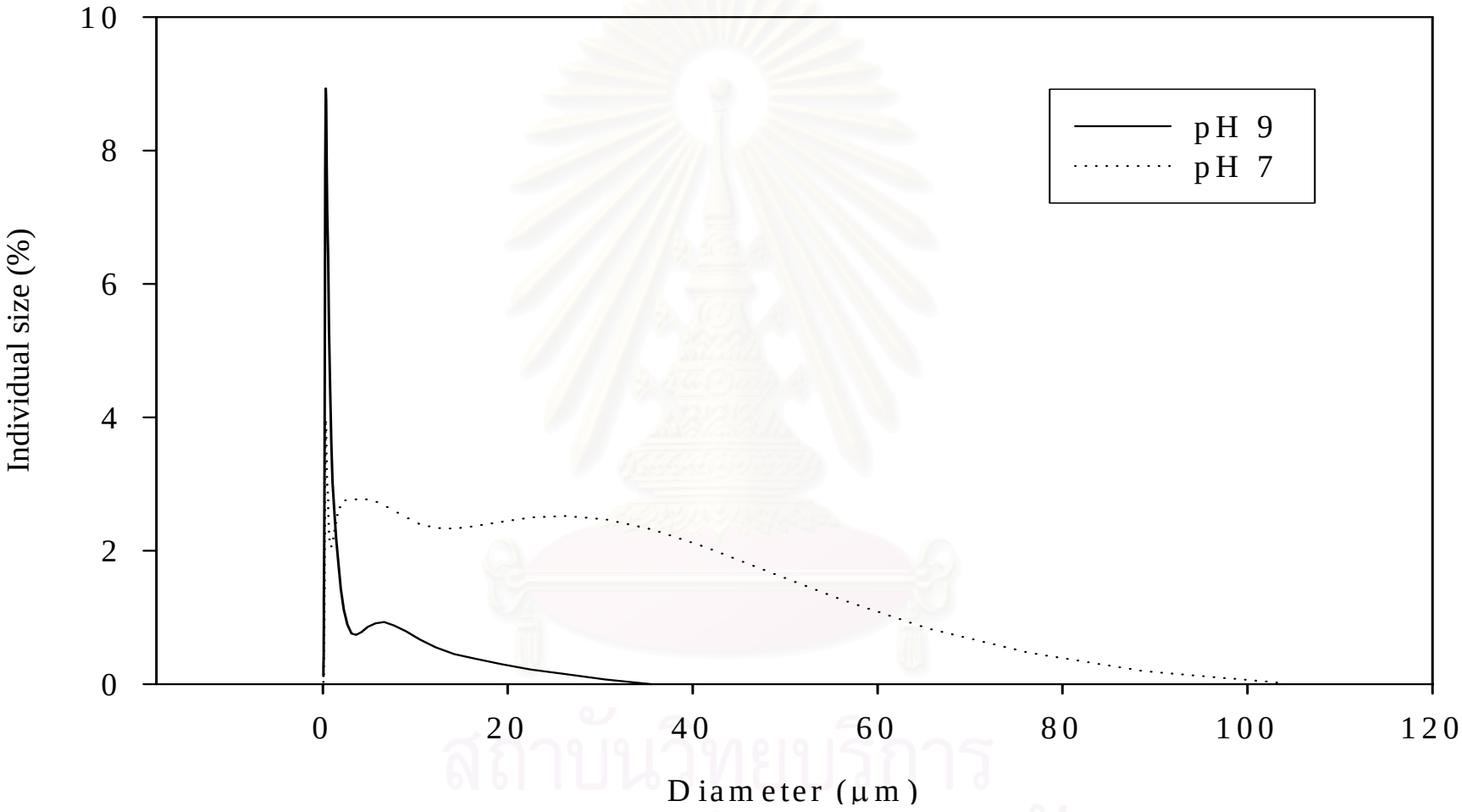

Figure 4.13 The particle size distribution of powder synthesized by precipitation method at various pH.

4.1.2.3 Effects of speed of mixing

Speed of mixing, including stirring speed and rate of reactant addition, is found to affect both particle size and size distribution of the obtained product, as seen in Figure 4.14-4.15. Figure 4.14 indicates that the higher speed of mixing, the smaller the particle and the more narrow the particle size distribution. The median diameter of the powder obtained from the reaction using various stirring speed are summarized in Table 4.5. At the highest stirring speed, the median diameter is the smallest. Since the reaction between AHC and AAS to form ammonium aluminum carbonate hydroxide particles is rapid, evidenced by the fact that white precipitates are observed immediately after AAS solution is mixed with AHC solution, the mixing speed is mainly associated with crystal growth and agglomeration of the particles. The high stirring speed prevents agglomeration of the precipitate. Moreover, it facilitates the dispersion of the ammonium aluminum carbonate hydroxide particles formed and therefore minimizes the growth of ammonium aluminum carbonate hydroxide on large existing seeds.

Table 4.5 Median diameter at various stirring speed

Stirring speed (rpm)	Median diameter (μm)
0	0.95
300	0.68
450	0.42

When the stirring speed is fixed at 450 rpm and the addition rate of AAS solution into AHC solution is varied, the effect of adding rate to particle size distribution and median diameter can be observed. The result shown in Figure 4.15 indicate the same phenomena as observed from varying the stirring speed. The lower adding rate, the smaller range of particle size distribution. When AAS solution is pour into AHC solution directly, the particle size is large and their distribution is apparently bimodal, which is undesirable characteristic for powder in ceramic field. Since AAS solution is acidic (pH = 3), while AHC solution is basic (pH = 9), sudden pouring of AAS to AHC solution cause

rapid fluctuation and nonuniformity in pH value of the system. Some regions in the system may be acidic, which results in undesired product trapped in ammonium aluminum carbonate hydroxide precipitates, as discussed earlier in section 4.1.2.2. This trapped species acts as impurity in alumina and initiates rapid crystal growth upon the calcination. On the contrary, at low adding rate of 1, 3 and 10 cc/min, the stirring in the system is capable of homogenizing the pH of the system. By the nature of the reaction, the system can be maintained as basic solution if AAS is gradually added. The median diameters of powder obtained by using adding rate of 1, 3 and 10 cc/min are not different in size distribution.

Table 4.6 Median diameter at various rate of addition

Adding rate (cc/min)	Median diameter (μm)
1	0.38
3	0.42
10	0.38
pour directly	9.59

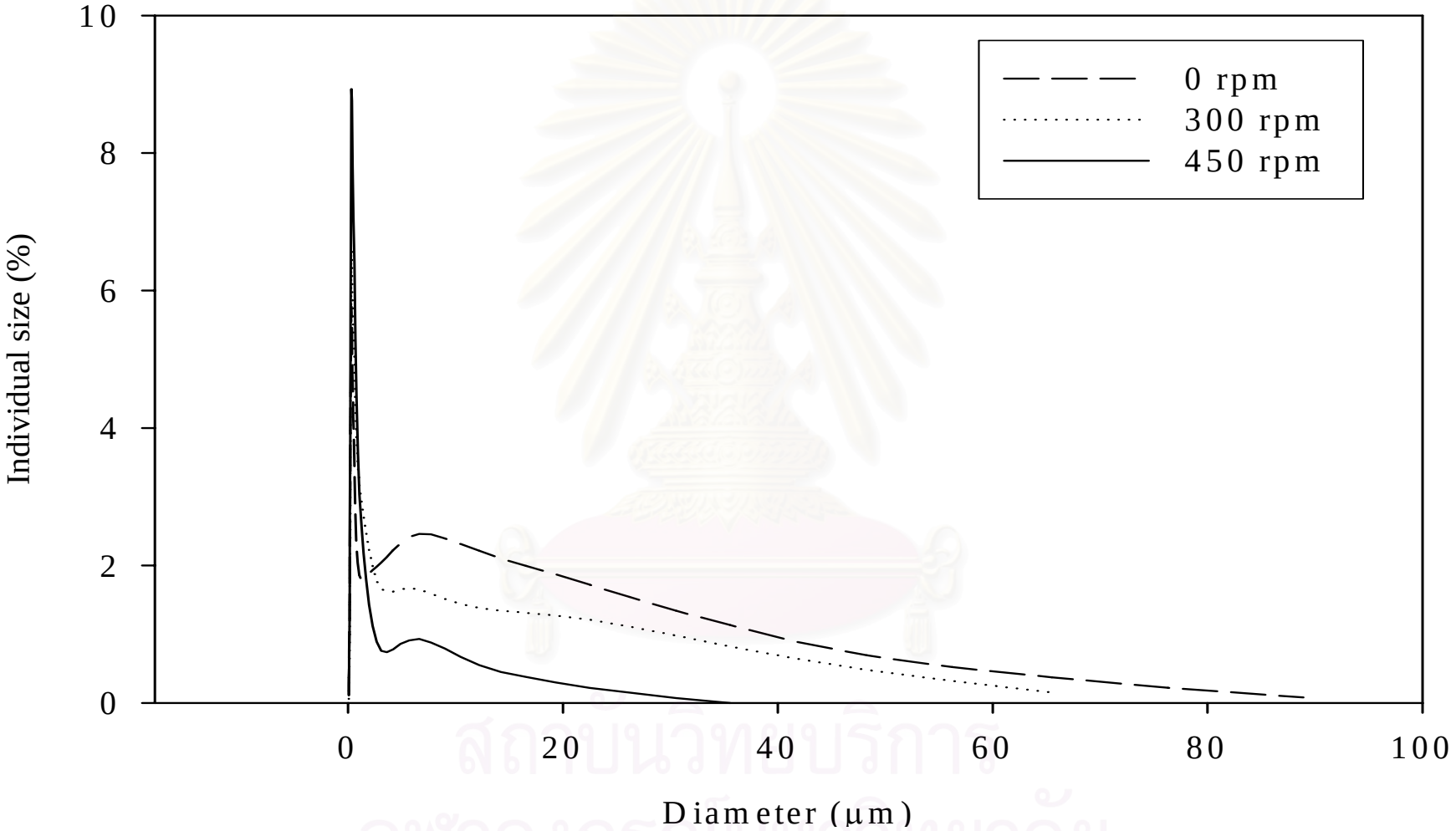

Figure 4.14 The particle size distribution of powder synthesized by precipitation method, using various speed of mixing.

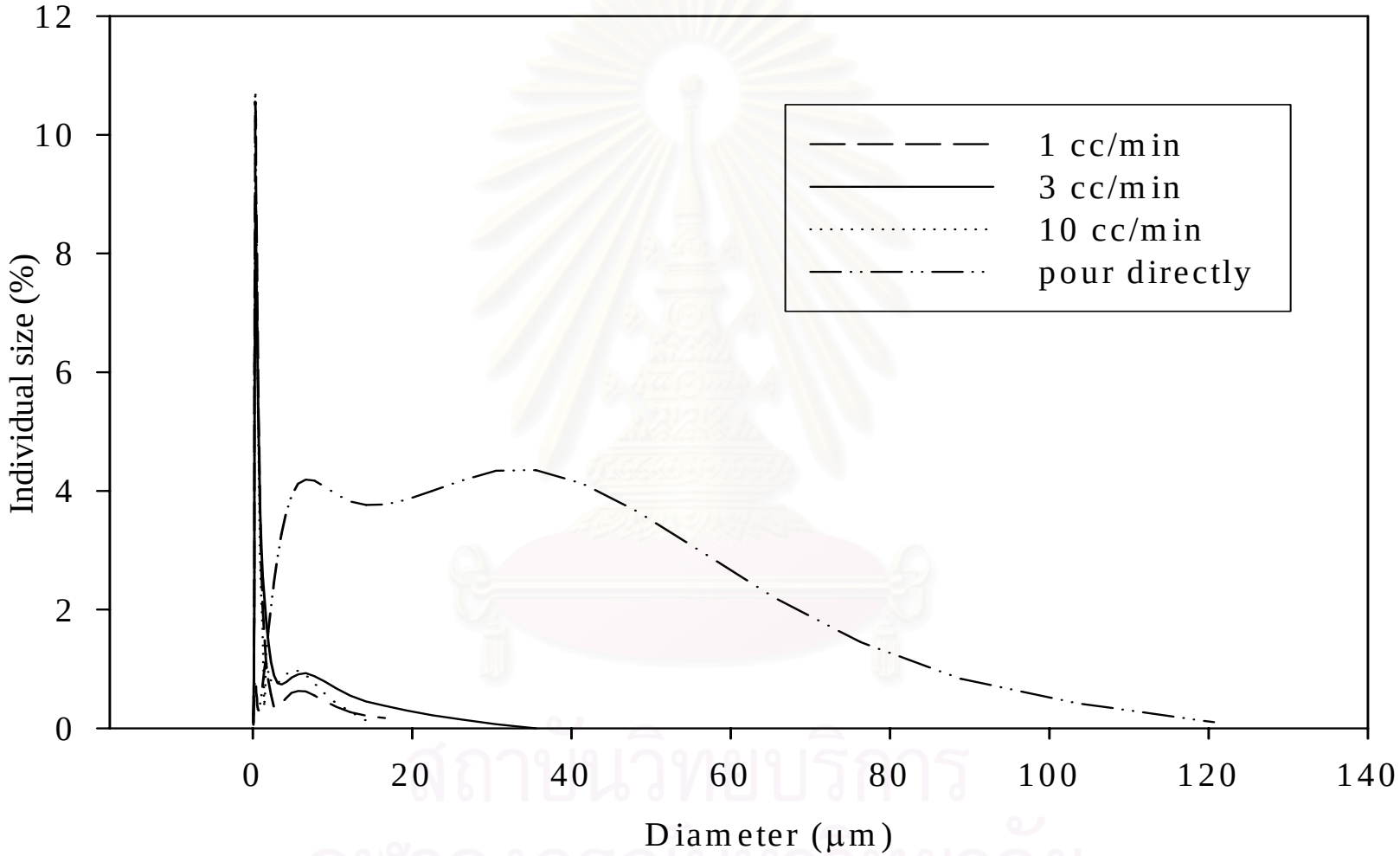

Figure 4.15 The particle size distribution of powder synthesized by precipitation method, using various rate of addition of AAS solution into AHC solution.

4.1.2.4 Effects of reaction temperature

The effects of reaction temperature are shown in Table 4.7 and Figure 4.16. Although the results in Table 4.7 imply that the reaction temperature has no significant effect on the size of particle synthesized, the distribution curves in Figure 4.16 indicated otherwise. The reaction at high temperature (80^{o}C) results in powder with broad bimodal distribution, while powder synthesized at low temperature (30^{o}C) is uniform in size. It should be noted that yield of ammonium aluminum carbonate hydroxide increases with the increase in reaction temperature. However, if the temperature is higher than the range investigated, the decomposition of ammonium hydrogen carbonate is so accelerated that the reaction fails to proceed affectively and the product suffers from excessive crystal growth. Therefore, it can be concluded from the observation that the formation of ammonium aluminum carbonate hydroxide is more spontaneous at high temperature. Nevertheless, rate of the reaction that is too fast also increases the potential for agglomeration of the particles under the same stirring speed.

Table 4.7 Median diameter at various reaction temperature

Temperature (^{o}C)	Median diameter (μm)
30-35	0.34
40-45	0.42
75-80	0.42

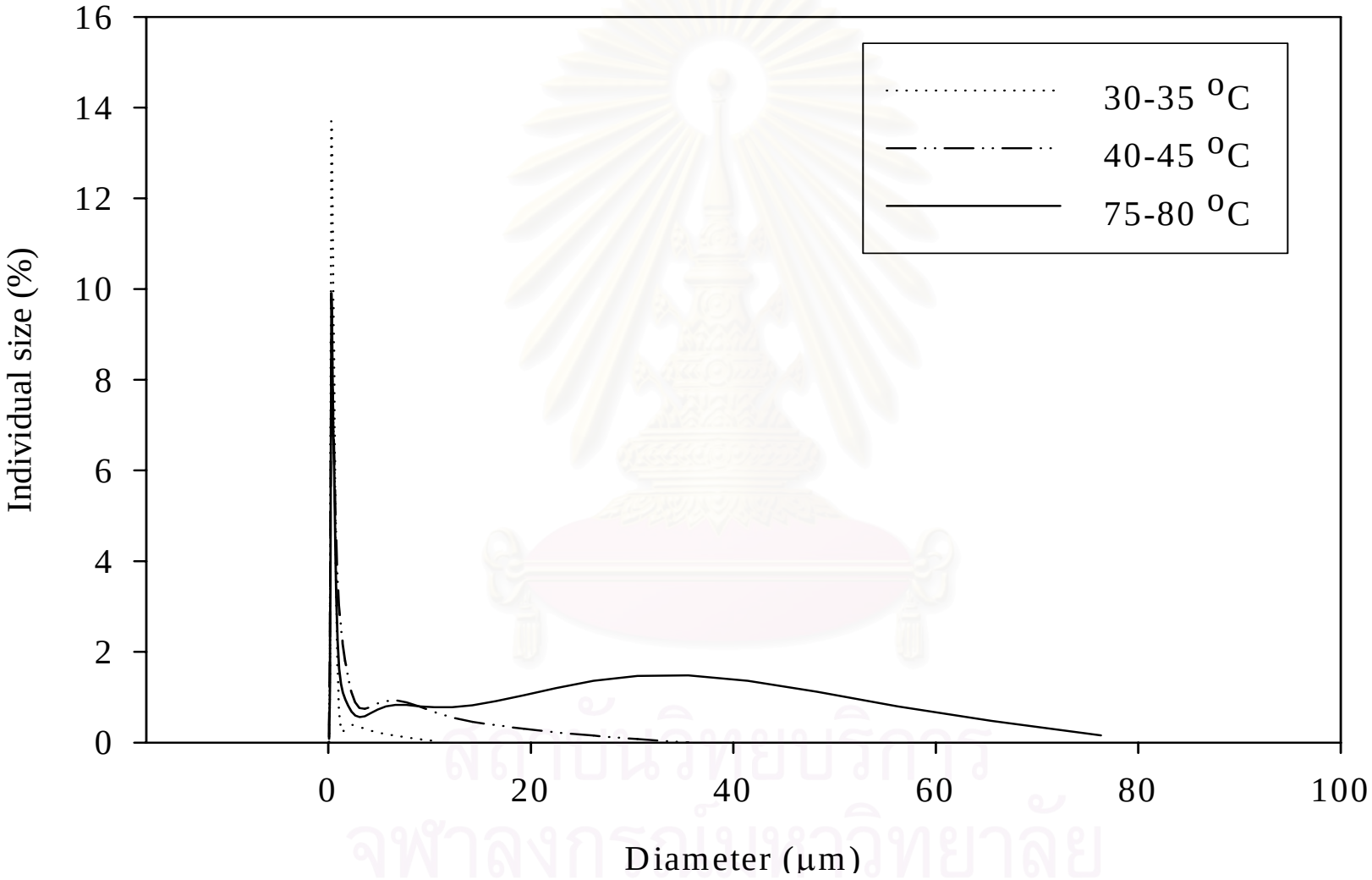

Figure 4.16 The particle size distribution of powder synthesized by precipitation method at various reaction temperature.

4.2 Chromium Doped Alumina

4.2.1 Structure and morphology of Cr-doped alumina

Chromium is doped into α-Al_2O_3 according to the procedures described earlier. XRD analysis has confirmed that although chromium is added, the crystal structure of the product remains as corundum. Different contents of chromium precursor give the same pattern of the X-ray diffraction. Figure 4.17 shows examples the XRD pattern of alumina doped chromium precursor at the concentration of 0.5 wt% produced by different methods. It should be noted that small amount of silicon is added to the sample as internal standard for XRD analysis, in order to verify the position of peaks of doped samples.

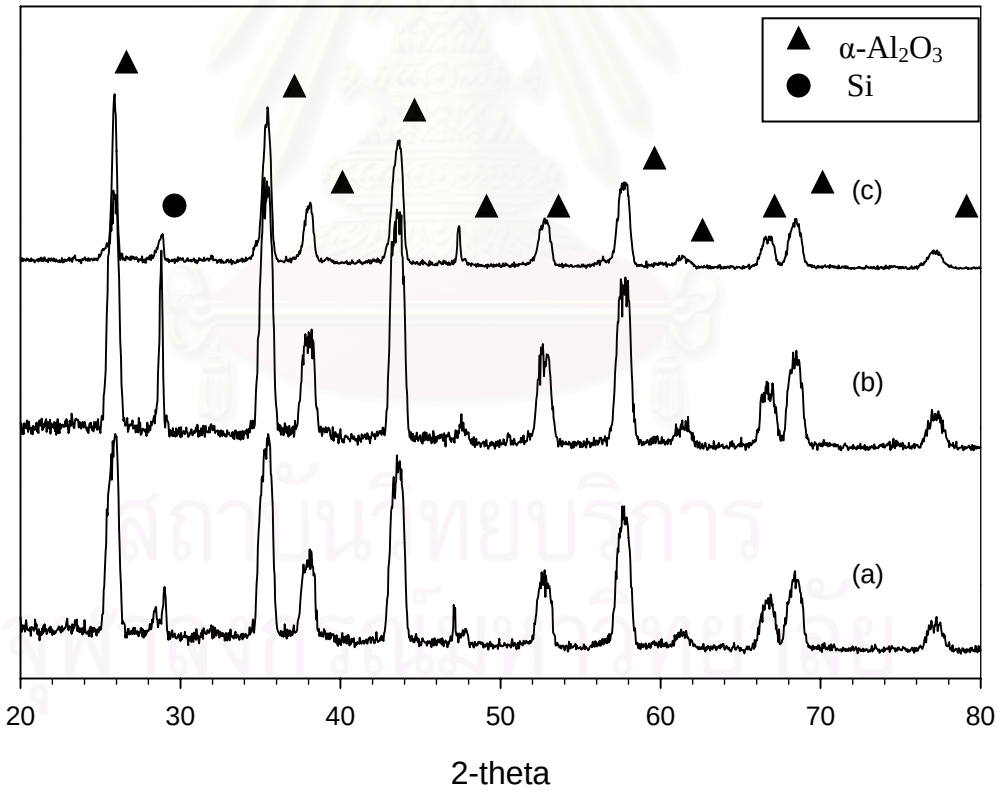

Figure 4.17 The XRD patterns of 0.5 wt% chromium doped-alumina produced by : (a) precipitation method, (b) sol-gel method, (c) solvothermal method.

As shown in Figure 4.17, no diffraction peak of chromium oxide is detected. It implies that no chromium is left on the surface of alumina particle. Instead, chromium ions are incorporated into alumina structure. This is also evidenced by the pink color of the calcined-powder.

The morphology of alumina powders doped with chromium ions can be described by SEM images shown in Figure 4.18.

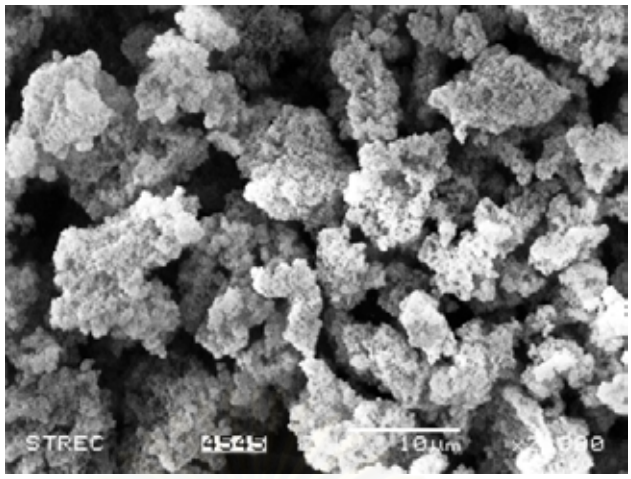

(a) Precipitation method

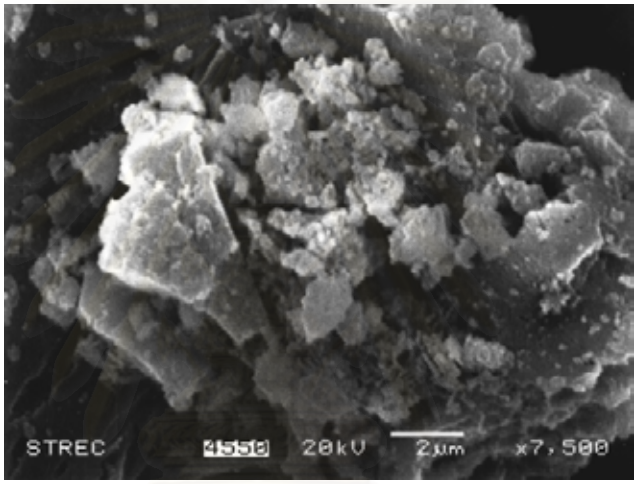

(b) Sol-gel method

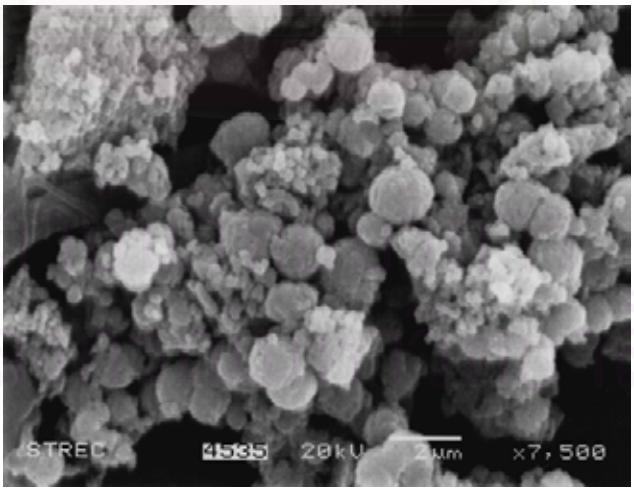

(c) Solvothermal method

Figure 4.18 SEM images of 0.5 wt% chromium doped-alumina powder produced from various techniques.

By comparing SEM images of 0.5 wt% chromium-doped alumina (Figure 4.18) to those of undoped alumina (Figure 4.5), it can be seen that shape and size of doped alumina particles produced from the same method are not different from undoped alumina. Noted that 0.5 wt% is the maximum doping investigated in this work. Therefore, the chromium ions diffusing into alumina structure have no effect on morphology and size of the secondary aggregation of alumina powders.

4.2.2 Effects of chromium ions in alumina structure

In this work, chromium doping takes place during synthesis procedures. Calcination of the as-obtained powder results in the formation of a Cr-corundum solid solution. Although the XRD pattern confirms that their crystal structure remains as corundum, the crystallite size of calcined-powder from various technique is shown in Table 4.8.

Table 4.8 The crystallite size of doped and undoped powder by various techniques after calcination.

Synthesis technique	Crystallite size (nm)
Precipitation method	
undoped	9.65
0.05 wt%	9.63
0.1 wt%	9.82
0.5 wt%	9.79
Sol-gel method	
undoped	9.52
0.05 wt%	32.32
0.1 wt%	14.66
0.5 wt%	28.49
Solvothermal method	
undoped	9.74
0.05 wt%	10.77
0.1 wt%	10.40
0.5 wt%	10.19

The crystallite size of Cr-doped and undoped powder from precipitation and solvothermal method after calcination are not different, while the crystallite size of calcined-powder of Cr-doped powder is much higher than undoped powder after calcination. This attribute to chromium ion dissolved into amorphous gel during gelation and chromium act as the initiation site for rapid growth of crystal during heat treatment at high temperature. Furthermore, detailed observation from XRD diffraction peaks has indicated slight change in lattice parameters after chromium is incorporated. The lattice parameters calculated from XRD pattern are shown in Table 4.9.

Table 4.9 Lattice parameters of 0.1 wt% chromium doped alumina prepared by various methods

Sample	*a* and *b*[A^o]	*c* [A^o]
α–Al_2O_3 (undoped)	4.749	12.9219
Precipitation method	4.7403	12.8695
Sol-gel method	4.7388	12.8670
Solvothermal method	4.7335	12.7987

The change in lattice parameter indicates that after chromium doping, chromium ions occupy parts of alumina structure, which supports the XRD analysis results that no chromium oxide is detected. The presence of Cr ions in the powder is also confirmed by XRF and XPS analyses. The oxidation state of chromium in alumina structure is verified by Electron Spin Resonance (ESR) analysis. After chromium ions diffuse into alumina structure, their oxidation state presented in to be Cr^{3+} form, which is indicated by peaks at g-values of 3.6531, 1.4366, and 1.1857 in the ESR spectra, respectively. The intensities of peak at specific g-value (3.6531) in the ESR spectra from various Cr-doped alumina samples, which are indirectly related to concentration of Cr^{3+} in the sample, are compared as shown in Figure 4.19.

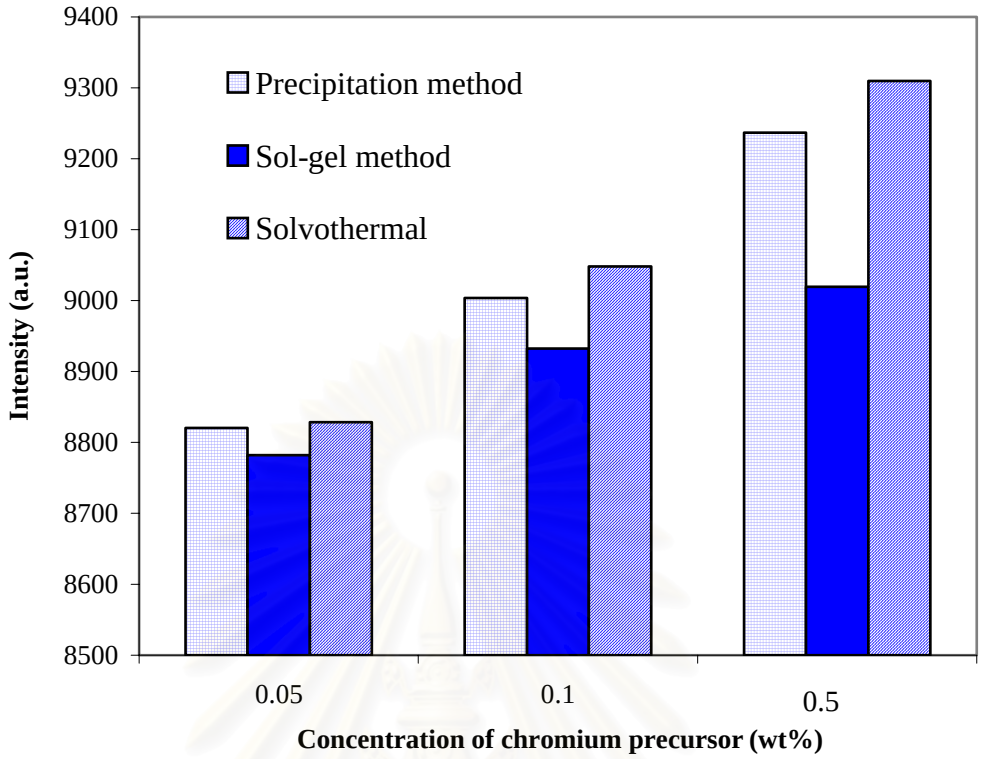

Figure 4.19 Intensity of ESR spectra at g-values of 3.6531 for alumina powder doped with various concentration of chromium.

Figure 4.19 clearly illustrates that the intensity of ESR peak increases with an increasing in chromium content, regardless of the synthesis technique. It implies that with in the range of doping investigated, the more chromium doped, the higher concentration of chromium in alumina structure. This figure also indicates that the amount of Cr^{3+} in alumina prepared by solvothermal technique is higher than that prepared by precipitation and sol-gel method. This result supports the finding that lattice parameters of doped alumina prepared by solvothermal technique are most deviated from the values of the undoped alumina, comparing with other synthesis techniques.

As mentioned earlier, doping of chromium results in colored alumina. The color of the powder depends upon oxidation states of chromium ions in the structure. In the precipitation technique, where chromium precursor is added to the AAS solution before dropping into AHC solution, the color of the precipitates obtained in

light blue. It has the same color as the powder obtained by impregnation of the undoped precipitates by chromium precursor. After calcination, both powders turn pink. This indicates that chromium coprecipitates with ammonium aluminum carbonate hydroxide powder during the precipitation step. Then, chromium ions diffuse into alumina lattice, while ammonium aluminum carbonate hydroxide decomposes into corundum. The pink color of the calcined product is mainly due to Cr^{3+} species dissolved in the corundum lattice. The same observation is formed in solvothermal method. The as-synthesized product (χ-alumina) is light blue in color, when chromium precursor is added into the autoclave. This indicates that chromium ions have not been incorporated into χ-alumina structure as Cr^{3+}. However, subsequent calcination results in reconfiguration of both alumina structure (from χ- to α-phase) and oxidation state of chromium ions.

For sol-gel method, the obtained gel, which is doped with chromium nitrate in the initial stage, is light purple. The calcination of pink and blue color of the gel suggests that parts of chromium ions penetrates into the structure of amorphous gel during gelation. After calcination, pink powder is obtained.

4.3 Fabrication of alumina powder

The particle size, size distribution and state of agglomeration of powder are important factors for fabrication of advanced ceramic, as mentioned earlier. To ensure the homogeneity of the starting material, soft agglomerated powders are broken by milling in ball mill to decrease the particle size as well as control the size distribution into narrow range.

The proper milling time depends upon the nature of powder. For alumina powder synthesized from different techniques, the reasonable milling time is selected according to the findings in Section 4.1.1. The same milling time selected is applied to both undoped and chromium-doped alumina powder, as long as they are prepared by the same technique. Morphologies of chromium doped powder after milling are shown in Figure 4.20. Also shown in Figure 4.20 is SEM image of commercial pure α-phase alumina, which is used as reference in this study.

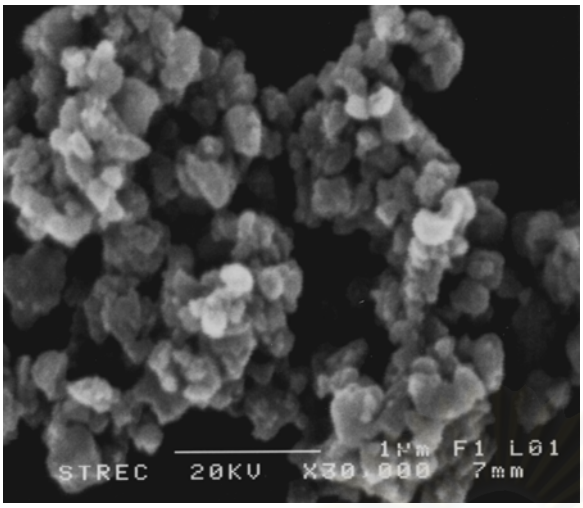

(a) Precipitation method
(24 h milling time)

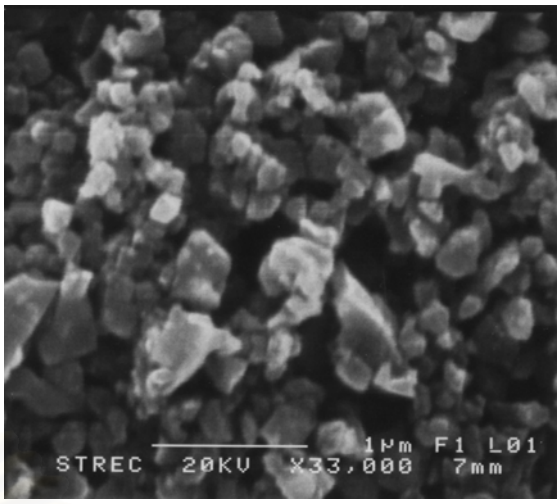

(c) Solvothermal method
(48 h milling time)

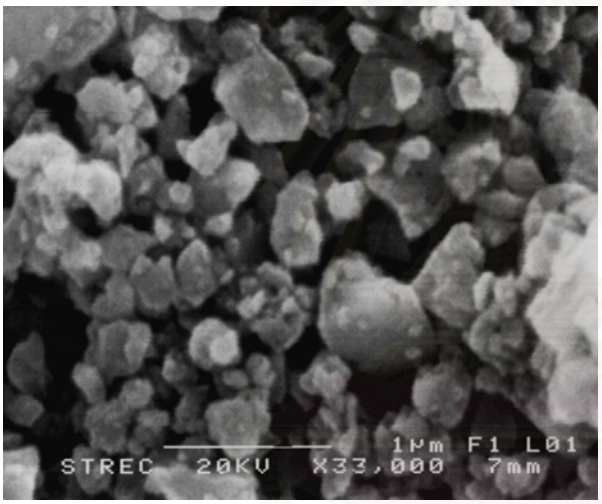

(b) Sol-gel method
(24 h milling time)

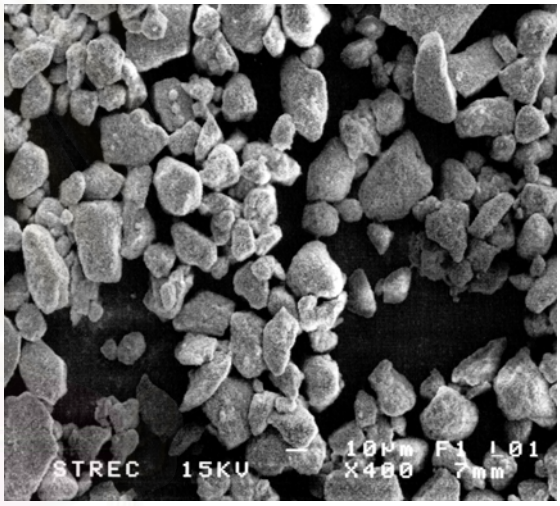

(d) Commercial powder

Figure 4.20 SEM images of chromium doped-alumina powder after milling and commercial alumina.

SEM image in Figure 4.20(d) shows that commercial alumina powder consists of small and uniform particles. This supports the fact that the particle size distribution curve, shown in Figure 4.21, is apparently unimodal with very narrow size distribution around the median diameter of 0.31 μm. Figure 4.21 also compares the size distribution among powders synthesized from various techniques. It shows that commercial powder has better characteristics, such as narrow size distribution and smaller median diameter, than the powder synthesized from precipitation, sol-gel and solvothermal methods.

After milling, the powder is fabricated into pellet according to the procedures decribed in Chapter III. The bulk density and relative density of the sintered specimen fabricated from undoped alumina powder are reported in Table 4.10.

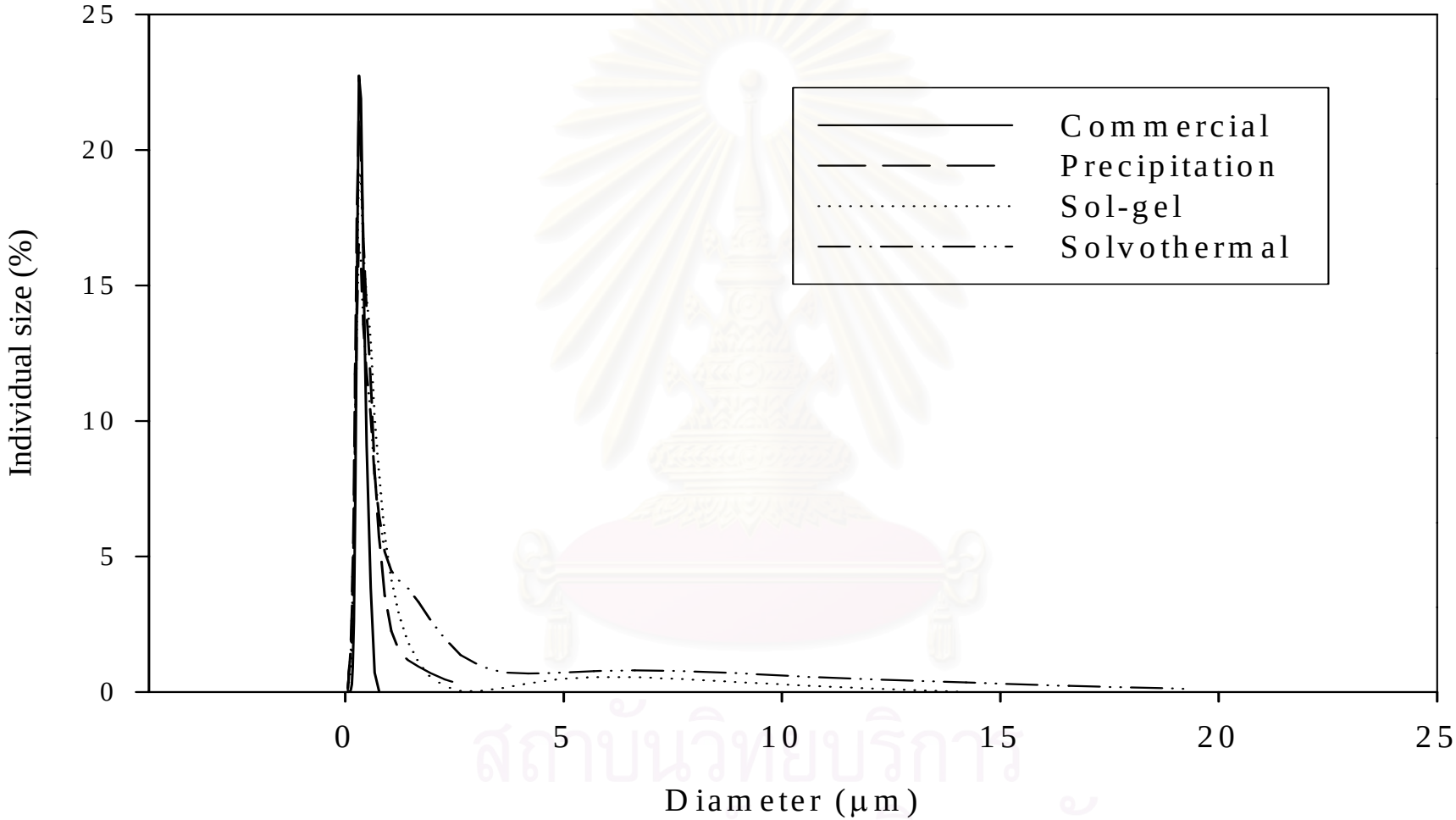

Fig. 4.21 The particle size distribution of powder synthesized from various techniques, comparing with commercial powder.

Table 4.10 Density of sintered specimen fabricated from undoped alumina.

Powder synthesis technique	Sintered in air		HIP	
	Bulk density [g/cm^3]	Relative density [%]	Bulk density [g/cm^3]	Relative density [%]
Precipitation method	3.88	97.5	3.90	98.1
Sol-gel method	3.69	92.7	3.70	93.1
Solvothermal method	3.84	96.5	3.87	97.3
Commercial powder	3.95	99.3	3.95	99.2

It can be seen from Table 4.10 that the density of the specimen fabricated from commercial powder is higher than other samples. This is attributed to small particle size and narrow size distribution of the powder. SEM image in Figure 4.20 (d) reveals that the commercial alumina powder is hardly aggregated. On the contrary, all powders synthesized in this work show certain level of agglomeration and presence of large particles, which may results in entrapped pores in the specimen. Among powders synthesized, alumina synthesized from precipitation method has more narrow size distribution. Consequently, the sintered article using this powder has density closest to that of the commercial alumina. Nevertheless, the size distribution is not the only factor affecting the density of the sintered article. Powder synthesized by sol-gel method has more narrow size distribution than the powder from solvothermal method, but the density of the sintered body is significantly lower. This is corresponding to the fact that the secondary particles in the powder from solvothermal method are consisted of tightly packed crystals, while the particles from sol-gel method is not as tightly packed, as discussed earlier in Section 4.1.1. Tight packing of crystallite grains within the secondary particles may responsible for higher density of the sintered article using powder synthesized from solvothermal technique. After the specimen is pressed by hot isostatic pressing (HIP), bulk density is increased because the trapped pores are partially eliminated by high pressure (150 MPa) high temperature (1300^{o}C) pressing.

Table 4.11 shows the density of specimen fabricated from chromium doped alumina powder. It is shown that the density of Cr-doped alumina is not considerably different from undoped alumina, if the powders are prepared by the same method. Hot isostatic pressing also increases the density of the specimen in the same manner as the

undoped alumina. After fabrication procedure, it is found that the apparent color of the specimen is changed. The color of the specimen can be examine by UV spectra, as shown in Figure 4.22-4.24.

Table 4.11 Density of sintered specimen fabricated from chromium doped alumina.

Cr-doped alumina	Sintered in air		HIP	
	Bulk density [g/cm^3]	Relative density [%]	Bulk density [g/cm^3]	Relative density [%]
Precipitation method				
0.05 wt% Cr	3.83	96.3	3.90	97.9
0.1 wt% Cr	3.87	97.1	3.90	98.0
0.5 wt% Cr	3.85	96.8	3.87	97.2
Sol-gel method				
0.05 wt% Cr	3.80	95.5	3.85	96.8
0.1 wt% Cr	3.84	96.5	3.89	97.7
0.5 wt% Cr	3.73	93.7	3.71	93.2
Solvothermal method				
0.05 wt% Cr	3.82	96.0	3.84	96.4
0.1 wt% Cr	3.86	96.9	3.88	97.6
0.5 wt% Cr	3.80	95.6	3.91	98.2

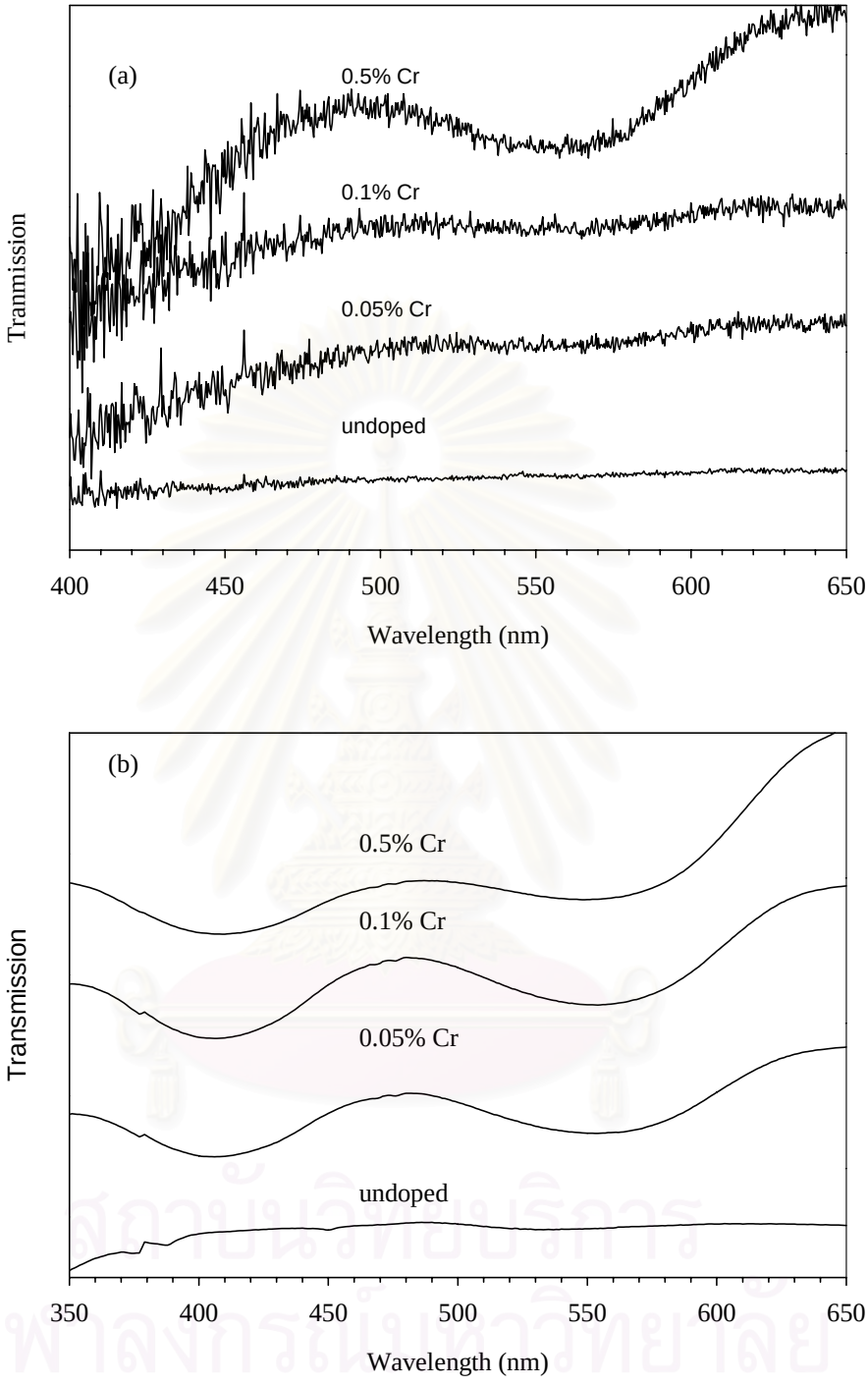

Figure 4.22 Reflective UV/visible spectra of chromium doped alumina synthesized by precipitation method : (a) starting powder, (b) sintered specimen.

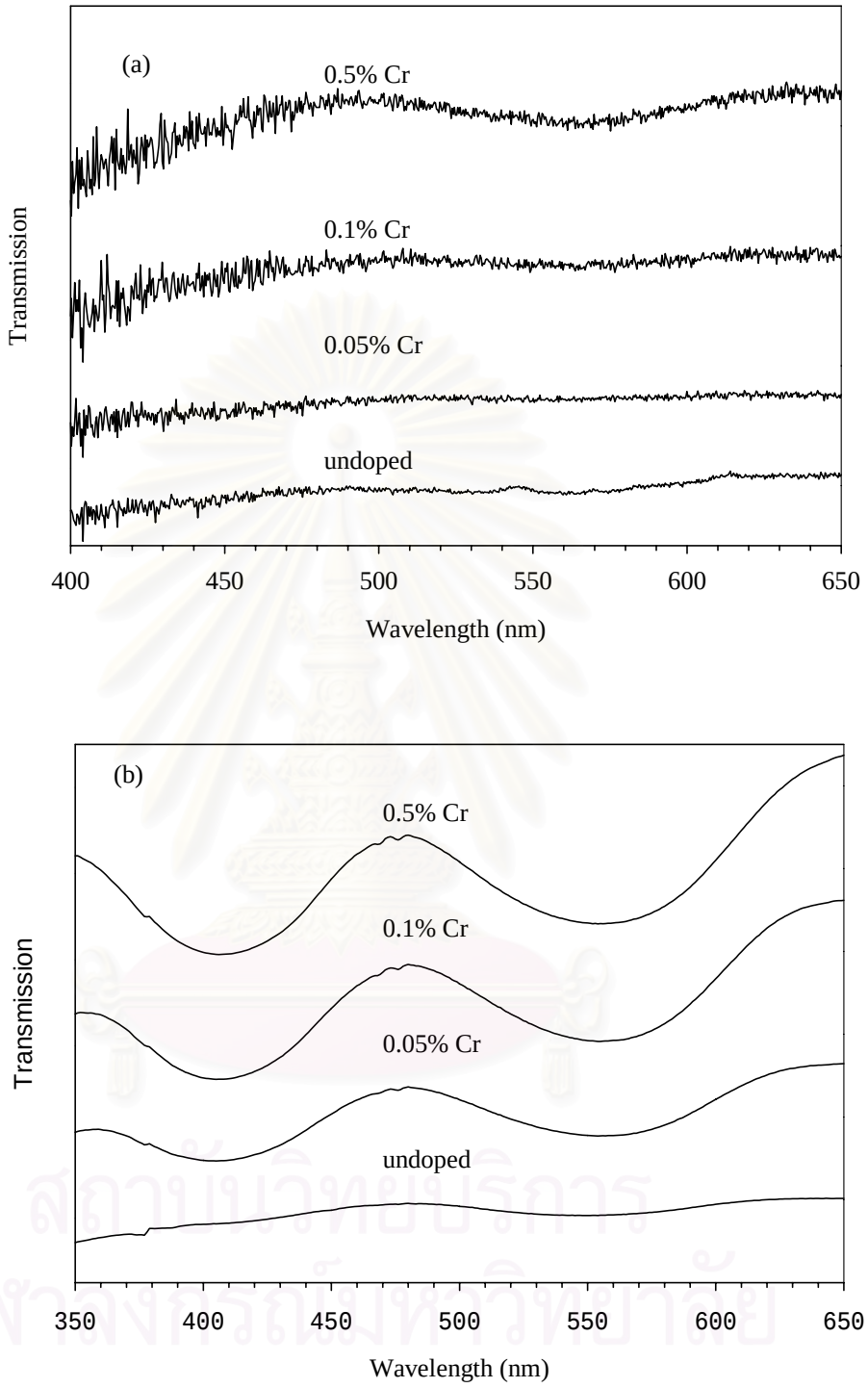

Figure 4.23 Reflective UV/visible spectra of chromium doped alumina synthesized by sol-gel method : (a) starting powder, (b) sintered specimen.

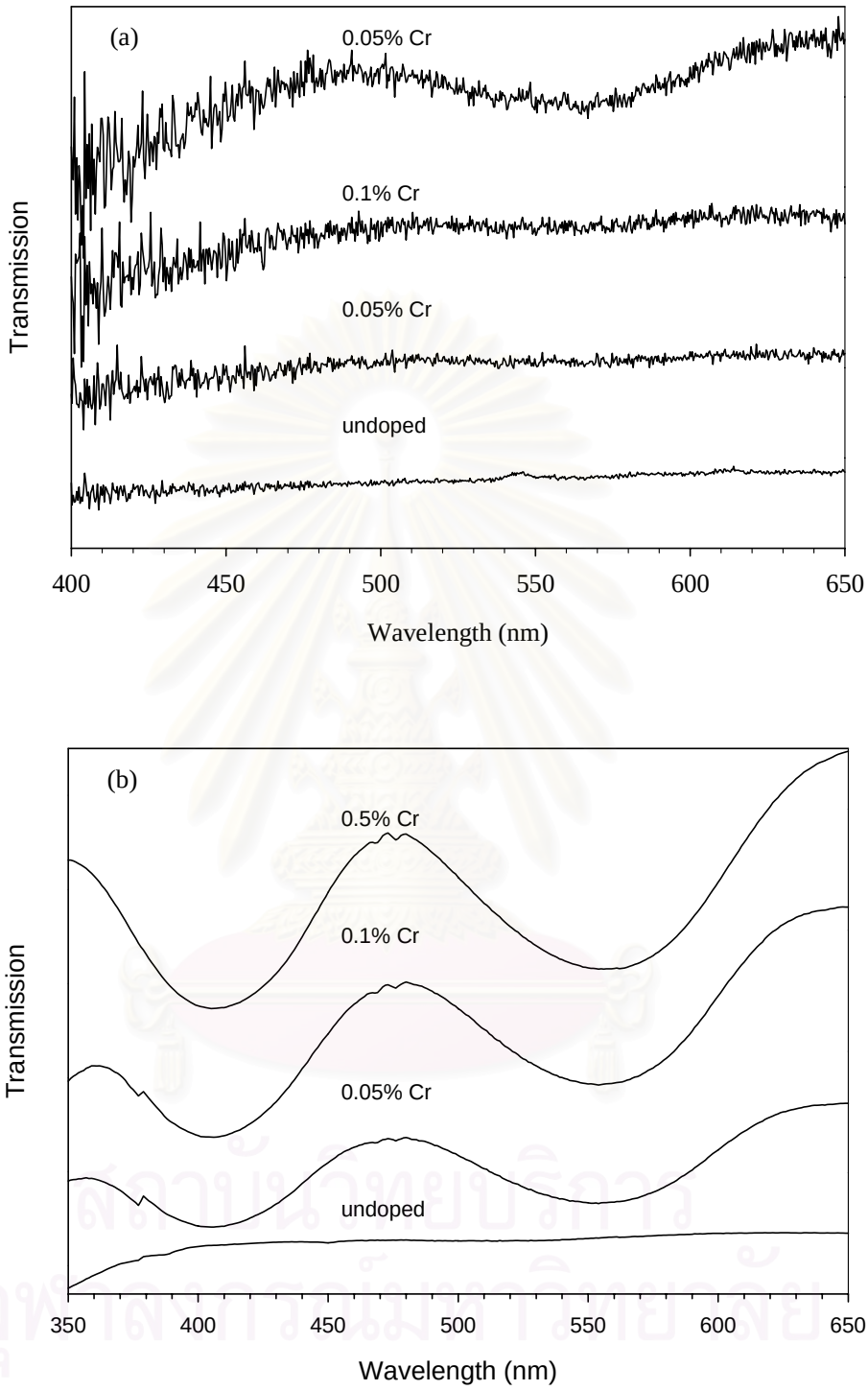

Figure 4.24 Reflective UV/visible spectra of chromium doped alumina synthesized by solvothermal method : (a) starting powder, (b) sintered specimen.

Figure 4.22 shows the comparison between the reflective UV/Visible spectra of the starting powder and the fabricated specimen, using precipitation method. It can be seen that the transmission peaks appear at wavelength around 480 and 650 nm, which result mainly in the blue and red color, regardless of the amount of chromium doped. These peaks are more apparent from the sintered specimens. It is also found that, at different concentration of chromium precursor, the intensities of the transmission peak, i.e. color of the specimen, are different. Therefore, high content of chromium results in more intense color of the specimen without changing the shade of color. Higher intensity is due to the incorporation of higher amount of Cr ions to the alumina lattice. This supports the findings from ESR spectra that higher intensity of Cr^{3+} signal in ESR spectra is detected after doping with higher content of chromium. The same observation is also found in alumina synthesized by sol-gel (Figure 4.23) and solvothermal (Figure 4.24). The UV/Visible spectra in Figure 4.22-4.24 confirm that the apparent color of Cr-doped alumina in fabricated form and in powder form are the same, since the same transmission ranges are detected. Nevertheless, the intensity of the fabricated sample is higher than the starting powder because of the densification, which brings colored grains close together.

Transparency of specimen sintered in air is also investigated by measuring transmission of light at different wavelength through thin pellet of fabricated sample. The transmittance of the undoped and 0.5% Cr-doped alumina specimens sintered in air are shown in Figure 4.25-4.26, respectively.

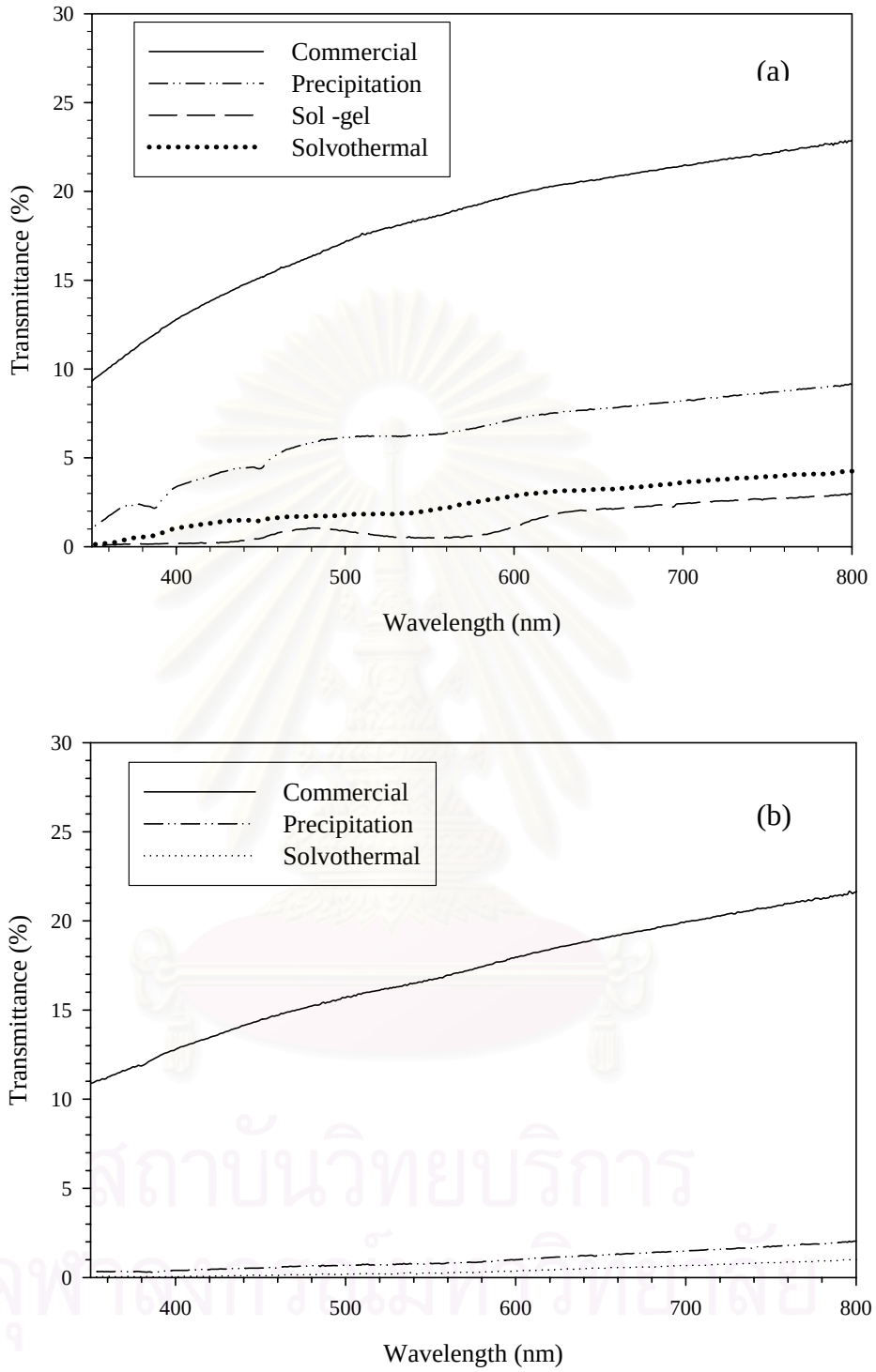

Figure 4.25 Transmittance of undoped alumina specimens prepared from alumina powder synthesized by various techniques :
(a) sintered in air, (b) sintered in air and HIP.

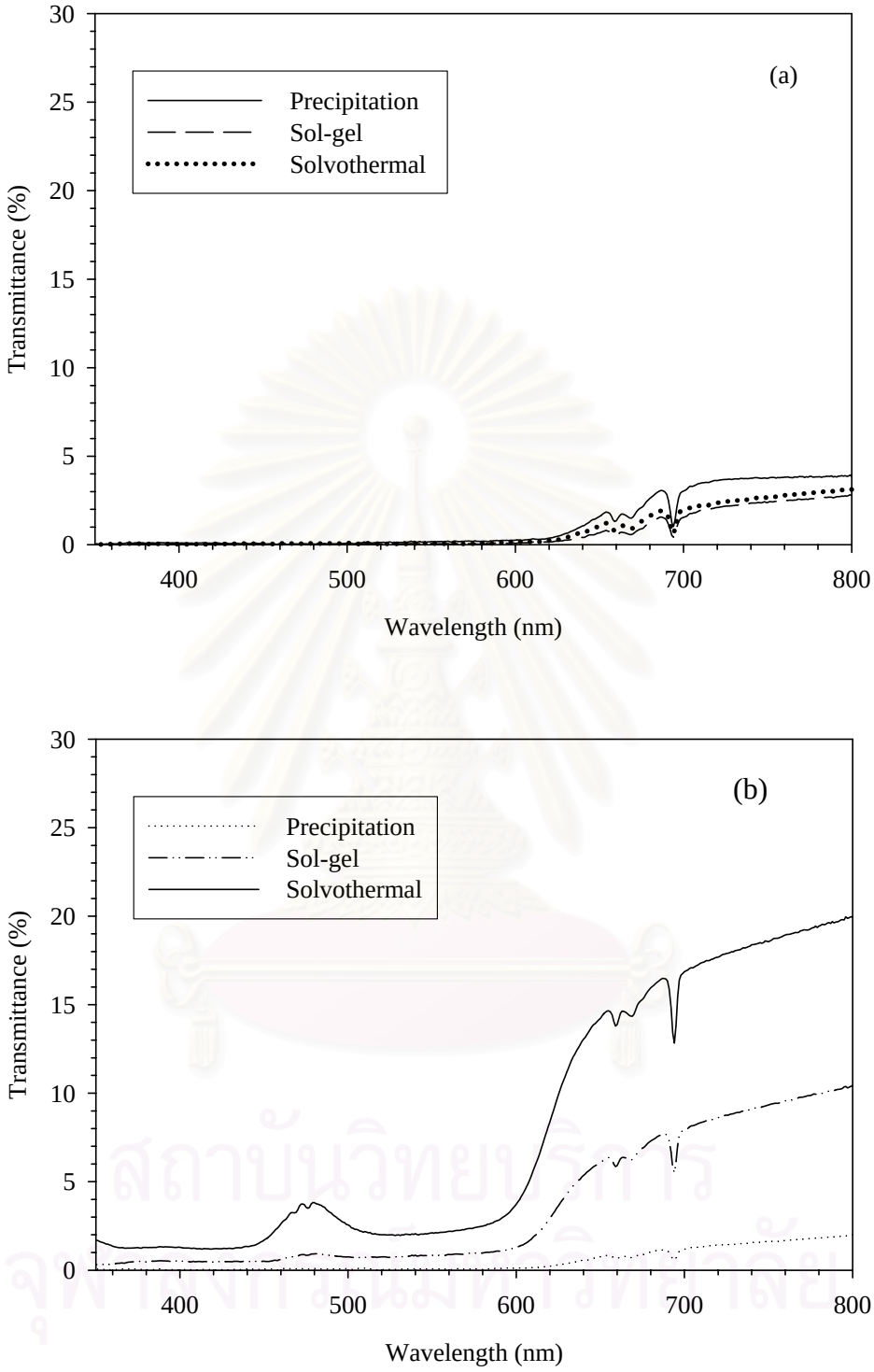

Figure 4.26 Transmittance of specimens fabricated from alumina powder doped with 0.5 wt% chromium precursor prepared by various techniques : (a) sintered in air, (b) sintered in air and HIP.

According to Figure 4.25, for undoped alumina, it is apparent that the transmittance of the commercial alumina is the highest because of the highest bulk density as reported in Table 4.10. Although the specimen is far from becoming transparent, its light transmittance is much higher than sample prepared from precipitation, solvothermal and sol-gel method, respectively. It should be noted that bulk density of sample fabricated from alumina synthesized by precipitation method is not significantly different than that of commercial powder. Yet, the transmittance of the sample prepared from precipitation technique is much lower than that of the commercial alumina. Therefore, bulk density is not a sole factor responsible for the transparency of the specimen. Grain size is also very important. Large grain size allow only slight transmission of light through the material, which makes the specimen semi-translucent. No object can be seen through this specimen.

Considering transparency of the fabricated Cr-doped alumina, the transmittance of sample from precipitation is higher than those from solvothermal and sol-gel methods, because the sample has higher bulk density. However, the value of transmittance is incomparable to that from undoped alumina. This behavior can be explained from the fact that chromium may act as the initiation site for rapid growth during sintering at high temperature, which results in large grain size of specimen. As mentioned that the large grain size cause low light transmission and give the sample lower transmittance as compared with specimen shown in Figure 4.26.

After pressing all chromium-doped samples by HIP, the transmittance is increased. The transmittance of sample from solvothermal method is higher than those from sol-gel and precipitation method, respectively because crystals from solvothermal are tightly packed which can cause the lower grain growth when compare with other methods. In the contrary, the sample from precipitation is loosely packed, which result in rapid grain growth and make it appears in lower transmittance.

CHAPTER V

CONCLUSIONS AND RECOMMENDATIONS

5.1 Conclusions

In this work, preparation of α-alumina using various techniques, doping of chromium ions into alumina during preparation procedure, the effect of chromium ion on alumina structure and density of fabricated sample are investigated. The conclusion can be drawn as follows:

1. α-alumina with nanocrystallite size can be successfully synthesized by sol-gel, precipitation and solvothermal method.

2. The secondary particle of the calcined alumina powder are soft agglomeration and can be broken off by milling. The reasonable milling time for powder from precipitation and sol-gel are 24 h while 48 h is suitable for powder from solvothermal method.

3. In precipitation technique, concentration of the reagents has no significant effect on particle size, but it affect size distribution of powder. Speed of mixing, temperature and pH of the reaction system affect both size and size distribution of powder.

4. Chromium doping into alumina matrix can be achieved in all synthesis techniques. For precipitation and solvothermal methods, chromium ions diffuse into alumina structure during calcinations procedure while, for sol-gel method, chromium ions penetrate into structure of amorphous gel during gelation step.

5. Chromium ion doping has no effect on morphology of alumina powder, although chromium resides in alumina structure as Cr^{3+}.

6. Solvothermal method is more effective in incorporating Cr^{3+} into alumina structure, comparing to precipitation and sol-gel method.

7. Semi-translucent chromium doped alumina specimen can be fabricated from alumina powder synthesized by all techniques investigated.

8. Bulk density of specimen depends on size, size distribution and particle shape of powder.

5.2 Recommendations

1. More characterization techniques such as Rietveld refinement for refining the crystalline structures, Synchrotron radiation SAXS for measuring size distribution of the crystal, and XANES spectroscopy for more precise determination of the Cr chemical state are required.

2. Phase transformation of synthesized product from precipitation and sol-gel method should be investigated.

3. Doping with other metals to study their effects on alumina structure is also recommended.

REFERENCES

1. Brinker, C.J., and Scherrer, G.W., Sol-Gel Science : The Physics and Chemistry of Sol-Gel processing : Academic Press. (1990).
2. Dawson, W.H., Journal of American Ceramic Society Bulletin. 67 (1988): 1673.
3. Deng, S.G., and Lin, Y.S., Microwave Synthesis of Mesoporous and Microporous Alumina powders. Journal of Materials Science Letters. 16 (1997): 1291.
4. Sarikaya, Y., Sevinc, I., and Akinc, M., The effect of calcinations temperature on some of the adsorptive properties of fine alumina powders obtained by emulsion evaporation technique. Powder Technology, 116 (2001): 109-114.
5. Sevinc, I., Sarikaya, Y., and Akinc, M., Adsorption characteristics of alumina powders produced by emulsion evaporation. Ceramic International. 17 (1991): 1-4.
6. Scott, W.B., and Matijevic, E., Aluminum hydrous oxide sols : III. Preparation of uniform particles by hydrolysis of aluminum chloride and perchlorate salts. Journal of Colloid and Interface Science. 66 (1978): 447.
7. Inoue, M., Kominami, H., and Inui, T., Thermal Reaction of Aluminum Alkoxide in Glycol. Journal of American Ceramic Society. 73 (1990): 1100-1102.
8. Inoue, M., Kominami, H., and Inui, T., Thermal Reaction of Aluminum Alkoxide in Various Glycols and the Layer Structure of Their Products. Journal of the Chemical Society, Dalton Transactions. (1991): 3331-3336.
9. Inoue, M., Kominami, H., Inui, T., Thermal Transformation of χ- alumina Formed by Thermal Decomposition of Aluminum Alkoxide in organic Media. Journal of American Ceramic Society. 75 (1992):2597-98.
10. Inoue, M., Kominami, H., and Inui, T., Novel Synthesis Method for The Catalytic Use of Thermally Stable Zirconia: Thermal Decomposition of Zirconium Alkoxide in Organic Media. Applied Catalyst. A 77 *(*1993): L25-L30.

11. Inoue, M., Kominami, H., and Inui, T., Novel Synthesis Method for The Thermally Stable Zirconia : Hydrolysis of Zirconium Alkoxide at High Temperature With a Limited Amount of Water Dissolved in Inert Organic Solvent from The Gas Phase. Applied Catalyst. A 121 (1995): L1-L5.
12. Inoue, M., Kominami, H., and Inui, T., Thermal Decomposition of alkoxides in an inert organic solvent : nevel method for the synthesis of homogeneous mullite precursor. Journal of American Ceramic Society. 75 (1996): 2597-98.
13. Inoue, M., Kondo, Y., and Inui, T., Ethylene Glycol Derivative of Boehmite. Inorganic Chemistry Industry. 27 (1988): 215-221.
14. Inoue, M., Otsu, H., Kominami, H., and Inui, T., Synthesis of Thermally Stable, Porous Silica-Modified Alumina Via Formation of a Precursor in an Organic Solvent. Industrial and Engineerig Chemistry Research. 35 (1996): 295-306.
15. Hugo, P., and Koch, H., Ger. Chem. Eng. 2 (1979): 24.
16. Dynys, F.W., and Hallora, J.W., Journal of American Ceramic Society. 66 (1983): 655.
17. Vogel, RF., Marcellin, G., and Kehl, W.L., The prepation of coltrolled pore alumina. Applied Catalyst. 12 (1984): 237-248.
18. Trimm, D.L., and Stainslaus, A., The control of pore size in alumina catalyst supports. Applied Catalyst. 21 (1986): 215-238.
19. Ueyama, T., Wada, H., and Kaneko, N., Journal of American Ceramic Society. 71 (1988): C-74.
20. Rajendran, S., Production of ultrafine alpha-alumina powders and frabication of fine-grained strong ceramics. Journal of Materials Science. 29 (1994): 5664.
21. Androff, N.W., Francis L.F., and Velmakanni B.V., Macroporous ceramics from ceramic polymer dispersion methods. AIChE Journal. 43 (1997): 2878-2888.
22. Hellgardt, K., and Chadwick, D., Effect of pH of precipitation on the preparation of high surface area aluminas from nitrate solutions. Industrial and Engineering Chemistry Research. 37 (1998): 405-411.
23. Fremy, E., and Feil, E. Comp.rend 85 (1877): 1029.
24. Kronberg M.L., Plastic deformation of Single crystals of sapphire. Acta Materialia. 5 (1957): 507-524.

25. Lippens, B. D. and J. H. De. Boer ., Study of phase transformations during calcination of aluminum hydroxides by selected area electron diffraction. Acta Crystallography. 17 (1964) :1312.

26. Wilson, S. J., Phase transformations and development of microstructure in-derived transition aluminas. Proceedings of the British Ceramic Society. 28 (1979) : 281-94.

27. Gitzen W.H., Alumina as a ceramic material. 1970.

28. Dynys, F.W., and Halloran, J.W., Alpha alumina Formation in Alum-Derived Gamma Alumina. Journal of American Ceramic Society. 65 (1982): 442-448.

29. Simpson, T.W., Wen, Q.Z., YU, N., and Clarke, D.R., Kinetics of the Amorphous - > γ - > α Transformation in Aluminum oxide : Effect of Crystallography Orientation. Journal of American Ceramic Society. 1998, 81:1995.

30. Levin, I., and Brandon, D., Metastable Alumina Polymorph: Crystal Structures and Transition Sequences. Journal of American Ceramic Society. 81 (1998): 61.

31. Morinaga, K., Torikai, T., Nakagawa, K., and Fujino, S., Fabrication of fine α-alumina powders by thermal decomposition of ammonium aluminum carbonate hydroxide(AACH). Acta Materialia. 48 (2000): 4735-4741.

32. Mekasuwandumrong, O., Silveston, P.L., Praserthdam, P., Inoue, M., Pavarajarn, V., and Tanakulrungsank, W., Synthesis of thermally stable micro spherical χ-alumina by thermal decomposition of alumina isopropoxide in mineral oil. Inorganic Chemistry Communications. 6 (2003): 930-934.

33. Aegerter, M.A., Jafelicci Jr, M. Souza, D.F., and Zanotto, E.D., SOL-GEL SCIENCE and TECHNOLOGY. World Scientific.

34. Ertl, G., Knozinger, H., and Weitkamp, J., Preparation of Solid Catalysts. Wiley-VCH. (1997).

35. Yoldas, B.E., Journal of Applied Chemistry and Biotechnology. 23 (1973): 803-809.

36. Yoldas, B.E., Journal of Materials Science. 10 (1975): 1856-1860.

37. Wakao, Y., and Hibbino, T., Effect of Metallic Oxides on Alpha Transformation of Alumina. Nagoya Hogyo Gijutsu Shikensko Hokoku 11 (1962): 588-95.

38. Bye, G.C., and Simkin, G.T., Effect of Cr and Fe on Formation of α-Al_2O_3 from γ- Al_2O_3. Journal of American Ceramic Society. 57 (1974): 367-71.

39. Okada, K., Hattori, A., Tanigushi, T., Nikui, A., and Das, R.N., Effect of Divalent Cation Additives on the γ- $Al_2O_3$to α-Al_2O_3 Phase Transition. Journal of American Ceramic Society. 83 (2000): 928-32.

40. Kumagai, M., and Messing G.L., Controlled Transformation and sintering of a Boehmite Sol-Gel by α-alumina Seeding. Journal of American Ceramic Society. 68 (1985): 500-505.

41. Srdic, V., and Radonjic L., Seeded Sol-Gel Derived Alumina-Zirconia Composites. Ceramic International. 21 (1995): 5-11.

42. Kao, H.-C., and Wei, W.-C., Kinetics and Microstructural Evolution of Heterogeneous Transformation of θ-alumina to α-alumina. Journal of American Ceramic Society. 83 (2000): 362-68.

43. Han, K.R., Lim, C.S., Hong, M.J., Jan, J.W., and Hong, K.S., Preparation Method of Submicrometer-Sized α- alumina by Surface Modification of γ-alumina with Alumina Sol. Journal of American Ceramic Society. 83 (2000): 750-54.

44. Resgui, S., and Gates,B.C., Control of Magnesia-Alumina Properties by Acetic Acid in Sol-Gel Synthesis. J. Non-Crystalline Solids. 210 (1997): 287-97.

45. Nair, J., Nair, P., Ommen, J.G.V., Ross, J.R.H., Burggraaf, A.J., and Mizukami, F., Influence of Peptization and Ethanol Washing in the Pore-Structure Evolution of Sol-Gel-Derived Alumina Catalyst Supports. Journal of American Ceramic Society. 81(1998): 2709-12.

46. Yoldas, B.E., Effect of Variations in Polymerized Oxides on Sintering and Crystalline Transformations. Journal of American Ceramic Society. 65 (1982): 387-393.

47. Tsay, C.S., Lee, C.K., and Chiang, A.S.T., The Fractal and Percolation Analysis of a Polymeric alumina gel. Chemical Physics Letters. 278 (1997): 83-90.

48. Masalski, J., Gluszek, J., Zabrzeski, J., Nitsch, K., and Gluszek,P., Improvement in corrosion resistance of the 3161 stainless steel by means of alumina coatings deposited by the sol-gel method. Thin Solid Films. 349 (1999): 186-90.

49. Bahlawane, N., and Watanabe, T., New Sol-Gel Route for the Preparation of Pure α-Alumina at 950^{o}C. Journal of American Ceramic Society. 83 (2000): 2324-26.

50. Lin, C.-P., Wen, S.-B., and Lee, T.-T., Preparation of Nanometer-Sized α-alumina Powders by Calcining an Emulsion of Boehmite and Oleic Acid. Journal of American Ceramic Society. 85 (2002): 129-33.

51. Buelna, G., Lin, YS., Sol-gel mesoporous γ-alumina granules. Microporous and Mesoporous Materials. 30 (1999):359-369.

52. Hen, P.-, L., and Chen, J.-W., Reactive Cerium (IV) Oxidase Powders by the Homogeneous Precipitation Method. Journal of American Ceramic Society. 76 (1993): 1577.

53. Nagai, H., Oshima, Y., Hirano, K., and Kato, A., Sintering Behavior of Aluminum-oxide Derived from Aluminum Hydroxides with Various Morphologies. British Ceramic Society. 93 (1993): 114.

54. Nagai, H., Oshima, Y., Hirano, and K., Kato, A., Synthesis of Aluminium Hydroxide by a Homogeneous Precipitation Method. I. Effect of Additives on the Morphology of Aluminium Hydroxide. Transactions of the British Ceramic Society. 90 (1991): 44.

55. Ertl, G., Knozinger, H. and Weitkamp, J., Preparation of Solid Catalysts. Wiley-VCH. (1997).

56. Shuzo, K., Takeo, I., Shogo, H., and Yuichi, I., Method for manufacture of sintered alumina from ammonium aluminum carbonate hydroxide. U.S. Patent : 45053579. (1975).

57. Dorre, E., and Hubner,H. Alumina, Processing, Properties, and Applications. Springer-Verlag. (1984).

58. Smith, F. Principles of materials science and engineering. McGraw-Hill. (1996).

59. Brophy, J.H., Rose, R.M., and Wulff, J., The structure and Properties of Materials. Wiley. (1964).

60. Wong, B., and Pask,J.A., Journal of American Ceramic Society. 62 (1979): 141-144.

61. Rahaman ,M., Ceramic processing and sintering. Marcle Dekker. (1995).

62. Hughes, R.W., Ruby & Sapphire. RWH. (1997).

63. Fritsch, E. and Rossman, G.R. (1987, 1988), An update on color in gems. Gems & Gemology ; Part I : Introduction and colors caused by dispersed metal ions. 23, No.3 :126-139; Part II : Colors involving multiple atoms and color centers. 24 No.1: 3-15; Part III : Colors caused by band gaps and physical phenomena. 24 No.2 :81-103. RWHL.

64. Schmetzer, K., Zur deutung der farbursache blauer Saphire-Einc discussion. Neues Jahrobuch für Mineralogie. Monatshefte. No.8: 337-343.

65. Ferguson, J.C., and Fielding, P.E., The origins of the colours of natural yellow, blue and green sapphires. Australian Journal of Chemistry. 25 (1972): 1371-1385.

66. Emmett, J.L., and Douthit, T.R., Heat treating the sapphires of Rock Creek, Montana. Gems & Gemology. 29 (1993): 250-272.

67. Nassau, K., and Valente ,K., The seven types of yellow sapphire and their stability to light. Gems & Gemology. 23 (1987): 222-231.

68. Koivula,J.I., Internal diffusion. Journal of Gemmology. 20 (1987): 474-477.

69. Nassau,K., Gems Made by Man. Chilton. (1980).

70. Schmetzer, K., and Bank ,H., Explanation of the absorption spectra of natural and synthetic Fe- and Ti containing corundums. Neues Jahrbuch fur Mineralogic. 139 (1980): 216-225.

71. Weibel, M., and Wessicken, R., Hamatit als Einschluss im schwarzen Sternsaphir. Zeitschrift der Deutschen Gemmologischen Gesellschaft. 30 (1981): 170-176.

72. Webster ,R., GEMS Their sources, Descriptions and identification. (1994).

73. Ballman ,A.A., Method of Growing Corundum Crystals. (1961).

74. López-Navarrete, E., Gonzălez-Elipe, AR., Ocaňa, M., Nonconventional synthesis of Cr-doped SnO_2 pigments. Ceramic International. 29 (2003) : 385-392.

75. López-Navarrete, E., Ocaňa, M., A simple procedure for the preparation of Cr-doped tin sphene pigments in the absence of fluxes. Journal of the European Ceramic Society. 22 (2002): 353-359.

76. López-Navarrete, E., Caballero, A., Gonzălez-Elipe, AR., Ocaňa, M., Low temperature preparation and structural characterization of Pr-doped ceria solid solution. Journal of Materials Research. 17 (2002) : 797-804.

77. López-Navarrete, E., Caballero, A., Gonzălez-Elipe, AR., Ocaňa, M., Chemical state and distribution of Mn ions in Mn-doped alpha-Al_2O_3 solid solution prepared in the absence and the presence of fluxes. Journal of the European Ceramic Society. 24 (2003) : 3057-3062.

78. Ma, C-C., Zhou, X-X., Xu, X., Zhu, T., Synthesis and thermal decomposition of ammonium aluminum carbonate hydroxide (AACH). Material Chemistry and Physics. 72 (2001) : 374-379.

APPENDICES

APPENDIX A

CALCULATION OF CONCENTRATION OF BOTH REACTANTS IN PRECIPITATION METHOD

In this study, ammonium aluminum carbonate hydroxide ($NH_4AlCO_3(OH)_2$) has been produced by the reaction of ammonium aluminum sulfate solution (AAS solution) and ammonium hydrogencarbonate solution (AHC solution) as following equation :

$$8NH_4HCO_3 + 2(NH_4)\,Al\,(SO_4)_2 \longrightarrow 2NH_4AlCO_3(OH)_2 + 4(NH_4)_2SO_4 + 6CO_2 + 2H_2O$$

Ammonium aluminum carbonate hydroxide(AACH) was prepared with the molar ratio of AAS solution to AHC solution equal to 1:4 as the above reaction and calculation procedure is given here.

Calculation of the amount of ammonium hydrogencarbonate (AHC) and ammonium aluminum sulfate (AAS) for AACH preparation

Ammonium aluminum sulfate (AAS) and ammonium hydrogencarbonate (AHC) are used as reactants to prepare AACH.

10. Ammonium aluminum sulfate ($NH_4Al(SO_4)_2.12H_2O$) has an molecular weight of 237.18 g/mol (not included molecule of water)
11. Ammonium hydrogencarbonate (NH_4HCO_3) has an molecular weight of 79.06 g/mol.

Example : Calculation of AACH preparation with concentration of AAS solution to AHC solution equal to 0.2 : 2.0 mol/l and molar ratio of AAS solution to AHC solution is 0.05 : 0.2 , which is equal to 1:4 as mentioned before, are as following :

AAS solution 0.05 mol consists of :

AAS 0.05 x 237.18 = 11.859 g

To get concentration 0.2 mol/l

Distilled water = 250 cm^3

AHC solution 0.2 mol consists of :

AHC 0.2 x 79.06 = 15.812 g

To get concentration 2.0 mol/l

Distilled water = 100 cm^3

APPENDIX B

CALCULATION OF AMOUNT OF CHROMIUM PRECURSOR FOR CHROMIUM DOPED ALUMINA

For precipitation and sol-gel method, Chromium (III) nitrate nonahydrate was used as chromium precursor and Chromium (III) acetylacetonate was employed in solvothermal method as chromium precursor.

Reagents : Ammonium aluminum sulfate ($NH_4Al(SO_4)_2.12H_2O$)
Molecular weight = 237.18 g/mol
(not included molecule of water)
Aluminium nitrate nonahydrate ($Al(NO_3)_3.9H_2O$)
Molecular weight = 212.98 g/mol
Aluminum isopropoxide ($((CH_3)_2CHO)_3Al$)
Molecular weight = 203.98 g/mol

Precursors : Chromium (III) nitrate nonahydrate ($Cr(NO_3)_3.9H_2O$)
Molecular weight = 238 g/mol (do not include H_2O molecule)
Chromium (III) acetylacetonate ($(CH_3COCHCOCH_3)_3Cr$)
Molecular weight = 349.33 g/mol

Calculation :

Precipitation method

From Appendix A, concentration of AAS solution to AHC solution equal to 0.2 : 2.0 mol/l and molar ratio of AAS solution to AHC solution is 0.05 : 0.2, then AAS 11.859 g was required.

- For 0.05% Chromium precursor/Aluminium precursor
  Chromium (III) nitrate nonahydrate = (0.05/100) x 11.859 = 5.9295×10^{-3} g consisted of chromium equal to :
  Chromium = (52/238) x 5.9295×10^{-3} = 1.2955×10^{-3} g = 2.4914×10^{-5} mol
  AAS 11.859 g consisted of aluminium equal to :
  Aluminium = (26.98/237.18) x 11.859 = 1.349 g = 0.05 mol

The mol ratio of Cr/Al = $2.4914 \times 10^{-5}/0.05 = 4.9828 \times 10^{-4}$

= 0.05 mol % Cr/Al

- For 0.1% Chromium precursor/Aluminium precursor

  Chromium (III) nitrate nonahydrate = (0.1/100) x 11.859 = 0.011859 g

  consisted of chromium equal to :

  Chromium = (52/238) x 0.011859 = 2.5910×10^{-3} g = 4.9828×10^{-5} mol

  AAS 11.859 g consisted of aluminium equal to :

  Aluminium = (26.98/237.18) x 11.859 = 1.349 g = 0.05 mol

  The mol ratio of Cr/Al = $4.9828 \times 10^{-5}/0.05 = 9.9655 \times 10^{-4}$

  = 0.1 mol % Cr/Al

- For 0.5% Chromium precursor/Aluminium precursor

  Chromium (III) nitrate nonahydrate = (0.5/100) x 11.859 = 0.059295 g

  consisted of chromium equal to :

  Chromium = (52/238) x 0.059295 = 0.01296 g = 2.2914×10^{-4} mol

  AAS 11.859 g consisted of aluminium equal to :

  Aluminium = (26.98/237.18) x 11.859 = 1.349 g = 0.05 mol

  The mol ratio of Cr/Al = $2.2914 \times 10^{-4}/0.05 = 4.9828 \times 10^{-3}$

  = 0.5 mol % Cr/Al

Solgel method

For sol-gel method, 24.0729 g of Aluminium nitrate nonahydrate was used as aluminium precursor.

- For 0.05% Chromium precursor/Aluminium precursor

  Chromium (III) nitrate nonahydrate = (0.05/100) x 24.0729 = 0.012 g

  consisted of chromium equal to :

  Chromium = (52/238) x 0.012 = 2.6218x 10^{-3} g = 5.042 x 10^{-5} mol

  Aluminium nitrate nonahydrate 24.0729 g consisted of aluminium equal to :

  Aluminium = (26.98/212.98) x 24.0729 = 3.0495 g = 0.1130 mol

  The mol ratio of Cr/Al = 5.042x 10^{-5}/0.1130 = 4.4619 x 10^{-4}

  = 0.045 mol % Cr/Al

- For 0.1% Chromium precursor/Aluminium precursor

  Chromium (III) nitrate nonahydrate = (0.1/100) x 24.0729 = 0.0240729 g

  consisted of chromium equal to :

  Chromium = (52/238) x 0.0240729 = 5.2596 x 10^{-3} g = 1.0115 x 10^{-4} mol

  Aluminium nitrate nonahydrate 24.0729 g consisted of aluminium equal to :

  Aluminium = (26.98/212.98) x 24.0729 = 3.0495 g = 0.1130 mol

  The mol ratio of Cr/Al = 1.0115 x 10^{-4}/0.1130 = 8.9510 x 10^{-4}

  = 0.09 mol % Cr/Al

- For 0.5% Chromium precursor/Aluminium precursor

  Chromium (III) nitrate nonahydrate = (0.5/100) x 24.0729 = 0.1203645 g

  consisted of chromium equal to :

  Chromium = (52/238) x 0.1203645 = 0.026298 g = 5.0573 x 10^{-4} mol

  Aluminium nitrate nonahydrate 24.0729 g consisted of aluminium equal to :

  Aluminium = (26.98/212.98) x 24.0729 = 3.0495 g = 0.1130 mol

  The mol ratio of Cr/Al = 5.0573 x 10^{-4} /0.1130 = 4.4755 x 10^{-3}

  = 0.45 mol % Cr/Al

Solvothermal method

Aluminum isopropoxide 25 g was used as aluminium precursor while Chromium (III) acetylacetonate was used as chromium precursor.

- For 0.05% Chromium precursor/Aluminium precursor
  Chromium (III) acetylacetonate = (0.05/100) x 25 = 0.0125 g
  consisted of chromium equal to :
  Chromium = (52/349.33) x 0.0125 = 1.8607×10^{-3} g = 3.5783×10^{-5} mol
  Aluminum isopropoxide 25 g consisted of aluminium equal to :
  Aluminium = (26.98/203.98) x 25 = 3.30669 g = 0.12256 mol
  The mol ratio of Cr/Al = $3.5783 \times 10^{-5}/0.12256 = 2.9196 \times 10^{-4}$
  = 0.03 mol % Cr/Al

- For 0.1% Chromium precursor/Aluminium precursor
  Chromium (III) acetylacetonate = (0.1/100) x 25 = 0.025 g
  consisted of chromium equal to :
  Chromium = (52/349.33) x 0.025 = 3.7214×10^{-3} g = 7.1566×10^{-5} mol
  Aluminum isopropoxide 25 g consisted of aluminium equal to :
  Aluminium = (26.98/203.98) x 25 = 3.30669 g = 0.12256 mol
  The mol ratio of Cr/Al = $7.1566 \times 10^{-5}/0.12256 = 5.8392 \times 10^{-4}$
  = 0.06 mol % Cr/Al

- For 0.5% Chromium precursor/Aluminium precursor
  Chromium (III) acetylacetonate = (0.5/100) x 25 = 0.125 g
  consisted of chromium equal to :
  Chromium = (52/349.33) x 0.125 = 0.0186 g = 3.5783×10^{-4} mol
  Aluminum isopropoxide 25 g consisted of aluminium equal to :
  Aluminium = (26.98/203.98) x 25 = 3.30669 g = 0.12256 mol
  The mol ratio of Cr/Al = $3.5783 \times 10^{-4}/0.12256 = 2.9196 \times 10^{-3}$
  = 0.3 mol % Cr/Al

APPENDIX C

CALCULATION OF THE CRYSTALLITE SIZE

Calculation of the crystallite size by Debye-Scherrer equation

The crystallite size was calculated from the half-height width of the diffraction peak of XRD pattern using the Debye-Scherrer equation.

From Scherrer equation:

$$D = \frac{K\lambda}{\beta \cos \theta} \qquad \text{(C.1)}$$

where D = Crystallite size, Å

K = Crystallite-shape factor = 0.9

λ = X-ray wavelength, 1.5418 Å for CuKα

θ = Observed peak angle, degree

β = X-ray diffraction broadening, radian

The X-ray diffraction broadening (β) is the pure width of a powder diffraction free from all broadening due to the experimental equipment. α-Alumina is used as a standard sample to observe the instrumental broadening since its crystallite size is larger than 2000 Å. The X-ray diffraction broadening (β) can be obtained by using Warren's formula.

From Warren's formula:

$$\beta = \sqrt{B_M^2 - B_S^2} \qquad \text{(C.2)}$$

Where B_M = The measured peak width in radians at half peak height.

B_S = The corresponding width of the standard material.

Example: Calculation of the crystallite size of α-alumina

The half-height width of 012 diffraction peak = 0.88^o (from the figure C.1)

= $(2\pi x 0.88)/360$

= 0.0154 radian

The corresponding half-height width of peak of α-alumina (from the Bs value at the 2θ of 25.92^o in figure C.2) = 0.0041 radian

The pure width, $\beta = \sqrt{B_M^2 - B_S^2}$

$= \sqrt{0.0154^2 - 0.0041^2}$

= 0.0148 radian

B = 0.0148 radian

2θ = 25.92^o

θ = 12.96

λ = 1.5418 Å

The crystallite size $= \frac{0.9x1.5418}{0.0148\cos 12.96}$ = 96.21 Å = 9.62 nm

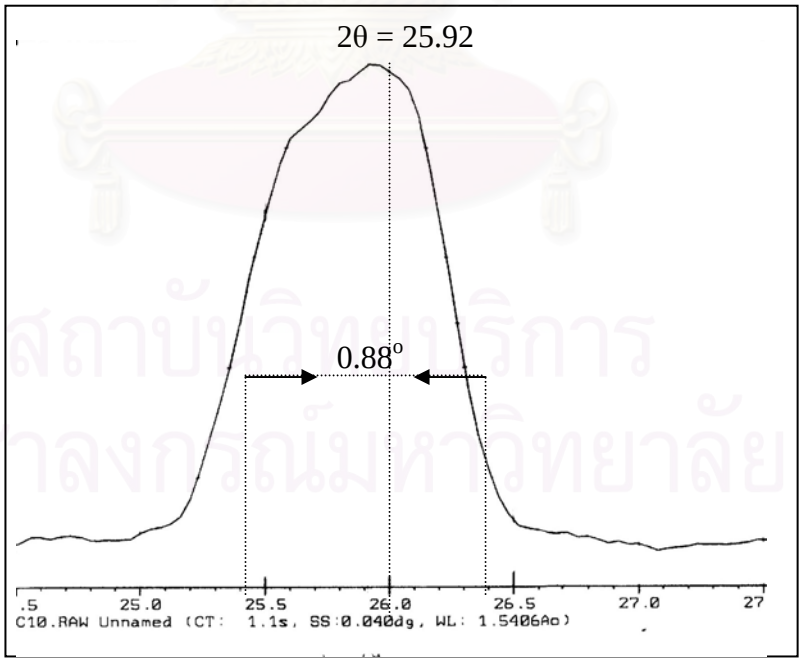

Figure C.1 The observation peak of α-alumina for calculating the crystallite size.

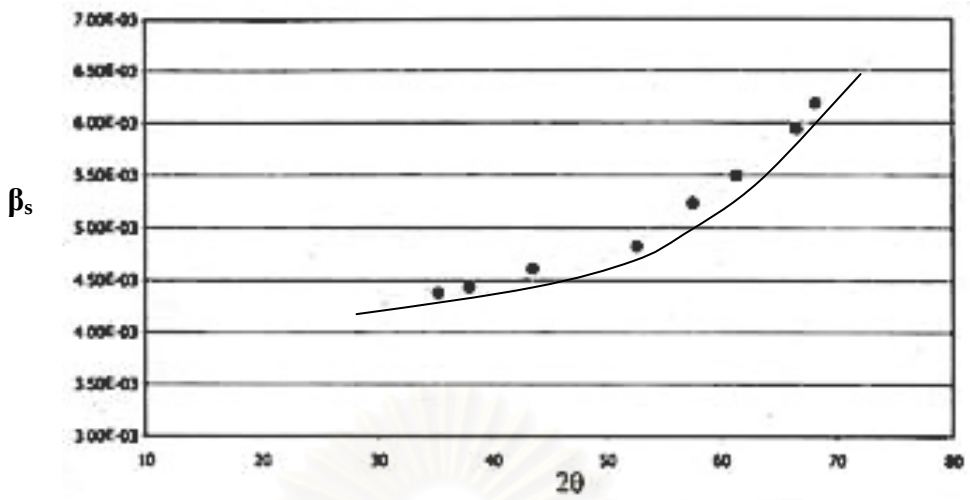

Figure C.2 The graph indicating that value of the line broadening attribute to the experimental equipment from the α-alumina standard.

APPENDIX D

CONDITIONS FOR BALL MILL AND DISPERSION OF POWDER

Ball mill

The particles size can be reduced a by breaking some soft agglomeration of powders by using polypropylene bottle and high purity alumina balls.

Place high purity alumina ball 362 g or half of bottle, alumina powder, and ethanol solution 100 cc into the polypropylene bottle which has volume 250 cc. Mill this bottle with rotating speed 150 rpm at desired time. After milling with ball mill, filter the solution of powder and dry in the oven at 100^{o}C for 24 h.

Dispersion of powder

Before measuring a particle size distribution of alumina powder, all powders should to be dispersed by following steps :

1. Preparation of dispersion solution with concentration 0.2 wt% by dissolving NaHMP (Sodium Hexa Methaphosphate) 0.2 g in distilled water 99.8 g.
2. Use this solution 50 cc for 0.5 g of powder, then mix this solution with magnetic stirrer for 30 minutes.

After mixing by magnetic stirrer, pour the solution into a bottle and sealed with para-film and place it into ultrasonic apparatus for 30 minutes before measuring their particle size distribution by using Laser Particle Size Distribution Analyzer.

APPENDIX E

DENSITY

- **Bulk density**

The bulk density of specimens was measured according to Archimedes' method. The air in open pores of specimen was removed by applying vacuum for 30 min and then water was poured onto specimens until submerged in water. Water was further forced into the opened pores by applying vacuum for 2 h. The dry weight W_d were measured and used to calculate the bulk density using equation (E.1) following ASTM standard (Designation : C830-93).

$$\text{Bulk density} = \frac{W_d}{W_{sat} - W_{sus}}\,\rho \qquad \text{(E.1)}$$

Where ρ is water density at the measurement temperature (0.996512 g/cm^3 at 27^{o}C)

- Theoretical density

The theoretical density of sintered pellets was calculated from real density using

the following equation ;

$$\text{Theoretical density} = \frac{W_{total}}{W_a/\rho_a + W_b/\rho_b + \ldots} \qquad \text{(E.2)}$$

Where W_{total} is total weight of used components.

W_a, W_b are weights of component, a and b, respectively.

ρ_a, ρ_b are real densities of component, a and b, respectively.

a, b,….. are used components.

In this experiment, the theoretical densities of pure Al_2O_3 = 3.98 g/cm^3 was used for calculation.

- Relative density

The relative density of the sintered specimens was calculated from its bulk density and theoretical density using the following equation :

$$\text{Relative density} = \frac{\text{Bulk density}}{\text{Theoretical density}} \qquad \text{(E.3)}$$

And % of theoretical density = Relative density x 100

LIST OF PUBLICATION

1. Tanitta Prasitwuttisak, Varong Pavarajarn, and Piyasan Praserthdam, “Comparative study of Nanoscaled Alumina and Chromium Doped Alumina Powder Prepared from Various Synthesis Techniques”, Proceedings of the Regional Symposium on Chemical Engineering 2004, Bangkok, Thailand, Dec. 1-3, 2004, Ref. No. LM-323.

Comparative Study of Nanoscaled Alumina and Chromium Doped Alumina Powders Prepared from Various Synthesis Techniques

Tanitta Prasitwuttisak, Varong Pavarajarn and Piyasan Praserthdam*
Center of Excellence on Catalysis and Catalytic Reaction Engineering, Department of Chemical Engineering, Faculty of Engineering, Chulalongkorn University, Bangkok 10330 Thailand
** Corresponding author (Tel: +66-02-2186890, Fax: +66-02-2186877, Email: fchvpv@eng.chula.ac.th)*

ABSTRACT

physical properties of nanoscaled alumina particles prepared by various techniques, i.e. sol-gel, precipitation and solvothermal method are investigated. Alumina obtained from these methods can be transformed to α-phase by heat treatment at 1150°C. It was found that the products from the sol-gel, precipitation and solvothermal method were nanoscaled alumina particles having crystallite size of 9.52, 9.65 and 9.74 nm, respectively. These methods are also employed for the preparation of chromium-doped alumina in various chromium concentrations, from 2 to 10% w/w. Heat treatment of the obtained samples results in wide range of red-colored alumina, which suggests different amount of chromium ions doped in α-alumina matrix. The samples were characterized by using X-ray diffraction (XRD), particle size distribution analyzer, scanning electron microscopy (SEM) and UV-Visible spectroscopy.

Keywords: Sol-gel, precipitation, solvothermal, alumina, chromium doped

INTRODUCTION

The α-alumina (α-Al_2O_3) is widely used in ceramics industry. It is one of the most stable crystalline phases of alumina, which has the highest density and high melting point (2050°C) [1]. Many techniques have been developed to synthesize alumina powders with required characteristics, such as sol-gel method, hydrothermal method, microwave synthesis, emulsion evaporation, precipitation from solution and solvothermal method.

It is well known that ruby is the single crystal of Al_2O_3 including small amount of chromium impurities. Such precious stone could not only be fabricated naturally but also synthesized artificially. Incorporation of chromium ions into the Al_2O_3 network at different oxidation states would results in wide range of colored alumina. In this work, nanoscaled alumina particles were prepared by sol-gel, precipitation and solvothermal method. These methods are also employed to synthesize of chromium-doped alumina containing different amounts of Cr in the range of 2-10 % w/w. The objective of this work is to investigate properties of chromium-doped alumina prepared from different synthesis techniques.

EXPERIMENTAL

For sol-gel method, aluminium nitrate nonahydrate was dissolved in ethanol at room temperature. The solution was then heated to 70-80°C in the reflux-condenser, after which urea solution was added to adjust pH to neutral for gellation. For Cr-doped alumina, chromium nitrate nonahydrate added to aluminium nitrate solution. Chromium concentration investigated was in the range of 2 to 10% w/w.

In precipitation method, ammonium aluminium sulfate and ammonium hydrogen carbonate aqueous solution in various concentration were gradually added together at temperature in the range of 40-45°C. White precipitates formed were separated from the solution. For Cr-doped alumina, chromium nitrate nonahydrate used as chromium source was added into ammonium aluminium sulfate solution.

Finally for solvothermal method, aluminum isopropoxide 25 g was suspended in 100 ml mineral oil in a test tube, which was then placed in autoclave. The autoclave was purged completely by nitrogen before heating up to the desired temperature at a rate of 2.5°C/min and holding at that temperature for 2 hours. After the system was cooled down, the resulting powders were repeatedly washed with acetone and dried in air. In this method chromium acetylacetonate was employed as chromium source, since chromium nitrate is insoluble in mineral oil.

The as-synthesized powders from all techniques were then calcined in a box furnace at 1150°C for 3 hours to transform the synthesized product to α-alumina. The calcined products were characterized by using X-ray diffraction (XRD), particle size distribution analyzer, scanning electron microscopy (SEM) and UV-Visible spectroscopy.

RESULTS AND DISCUSSION

The XRD analysis of synthesized products shows that although the as-synthesized products from each technique are different, all products are α-alumina after heat treatment at 1150°C for 3 hours. The crystallite size calculated from the Scherrer equation, summarized in Table 1, confirms that the grain sizes of all alumina crystals synthesized are in nanometer scale.

Table 1. Crystallite size and particle size of synthesized products.

Synthesized method	Phase of as-synthesized product	Crystallite size after calcination (nm)	Average particle size (μm)	
			before milling	after 72h-milling
Sol-gel	amorphous	9.52	4.07	0.36
Precipitation	amorphous	9.65	0.45	0.37
Solvothermal	χ-Al_2O_3	9.74	4.36	1.11*

* sample was milled for 48 hours.

SEM micrographs of the obtained samples indicate that grains of the alumina powders are agglomerated into larger particles, called secondary particles. However, since the average size of the secondary particles can be decreased by milling, it is suggested that the secondary particles are loosely agglomerated.

Figure 1 illustrates UV-Visible spectra of undoped and Cr-doped products, synthesized by various methods. Undoped α-alumina samples do not show any absorption peak, regardless of the synthesis method. Nevertheless, all chromium-doped samples show absorption peaks around 400 and 550 nm, which are the same as the absorption of ruby [2]. It should be noted that the product synthesized by sol-gel method has highest absorption intensity, suggesting that chromium ions diffused into the Al_2O_3 matrix more easily when sol-gel method is employed.

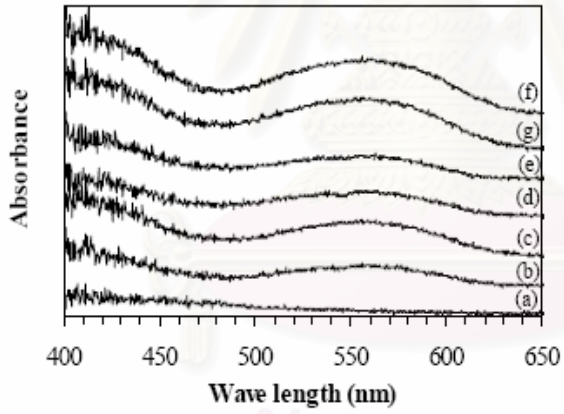

(a): undoped α-Al_2O_3,
(b) and (c): 2% and 5% Cr-doped Al_2O_3 using precipitation method, respectively,
(d) and (e): 2% and 5% Cr-doped Al_2O_3 using solvothermal method, respectively,
(f) and (g): 2% and 5% Cr-doped Al_2O_3 using sol-gel method, respectively.

Figure 1. UV-Visible spectra of synthesized samples.

CONCLUSION

α-alumina with nanosized grains can be successfully synthesized by sol-gel, precipitation and solvothermal method. Chromium doping into alumina matrix can be achieved by using all techniques. However, sol-gel method results in highest amount of chromium ions containing in the alumina matrix.

ACKNOWLEDGEMENT

The author would like to thank the Thailand Research Fund (TRF), the National Nanotechnology Center and the Thailand-Japan Technology Transfer Project (TJTTP) for their financial support.

REFERENCES

[1] Dorre, E. and Hubner, H. *Alumina, Processing, Properties, and Applications*, Springer-Verlag, (1984).

[2] Cornelis, K. and Cornelius, S. H., *Manual of Mineralogy*, John Wiley and Sons, New York, (1993).

VITA

Miss Tanitta Prasitwuttisak was born in Nan, Thailand, on February, 1981. She received bachelor's degree in Chemical Engineering from the department of Chemical Engineering, Faculty of Engineering, King Mongkut's Institute of Technology Ladkrabang, Bangkok, Thailand on May, 2003.